





This is to certify that the  
thesis entitled

SPECTROSCOPIC STUDIES OF POTASSIUM SALT SOLVATION  
AND COMPLEXATION IN VARIOUS SOLVENTS

presented by

Jeny-Shang Shih

has been accepted towards fulfillment  
of the requirements for

Ph.D degree in Chemistry

A handwritten signature in cursive script, appearing to read "Alexander D. Pope".

Major professor

Date July 25 1978

© 1978

JENY-SHANG SHIH

ALL RIGHTS RESERVED

SPECTROSCOPIC STUDIES OF POTASSIUM SALT SOLVATION  
AND COMPLEXATION IN VARIOUS SOLVENTS

BY

Jeny-Shang Shih

A DISSERTATION

Submitted to  
Michigan State University  
in partial fulfillment of the requirements  
for the degree of

DOCTOR OF PHILOSOPHY

Department of Chemistry

1978

ABSTRACT

SPECTROSCOPIC STUDIES OF POTASSIUM SALT SOLVATION  
AND COMPLEXATION IN VARIOUS SOLVENTS

BY

Jeny-Shang Shih

Potassium-39 and carbon-13 NMR measurements were applied as sensitive probes in the studies of solvation and complexation of potassium salts in nonaqueous solvents.

In most cases, the chemical shifts of  $^{39}\text{K}$  were found to be dependent on the concentration of  $\text{K}^+$  ion, which is indicative of the formation of contact ion pairs. The contact ion pairing formation was found to be dependent on the dielectric constant and also on the donicity of the solvents. Ion-solvent interaction was also studied by the extrapolation of the chemical shift to infinitely dilute concentration. In general, a correlation was observed between the  $^{39}\text{K}$  infinite dilute chemical shift with the Gutmann donor numbers of the solvents. A linear relation between the infinite dilution chemical shifts and the atomic numbers of alkali metals was found in some solvents such as acetonitrile, dimethylsulfoxide and nitromethane.

Preferential solvation of  $\text{K}^+$  ion in binary mixed solvents was studied qualitatively and quantitatively

by  $^{39}\text{K}$  NMR. The geometric equilibrium constant,  $K^{1/n}$  and the free energy of preferential solvation were obtained for each system by using Covington's treatment.

Complexation of potassium ion with macrocyclic cryptands and with crown ethers was investigated in several nonaqueous solvents by potassium-39 and carbon-13 NMR. The  $^{39}\text{K}$  chemical shifts for the  $\text{K}^+$  cryptate C222 was found to be solvent independent which is indicative of the formation of the inclusive complex. The cryptand C221 was found to form stable complexes with  $\text{K}^+$  in some nonaqueous solvents, but the solvent dependent  $^{39}\text{K}$  chemical shift for  $\text{K}^+\text{C221}$  complexes seems to suggest the formation of exclusive complexes. Carbon-13 NMR studies seem to indicate that the cryptand C221 forms less stable complexes with  $\text{K}^+$  than the cryptand C222.

The complexation of cryptand C211 with  $\text{K}^+$  in various solvents was studied by  $^{39}\text{K}$  NMR. The stabilities of  $\text{K}^+\text{C211}$  complexes among these solvents are in the order: acetone > acetonitrile > pyridine > dimethylformamide > dimethylsulfoxide. The cation selectivities of cryptands in nonaqueous solvents were monitored by C-13 NMR.

The complexation reactions of  $\text{K}^+$  with some macrocyclic crown ethers, such as 18-crown-6, dibenzo-18-crown-6, 15-crown-5, monobenzo-15-crown-5 and 12-crown-4 were investigated in various solvents by potassium-39 and carbon-13 NMR. The  $\text{K}^+$ -18-crown-6 complexes were

found to be quite stable in nonaqueous solvents. The stabilities of  $K^+$ -18-crown-6 complex decrease in the order: acetone > dimethylformamide > water > dimethylsulfoxide. No ion-pairing formation was found between the complex  $K^+$ -18-crown-6 and the anion.

In the complexation study of 15-crown-5 with  $K^+$  both 1:1 and 2:1 sandwich ligand/ $K^+$  complexes seem to be formed in all nonaqueous solvents used. The stability constants of 1:1 complexes in these solvents were always large. The solvent effect on the stability of 2:1 sandwich complexes is in the order: nitromethane > acetone > propylene carbonate > pyridine > acetonitrile > methanol > dimethylformamide > dimethylsulfoxide, which with the exception of pyridine, follows the inverse order of the donicities of these solvents. In the 2:1 complexes, the anions were insulated from the action of the solvent and the cation.

The complexation reactions of 12-crown-4 with  $K^+$  in various solvents were also studied by the same technique. In most cases no evidence was found for the formation of 2:1 sandwich complexes and the 1:1 complexes seem to be quite weak. Solvents influence on the stabilities of the 1:1 complexes are in the order: acetonitrile  $\geq$  acetone > nitromethane > methanol > dimethylsulfoxide.

Finally, a recovery process for the cryptand C222 and C211 from cryptates was developed.

## ACKNOWLEDGEMENTS

The author wishes to thank Professor Alexander I. Popov for his guidance, counseling and encouragement throughout this study.

The special contributions of Professor Michael J. Weaver as second reader are appreciated. Many thanks also go to all the members of Dr. A. I. Popov's research group for many months of friendship, and good times. And to Dianne, Fred, Mojtaba and Dale, special thanks for their friendship, discussion and stimulation.

Gratitude is also extended to the Department of Chemistry, Michigan State University and the National Science Foundation for financial aid.

Finally, I would like to acknowledge my parents and my wife for their constant encouragement and cordial consideration.

## TABLE OF CONTENTS

Chapter	Page
I HISTORICAL REVIEW	
INTRODUCTION.....	1
(A) STUDIES OF IONIC SOLVATION AND ASSOCIATION BY NMR.....	2
(B) POTASSIUM NUCLEAR MAGNETIC RESONANCE.....	8
(C) MACROCYCLIC CROWN ETHERS AND CRYPTATES.....	17
(a) MACROCYCLIC CROWN ETHERS.....	17
(b) MACROBICYCLE CRYPTANDS.....	24
III EXPERIMENTAL PROCEDURE	
(A) INSTRUMENTAL.....	28
(B) CHEMICAL SHIFT MEASUREMENTS.....	31
(C) POTASSIUM SALTS.....	34
(D) SOLVENTS.....	34
(E) PURIFICATION OF CRYPTANDS AND CROWN ETHERS.	35
(F) DATA HANDLING.....	36
III POTASSIUM-39 NUCLEAR MAGNETIC RESONANCE STUDIES OF IONIC SOLVATION AND ASSOCIATION OF POTASSIUM SALTS IN VARIOUS SOLVENT	
INTRODUCTION.....	37
(A) IONIC SOLVATION AND ASSOCIATION STUDIES OF THE POTASSIUM IONS IN NEAT SOLVENT.....	37
(B) IONIC SOLVATION OF THE POTASSIUM ION IN MIXED SOLVENTS.....	72

Chapter	Page
IV POTASSIUM-39 AND CARBON-13 NMR STUDIES OF POTASSIUM SALT COMPLEXATION IN VARIOUS SOLVENTS	
INTRODUCTION.....	89
(A) COMPLEXATION OF THE K <sup>+</sup> IONS BY CRYPTANDS..	89
(B) COMPLEXATION OF THE K <sup>+</sup> IONS BY CROWN ETHERS.....	113
V RECOVERY OF CRYPTAND FROM CRYPTATE.....	154
APPENDICES.....	164
APPENDIX I.....	164
APPENDIX II.....	169
APPENDIX III.....	171
APPENDIX IV.....	174
APPENDIX V.....	178
REFERENCES.....	183

## LIST OF TABLES

Table	Page
1	Nuclear properties of potassium isotopes..... 10
2	Diameters of selected cations and macrocyclic polyether cavities..... 20
3	Magnetic susceptibilities corrections to the $^{39}\text{K}$ chemical shifts..... 33
4	$^{39}\text{K}$ chemical shifts of potassium salt solutions. 39
5	Key solvent properties..... 46
6	The ion-pairing formation constants and limiting chemical shifts of potassium in various solvents 61
7	Potassium-39 chemical shifts at infinite dilution in various solvents..... 64
8	$^{39}\text{K}$ chemical of potassium salt solutions in mixed solvents..... 74
9	Summary of isosolvation point data for potassium salts in the Binary solvent mixtures ..... 77
10	The equilibrium constants and free energy change in the mixed solvents..... 85
11	The chemical shifts and line widths of potassium -39 of $\text{K}^+\text{C222}$ complexes at 0.5 mole ratio ( $\text{C222}/\text{K}^+$ )..... 93
12	Carbon-13 chemical shift of potassium cryptates C222..... 95
13	The change in $^{13}\text{C}$ chemical shift of cryptand C222 upon complexation..... 99

Table	Page	
14	Chemical shifts and line widths of K-39 of K <sup>+</sup> -C221 complexes at 0.5 mole ratio (C221/K <sup>+</sup> )....	103
15	Carbon-13 chemical shifts of potassium cryptate 221.....	104
16	Mole ratio study of cryptand C211 complexes with KPF <sub>6</sub> in various solvents.....	106
17	Formation constants and limiting chemical shift for complexation of KPF <sub>6</sub> by C211.....	109
18	Carbon-13 chemical shift ( $\Delta$ ppm) of Li, Na and Cs cryptates.....	110
19	Mole ratio studies of crown ethers complexes with KPF <sub>6</sub> in various solvents.....	114
20	Formation constants and limiting chemical shift for the complexation of KPF <sub>6</sub> by 18-crown-6 in various solvents.....	121
21	Formation constants of complexes of KPF <sub>6</sub> with dibenzo-18-crown-6 in various solvents .....	125
22	The elemental analysis for (15-crown-5) <sub>2</sub> KPF <sub>6</sub> sandwich complex.....	129
23	Formation constants and limiting chemical shifts for 1:1 and 2:1 15-crown-5-K <sup>+</sup> complexes in various solvents.....	133
24	The limiting chemical shifts of <sup>39</sup> K NMR for the complexes of potassium salts with 15- crown-5 in various solvents.....	137

Table	Page	
25	Elemental analysis of (monobenzo 15 C 5) <sub>2</sub> KPF <sub>6</sub> .....	139
26	Formation constants of complexes of KPF <sub>6</sub> with monobenzo-15-crown-5 in various solution.....	141
27	The C-13 NMR chemical shifts of M <sup>+</sup> -12-crown -4 complexes in various solvents (M <sup>+</sup> = K <sup>+</sup> , Cs <sup>+</sup> ).....	144
28	Formation constants for the 12-crown-4-K <sup>+</sup> complexes in various solvents.....	147
29	Limiting chemical shifts and line widths of K-39 for the complexation of KPF <sub>6</sub> by various macrocyclic ligands in acetone.....	152
30	Concentration of Na <sup>+</sup> and C222 in elution solutions .....	158
31	Carbon-13 chemical shifts of protonated cryptands.....	160

## LIST OF FIGURES

Figure		Page
1	Structure of crown ethers .....	18
2	Cryptands C222, C221 and C211 (with internal diameters) .....	25
3	The configurations of cryptand C222 .....	26
4	The structures of cylindrical macrotricyclic cryptands.....	27
5	Potassium-39 NMR resonance of 0.005 M $KPF_6$ in acetonitrile by Bruker 180 spectrometer. (1000 scans, 15 minutes, line width $\sim 10$ Hz) ..	30
6	K-39 chemical shifts of potassium salts in water and formamide.....	45
7	K-39 chemical shifts of potassium salts in dimethylformamide and dimethylsulfoxide .. ...	48
8	K-39 chemical shifts of potassium salts in propylene carbonate and formic acid.....	50
9	$^{39}K$ chemical shifts of potassium salts in methanol and acetonitrile.....	52
10	$^{39}K$ chemical shifts of potassium salts in acetone and ethylenediamine.....	53
11	$^{39}K$ chemical shifts of potassium iodide in various solvents.....	55
12	$^{39}K$ chemical shifts of potassium thiocyanate in various solvents .....	57

Figure	Page
13 $^{39}\text{K}$ chemical shifts of potassium hexafluoro-phosphate in various solvents.....	58
14 The temperature dependent ionic association of potassium salts in water and acetone.....	62
15 The plot of the infinite dilution chemical shift vs the Gutmann donor number.....	65
16 The range of infinite dilution chemical shifts between nitromethane and pyridine for $^{23}\text{Na}$ , $^{39}\text{K}$ and $^{133}\text{Cs}$ resonance.....	68
17 The plot of infinite dilution chemical shift vs atomic number of alkali metal ions.....	71
18 $^{39}\text{K}$ chemical shifts of $\text{KPF}_6$ in the Binary mixtures of acetone with nitromethane, acetonitrile, water and pyridine.....	76
19 $^{39}\text{K}$ chemical shifts of $\text{KPF}_6$ in the mixtures of acetonitrile with nitromethane, acetone and water.....	78
20 $^{39}\text{K}$ chemical shifts of $\text{KPF}_6$ in the acetonitrile-propylene carbonate mixtures.....	79
21 $^{39}\text{K}$ chemical shifts of $\text{KSCN}$ in the mixtures of DMSO with acetone, water and ethylenediamine.....	81
22 $^{39}\text{K}$ chemical shifts of $\text{KI}$ in mixtures of methanol with water and ethylenediamine.....	82
23 Convington plot for pyridine-acetone mixtures.....	86

Figure	Page
24	Convington plot for the acetonitrile- acetone mixtures..... 88
25	$^{39}\text{K}$ NMR spectra of $\text{KPF}_6$ -cryptand C222 solution. 91
26	$^{13}\text{C}$ NMR spectra of $\text{K}^+$ -cryptand C222 in acetone. 97
27	Potassium-39 spectra of potassium-C221 cryptate in various solvents; $[\text{C221}] = 0.01 \text{ M}$ $[\text{KPF}_6] = 0.02 \text{ M}$ 100
28	$^{39}\text{K}$ chemical shift vs mole ratio of C211/ $\text{K}^+$ in various solvents..... 107
29	$^{39}\text{K}$ chemical shift vs mole ratio of 18C6/ $\text{K}^+$ in various solvents..... 119
30	Chemical shifts of 18 C 6 $\text{K}^+$ complexes as function of concentration..... 122
31	$^{39}\text{K}$ chemical shifts vs mole ratio of dibenzo 18C6/ $\text{K}^+$ in various solvents..... 124
32	$^{39}\text{K}$ chemical shift vs mole ratio of 15C5/ $\text{K}^+$ in nitromethane, acetone, methanol and acetonitrile..... 127
33	$^{13}\text{C}$ spectrum of 15-crown-5 at mole ratio 0.75 of $\text{K}^+$ /15C5 in acetone..... 128
34	$^{39}\text{K}$ chemical shift vs mole ratio of 15C5/ $\text{K}^+$ in pyridine, propylene carbonate, dimethyl- formamide and dimethylsulfoxide..... 131
35	Computer fitting for the chemical shifts vs mole ratio of 15C5/ $\text{K}^+$ in methanol..... 132
36	carbon-13 chemical shift vs mole ratio of $\text{K}^+$ /15C5 in various solvents..... 136

Figure	Page
37	$^{39}\text{K}$ chemical shift variation with the concentration of 1:1 (15C5) $\text{KPF}_6$ complex and potassium salt in acetonitrile..... 138
38	$^{39}\text{K}$ chemical shifts vs mole ratio of MB 15C5 / $\text{K}^+$ in nitromethane and acetonitrile..... 140
39	$^{39}\text{K}$ chemical shift vs mole ratio of 12-crown -4/ $\text{K}^+$ in various solvents..... 143
40	Carbon-13 chemical shift vs mole ratio of $\text{K}^+$ / $^{12}\text{C}_4$ in various solvents..... 145
41	Carbon-13 chemical shift vs mole ratio of Cs/ligand in methanol..... 149
42	Mole ratio- $^{39}\text{K}$ chemical shift study for various ligands in acetone..... 151
43	Diagram for recovery of cryptand from cryptate..... 155
44	Elution curve for separation of $\text{C}_{22}\text{H}_{22}^{2+}$ from $\text{Na}^+$ ..... 157
45	Carbon-13 spectra of protonated and free cryptands..... 161
46	$^1\text{H}$ spectra of protonated and free cryptands... 162

## LIST OF ABBREVIATIONS

AC( $\text{Me}_2\text{CO}$ ): Acetone  
NM( $\text{MeNO}_2$ ): Nitromethane  
PC: Propylene carbonate  
ACN( $\text{Me}_2\text{CN}$ ): Acetonitrile  
DMF: N-N-Dimethylformamide  
DMSO: Dimethylsulfoxide  
HFor: Formic acid  
For $\text{NH}_2$ : Formamide  
PY: Pyridine  
EN: Ethylenediamine  
MeOH: Methanol

**CHAPTER I**  
**HISTORICAL REVIEW**

## INTRODUCTION

Potassium and other alkali metal ions play important roles in chemistry as well as in biological system. However, ionic interaction and binding process of these ions in solution and especially in nonaqueous solvents still remain largely unknown. The techniques usually applied to study complexation reactions and ionic solvation are potentiometric methods using cation-selective electrodes, calorimetry and conductometry.

Recently several new techniques which are very sensitive to change of ionic environments in solution have been developed. One of the most important techniques is Fourier-transform nuclear magnetic resonance. FTNMR method is now used to yield the qualitative information about the solvent-solute, solvent-solvent and solute-solute interactions, as well as quantitative data concerning ion-pair formation and complexation in alkali metal solutions.

## HISTORICAL REVIEW

(A) STUDIES OF IONIC SOLVATION AND ASSOCIATION BY NMR

Since both the chemical shift and the relaxation time of the nuclear resonances are very sensitive to change of ionic environments in solution, the nuclear resonance spectroscopy method has become a very powerful tool for the investigation of both ion-ion and ion-solvent interactions in alkali solutions.

The NMR studies of ionic solvation and association of alkali salt solution can be performed using alkali metal nuclei such as  ${}^7\text{Li}$ ,  ${}^{23}\text{Na}$ ,  ${}^{39}\text{K}$ ,  ${}^{87}\text{Rb}$  and  ${}^{133}\text{Cs}$ , anion nuclei such as  ${}^{19}\text{F}$ ,  ${}^{35}\text{Cl}$ ,  ${}^{81}\text{Br}$  and  ${}^{127}\text{I}$  and the solvents nuclei such as  ${}^{13}\text{C}$ ,  ${}^1\text{H}$ ,  ${}^{14}\text{N}$  and  ${}^{17}\text{O}$ . There are many studies of ionic solvation and association in alkali salt solutions performed by proton ( ${}^1\text{H}$ ) NMR (1-5) of the solvent. However, relatively few studies on other nuclei have been reported.

The pioneering NMR studies of ionic association in alkali solutions were done by Shoolery and Alder (1). They studied the ionic association in the KF aqueous solution and reported that  ${}^{19}\text{F}$  chemical shifts of KF were dependent on the concentration of potassium fluoride aqueous solution and suggested some small amount of ion-pairing formation. The same system was carefully studied by Connick and Poulson (6). They reported that the  ${}^{19}\text{F}$  chemical shift of KF aqueous solution moved down field

with increasing the potassium fluoride concentration at the concentration  $< 5.0 \text{ M}$ , and moved to high field at higher concentration. It was interpreted in terms of the formation of the solvent separated ion pairs at lower concentration while the formation of the contact ion-pairing formation at higher concentration. Recently, DeWitte and Popov (7) extended these  $^{19}\text{F}$  resonance studies of alkali hexafluorophosphate solutions to a wide range of nonaqueous media. They reported that in solvents of medium polarity and donicity such as propylene carbonate and acetonitrile, the  $^{19}\text{F}$  chemical shift for  $\text{NaPF}_6$  moved upfield with increasing concentration of the salt. The behavior is indicative of anion-cation interaction. However, potassium hexafluorophosphate solutions do not show any concentration dependence of  $^{19}\text{F}$  chemical shift, which indicates the absence of ionic association in these solutions.

The  $^{19}\text{F}$  chemical shift for potassium fluoride in water-organic solvent mixtures was monitored by Carrington and coworkers (8). The linear variation of chemical shifts of  $^{19}\text{F}$  with mole fraction of solvent were observed in mixtures of water with methanol and formamide. It indicated no preferential solvation of  $\text{F}^-$  ions in either mixtures. Similar results for the same system were also obtained by several authors (9-12). However, water was reported to appear strongly preferred in the primary solvation shell of  $\text{F}^-$  ion over acetone and acetonitrile (9). The

effect of paramagnetic ions on the transverse relaxation times of  $^{19}\text{F}$  of  $\text{PF}_6^-$  in aqueous solutions was observed by Stengle and Langford (12). The decrease in relaxation time of  $^{19}\text{F}$  was interpreted in terms of association between  $\text{PF}_6^-$  and the paramagnetic ion.

The chemical shifts of the nuclear resonance of  $^{35}\text{Cl}$ ,  $^{81}\text{Br}$  and  $^{127}\text{I}$  in aqueous solutions of alkali halides were studied by Deverell and Richards (13). They reported that the magnitude of the shift of halide nuclear resonance increases with increasing atomic number of the halide ion and generally the shielding by solvent showed dependence upon the partner cation:  $\text{Na}^+ > \text{K}^+ > \text{Li}^+ > \text{Rb}^+ > \text{Cs}^+$  while the order of magnetic solvent shielding effects produced by the anions was always found to be in the order  $\text{I}^- < \text{Br}^- < \text{Cl}^- < \text{F}^- < \text{NO}_3^-$ . Stengle, et al (14) monitored the  $^{35}\text{Cl}$ ,  $^{79}\text{Br}$  and  $^{127}\text{I}$  resonances of alkali halide solutions in water and in mixed solvents of water with methanol, acetonitrile, DMSO and DMF. The chemical shift of halide nuclear resonance was found to be strongly dependent on the solvent while the dependence on the cation  $\text{Li}^+$ ,  $\text{Na}^+$ ,  $\text{K}^+$  were comparatively weak. The NMR behavior of  $\text{Cl}^-$  and  $\text{I}^-$  ions in mixtures of DMSO with water indicated that there was no strong preference for either solvent. However, the strong preferential solvation of halide ions of water over acetonitrile was observed.

Recently,  $^{35}\text{Cl}$  was used to study quantitatively the

solvation of  $\text{LiClO}_4$  in acetone-nitromethane mixtures by Popov and Baum (15). In that work, the linewidth of the  $^{35}\text{Cl}$  resonance was monitored as a function of the acetone/ $\text{Li}^+$  mole ratio. They reported that the solvation number of  $\text{Li}^+$  by acetone is 4. The relaxation time of  $^{35}\text{Cl}$  nuclei has been used to study the ionic association of alkali chloride solution. Berman and Stengle (16) monitored the spin-lattice relaxation time ( $T_1$ ) of  $^{35}\text{Cl}$  to study the ionic association behavior of the  $\text{ClO}_4^-$  ion with  $\text{Li}^+$  in DMF, acetonitrile and DMSO.

Another anion resonance such as  $^{17}\text{O}$  and  $^{14}\text{N}$  NMR can be applied to the investigation of ionic solvation (17). However, the use of  $^{14}\text{N}$  and  $^{17}\text{O}$  NMR are limited by the need for special instrumentation due to their low magnetic moments.

Alkali nuclei resonances such as  $^7\text{Li}$ ,  $^{23}\text{Na}$ ,  $^{39}\text{K}$ ,  $^{87}\text{Rb}$  and  $^{133}\text{Cs}$  have also been applied as sensitive probes for the study of ionic association and solvation of alkali salt solutions. A review of the alkali nuclei resonance in alkali salt solutions was published by Popov (18).

Maciel and coworkers (19) monitored  $^7\text{Li}$  chemical shifts of  $\text{LiBr}$  and  $\text{LiClO}_4$  in several nonaqueous solutions. A linear correlation between chemical shifts of  $^7\text{Li}$  and Kosower's Z values (20) of the solvents was observed.

Recently, Popov and coworkers observed the chemical shifts of the  $^7\text{Li}$  resonance of Lithium salts in eleven

nonaqueous solvents (21)(22). They reported that in dimethylformamide and lesser extent in propylene carbonate, methanol and dimethylsulfoxide solution, the  $^7\text{Li}$  chemical shift were essentially independent of the counter ion and the salt concentration. The results indicated either that the salts were largely dissociated or that they exist in the form of solvents separated ion pairs.

Mishustin and Kessler (23) studied the lattice spin relaxation times ( $T_1$ ) of  $^7\text{Li}$  of lithium salt solutions for the investigation of the ion-solvent and ion-ion interaction. They reported the linear correlation between the relaxation time and Gutmann's donor number (24) of the solvents. The donor number of the solvents was defined as the negative enthalpy of the reaction between the solvent and antimony pentachloride in 1, 2 dichloroethane solution. Similar studies were made by Hertz and coworkers (25)(26), and similar results were obtained. The ionic association of organometallic lithium compounds such as  $\text{LiAlMe}_4$  was also studied using  $^7\text{Li}$  resonance by Covington and coworkers (27). Recently,  $^7\text{Li}$  has been used to study the preferential solvation of  $\text{Li}^+$  in mixed solvents. Covington, et al (28) studied the  $^7\text{Li}$  resonance of  $\text{LiNO}_3$  in DMSO- $\text{H}_2\text{O}$  mixture. They found that  $\text{NO}_3^-$  ion are preferentially solvated by DMSO and  $\text{Li}^+$  by water.

Sodium-23 NMR has been extensively investigated and a comprehensive review of the literature available to late 1974 is presented in the Ph.D thesis of M.S Greenberg

(29). Kessler, et al (30) studied the spin-lattice relaxation time ( $T_1$ ) of  $^{23}\text{Na}$  and  $^{133}\text{Cs}$  of alkali salts in eleven nonaqueous solvents. In the  $^{23}\text{Na}$  case they also found that values of  $1/T_1$  correlated with Gutmann's donor numbers for these solvents (24) with the only exception being  $\text{H}_2\text{O}$ . However, the correlation was less markedly in the case of  $\text{Cs}^+$ . In that work, values of donor number used for methanol (31) and water were 19 and 18 respectively. In a study of  $^{23}\text{Na}$  resonances of sodium salts in different solvents, Bloor and Kidd (32) found a correlation between the  $\text{pK}_a$  of the solvent and the chemical shift of the cation.

Of the heavier alkali nuclei (K, Rb, Cs), the  $^{133}\text{Cs}$  nucleus is the easiest to study by NMR technique. The signals were reported to be strong and sharp for the cesium samples in the concentration range of  $10^{-3}$  M (33).

Halliday (34) reported that  $^{133}\text{Cs}$  chemical shift changed nonlinearly with Cs salt concentration in water and several nonaqueous solvents and the degree of nonlinearity depended upon the dielectric constants of the solvents, the  $^{133}\text{Cs}$  shifts were explained in terms of the cation-anion interaction. Recently Popov and DeWitte (33) studies the  $^{133}\text{Cs}$  chemical shift of cesium salts in water and eleven nonaqueous solvents. In all cases, the chemical shifts were found to be strongly concentration dependent indicating some contact ion pair formation. In that work, the chemical shift of the  $\text{Cs}^+$

at infinite dilution have been determined in these solvents. Comparison of the limiting chemical shifts with Gutmann's donor numbers for these solvents in general shows an adequate but not straight line correlation as was observed with solvent-dependent chemical shifts of the  $^{23}\text{Na}$  resonance (29)(35).

Since  $^{87}\text{Rb}$  nucleus has a large quadrupole moment, the natural line width for  $^{87}\text{Rb}$  is large which limit the use of  $^{87}\text{Rb}$  resonance for study on the ionic solvation and association. The studies of the ionic association of rubidium salt solution in water was reported by Deverell and Richards (36). A very broad  $^{87}\text{Rb}$  signal (line width  $\sim 400\text{Hz}$ ) for rubidium salts in dimethylsulfoxide have been observed by Crawford and Gasser (37). Recently, Neggla, et al (38) monitored the spin-lattice relaxation time of  $^{87}\text{Rb}$  in methanol-water mixture. The  $\text{Rb}^+$  were found to be preferentially solvated by methanol.

Carbon-13 NMR also can be applied to study the solvation of cation. Stockton (39) monitored the  $^{13}\text{C}$  chemical shift of ethanol in  $\text{AlCl}_3$  ethanol solution as a function of temperature, solvation shell signal appeared below  $-20^\circ$ , the  $\text{CH}_2$  carbon showed three solvation signals. At least two  $\text{CH}_3$  carbon solvation shell signals were discernible.

#### (B) POTASSIUM NUCLEAR MAGNETIC RESONANCE

There are three magnetic potassium nuclei ie:  $^{39}\text{K}$

$^{40}\text{K}$  and  $^{41}\text{K}$ . The nuclear properties of these nuclei are listed in Table 1.

As shown in the Table 1, all the potassium nuclei ( $^{39}\text{K}$ ,  $^{40}\text{K}$  and  $^{41}\text{K}$ ) have very low sensitivities and low frequencies as compared to  $^1\text{H}$ . The sensitivity (S) is function of natural abundance (No), magnetic moment ( $\mu$ ) and nuclear spin (I) by the relation:  $S = \text{No} \mu^3 (I + 1) / I^2$ . Although  $^{39}\text{K}$  has a high natural abundance, it also has a very low magnetic moment which leads to low sensitivity. Both  $^{40}\text{K}$  and  $^{41}\text{K}$  nuclei have a low natural abundance and a low magnetic moment. Due to the low sensitivities and low frequencies of potassium nuclei, the study of potassium nuclei resonance is largely determined by the sensitivity of the spectrometer. In the past rather sparse studies on the potassium resonance have been reported. In most cases, the measurements were performed at relatively low fields (<13 kilogauss) and continuous wave techniques were used, and therefore they were limited to solutions of fairly high concentration (>0.2 M) (36)(40-44). Fortunately, due to the development of Fourier transform NMR technique and the availability of high field superconductive solenoids, potassium NMR studies are becoming quite feasible.

Of the potassium nuclei,  $^{39}\text{K}$  has the highest sensitivity and the signal of  $^{39}\text{K}$  resonance is easiest to observe. First  $^{39}\text{K}$  resonance signal was observed at 1.59 MC at a

Table 1. Nuclear Properties of Potassium Isotopes

	$^{39}\text{K}$	$^{40}\text{K}$	$^{41}\text{K}$
Nuclear spin	3/2	4	3/2
Quadrupole moment (barn)	0.055	-0.07	0.067
Magnetic moment <sup>(a)</sup> ( $\mu\text{N}$ )	0.390	-1.296	0.214
Natural abundance	93.1%	0.012%	6.88%
Sensitivity <sup>(b)</sup>	$4.7 \times 10^{-4}$	$6.2 \times 10^{-7}$	$5.8 \times 10^{-6}$
Resonance at 4.23 Tesla <sup>(c)</sup>	8.4 MHz	10.4 MHz	4.6 MHz

(a) The magnetic moment of potassium ion purely surrounded by water molecules.

(b) Referred to the proton NMR signal of  $\text{H}_2\text{O}$  at the same magnetic field and with same probe volume.

(c) One Tesla = 10 kilogauss magnetic field. At the field of 4.23 Tesla,  $^1\text{H}$  resonates at 180 MHz.

field of 8000 gauss by Collins (40). He obtained the ratio of the magnetic moment of  $^{39}\text{K}$  to proton:

$\mu_{^{39}\text{K}} / \mu_{^1\text{H}} = 0.13999$ . The value of  $\mu_{^1\text{H}}$  was found to be  $2.79268 \mu\text{N}$  (41). The value of  $\mu_{^{39}\text{K}}$  was calculated to be  $0.39094 \pm 0.0007 \mu\text{N}$ . Brun, et al (42) measured the nuclear magnetic moments of  $^{39}\text{K}$ ,  $^{41}\text{K}$ ,  $^{89}\text{Y}$  and  $^{109}\text{Ag}$  at a magnetic field of about 9000 gauss. Resonances of the two potassium isotopes 39 and 41 were obtained in a 15 molar aqueous solution of potassium formate. For  $^{39}\text{K}$  the magnetic was found to be  $\mu_{39} = +0.390873 \pm 0.000013 \mu\text{N}$  in a agreement with the value of Collins's (40). The signal of  $^{41}\text{K}$  appeared with a signal to noise ratio of about 3:1. The ratio of the frequencies of the two isotopes is  $\nu_{41} / \nu_{39} = 0.54886 \pm 0.00008$ .

Hindman (43) studied the potassium-39 resonance in aqueous solution of potassium chloride. The  $^{39}\text{K}$  chemical shift was found to be independent of the concentration of potassium chloride. Deverell, et al (36) monitored the chemical shift of  $^{39}\text{K}$  in aqueous solution of potassium halides and nitrates from concentration of 0.2 molar up to saturation. The chemical shifts of the  $^{39}\text{K}$  nuclear resonance in salt solutions were found to depend strongly on the salt concentration in a non-linear manner. For all the salts studies, however, the chemical shift does vary linearly with the mean activity of the salt. This suggests that the shifts are strongly influenced by

interactions between  $K^+$  ions with other ions. The importance of ionic interactions is also shown by the strong dependence of the chemical shifts on the nature of the anions present. The authors also found that the effect of different anions on the  $^{39}K$  chemical shifts varied in the order  $I^- > Br^- > Cl^- > F^- > NO_3^-$ . They suggested that it was caused by direct collisional interactions between the cations and the anions.

Bloor and Kidd (44) monitored the  $^{39}K$  chemical shifts of several aqueous potassium salt solutions. They reported that in all cases the chemical shifts of  $^{39}K$  resonance varies linearly with the salt concentration. The paramagnetic shielding was decreased by the counter ions in the order:  $I^- > Br^- > CN^- > PO_4^{3-} > OH^- > Cl^- > CNO^- > CO_3^{2-} > CNS^- > CH_3COO^- > F^- > N_3^- > NO_2^- = H_2O > SO_4^{2-} > CrO_4^{3-} > NO_3^- > Cr_2O_7^{2-}$ . The shift was explained in terms of the short range overlapping of the outer electron orbitals of the anion and cation during random ionic collisions. The magnitudes of the chemical shifts were shown to be directly proportional to the effectiveness of this overlap interaction.

Recently, the signal of the rare isotope  $^{40}K$  was detected for the first time by Sahm and Schwenk (45). In their work, the NMR lines of  $^{39}K$  and  $^{41}K$  have also been investigated in solution of some potassium salts in  $H_2O$ ,  $D_2O$ , methanol and ethylenediamine. The potassium salt concentration range used in their work was from 0.2 M to

saturation. The magnetic moments of the  $^{39}\text{K}$ ,  $^{40}\text{K}$  and  $^{41}\text{K}$  ions completely surrounded by water molecules were found to be 0.391, 1.296 and 0.214  $\mu\text{N}$  respectively. The natural line width of  $^{39}\text{K}$  resonance was reported to be 12 Hz. At infinite dilution the spin-spin relaxation time ( $T_2$ ) for  $^{39}\text{K}$  in  $\text{H}_2\text{O}$  is 56 msec. The ratio of  $T_2(^{39}\text{K}) / T_2(^{41}\text{K})$  is 1.36. The shielding constant ( $\sigma$ ) of the  $^{39}\text{K}$ ,  $^{40}\text{K}$  and  $^{41}\text{K}$  ions by the surrounding water are  $-0.105 \times 10^{-3}$ ,  $0.13 \times 10^{-3}$ , and  $-0.105 \times 10^{-3}$  respectively.

Some studies of spin-lattice relaxation time of  $^{39}\text{K}$  resonance have been reported. Shporer and Luz (46) monitored the spin-lattice relaxation time ( $T_1$ ) of  $^{39}\text{K}$  resonance to study the kinetics of complexation of potassium ions with dibenzo-18-crown-6 (DB18C6) in methanol. They reported that in the solvated form, the NMR relaxation rate of  $^{39}\text{K}$  was relatively long ( $\sim 0.01$  sec), while in the ( $\text{K}^+\text{DB18C6}$ ) complex the symmetry around the  $\text{K}^+$  ion was considerably reduced and at same time the correlation time was increased resulting in a fast nuclear relaxation. The activation energy of the complexation of  $\text{K}^+$  with DB18C6 in methanol solution was 12.6 Kcal / mole.

A few  $^{39}\text{K}$  resonance studies on the biological system have been reported. Damadian and coworkers (47) found that the spin-spin relaxation time ( $T_2$ ) of  $^{39}\text{K}$  of potassium ions in packed bacteria was much shorter than free  $\text{K}^+$  in  $\text{H}_2\text{O}$ . They also studied (48)(49) the spin-lattice relaxation

time ( $T_1$ ) of  $^{39}\text{K}$  of potassium ions on several types of normal tissues and cancers of rats and mice. They reported that the  $^{39}\text{K}$  spin-lattice relaxation time ( $T_1$ ) for normal tissues was on the average 24% longer than that for the cancerous tissues. Both  $T_1$  and  $T_2$  of  $^{39}\text{K}$  in fresh excised rat muscle and brain were much shorter than for  $^{39}\text{K}$  in aqueous solution. The results were interpreted in terms of the association of  $\text{K}^+$  with fixed charges on macromolecules. They also studied the interaction of  $\text{K}^+$  with Dowex 50 exchange resin (50). They found both  $T_1$  and  $T_2$  of  $^{39}\text{K}$  resonance were shortened by the association of  $\text{K}^+$  with the exchange resin.

Although potassium-39 has low sensitivity and low resonance frequency, fortunately, the quadrupole moment of potassium is not large (0.055 barn) and it is smaller than that for  $^{23}\text{Na}$  or  $^{87}\text{Rb}$ . Therefore, the natural line width of the resonance is small ( $<12$  Hz) (45). As with all alkali nuclei, the chemical shift of potassium-39 is dominated by the paramagnetic term ( $\sigma_p$ ) in Ramsey equation (51). According to Ramsey equation the screening constant,  $\sigma$ , which determines the position of the resonance as the sum of various diamagnetic (shielding) and paramagnetic (deshielding) contribution:

$$\sigma = \sigma_p + \sigma_d \quad (\text{I.1})$$

$\sigma_d$  is the diamagnetic component and  $\sigma_p$  is the paramagnetic component. The theory of paramagnetic interaction

was proposed by Kondo and Yamashita (52), who suggested that the chemical shift of cations and anions in alkali halide crystals arises from the overlap repulsive forces between the closed shell of the ions. These forces cause the excitation of p orbital electrons of the alkali nuclei to higher states, the result being a decrease in the shielding of the nucleus. For potassium nuclei, the most important contribution to the chemical shift must come from the overlap between the 3p orbitals of the potassium ion and the outer s and p orbitals of anions or solvent atoms. The overlap repulsive forces will cause the excitation of electrons from the 3p to the 4p levels. This perturbation produces a paramagnetic (down field) contribution to the chemical shift. This shift can be written in the following equation:

$$\sigma_p = -16\alpha^2 \left\langle \frac{1}{r^3} \right\rangle_{np} \frac{1}{(\Delta E)_{np}} S^2 \quad (\text{I.2})$$

where  $S$  is the overlap integral between p orbital of the potassium ion and the orbitals of the neighboring ions.  $\left\langle \frac{1}{r^3} \right\rangle$  is the radial function which is the average over the outer p orbitals of the potassium,  $\Delta E$  is the mean excitation energy from the 3p to the 4p orbital,  $\alpha$  is a constant =  $\frac{e^2}{2mc^2}$  where  $m$  and  $e$  are the mass and charge of a electron respectively.

Since Kondo and Yamashita's theory made

satisfactory calculation of the chemical shifts not only for the alkali halide crystals but also for the hexahydrated  $^{87}\text{Rb}^+$  ion relative to the free ion (53).

Deverell and Richards (13) applied this theory to the interpretation of the chemical shift in solutions. They suggested that the chemical shift at concentration  $c$ , relative to the free ion can be written as :

$$\delta = -16\alpha^2 \frac{1}{\langle r^3 \rangle_{np}} \frac{1}{\Delta E} \left( \Lambda_{\text{ion-solvent}}^{(c)} + \Lambda_{\text{ion-ion}}^{(c)} \right) \quad (1.3)$$

where  $\Lambda$  is appropriate sum of the overlap integrals of the orbitals of the central ion and surrounding solvent molecules or neighboring ions. The values of  $\frac{1}{\langle r^3 \rangle_{np}} / \Delta E$  for alkali metal nuclei increase in the following order,  $^{23}\text{Na}(5.9) < ^{39}\text{K}(7.98) < ^{87}\text{Rb}(13.8) < ^{133}\text{Cs}(18.7)$ . Therefore, if the extents of both ion-solvent and ion-ion interactions are about the same for an alkali nuclei with same anion and the same solvent, the  $\delta_p$  will increase in this order  $^{133}\text{Cs} > ^{87}\text{Rb} > ^{39}\text{K} > ^{23}\text{Na}$ . This assumption consistent with their experimental results. They reported that the magnitudes of the chemical shifts increased considerably with increasing atomic number of the cation. Recently Sahn and Schwenk (45) reported that the shielding of alkali nuclei ie  $^{23}\text{Na}$ ,  $^{39}\text{K}$ ,  $^{87}\text{Rb}$  and  $^{133}\text{Cs}$  in water was a

nearly linear function of the atomic number.

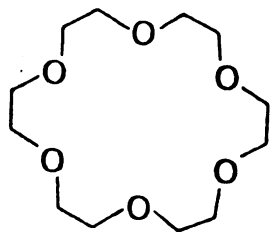
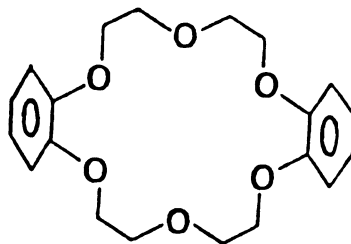
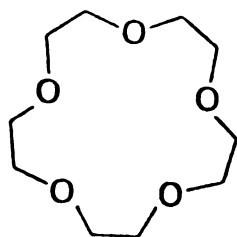
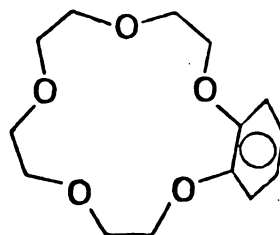
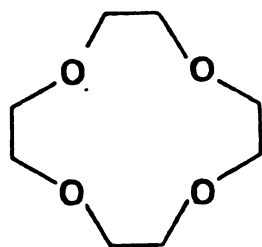
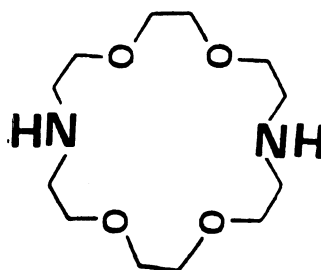
(C) MACROCYCLIC CROWN ETHERS AND CRYPTATES

(a) MACROCYCLIC CROWN ETHERS

Since Moore and Pressman (54) reported that the biological effects of some antibiotic substances such as valinomycin, nonactin and monensin depended on the presence or absence of specific alkali metal cations in the medium and suggested that these antibiotic substances acted as ion-carriers (ionophores) across membrane with different specificities for different ions.

After this discovery, the complexation of alkali metals with these naturally antibiotic carrier have been extensively investigated.

In 1967, the macrocyclic crown ethers which resemble the antibiotic ligand were synthesized by Pedersen (55). Since that time, Pedersen has reported the synthesis of over sixty macrocyclic crown ethers and discussed their abilities to complex alkali metal ions inside the two dimensional cavities (56). Several polyethers are shown in Figure 1. Generally, the alkali metal ions are regarded as poor complexing cations, and complexing of alkali cations by neutral molecules is an uncommon phenomenon. Because of these unusual complexation properties, many alkali salts can be dissolved in non polar organic solvents by forming

**18 CROWN 6****DIBENZO 18 CROWN 6****15 CROWN 5****MONOBENZO 15 CROWN 5****12 CROWN 4****CRYPTAND 22****Figure 1. Structure of Crown Ethers**

complexes with these macrocyclic polyethers. After this discovery, crown compounds and their complexes have been extensively investigated.

Crown compounds have been studied as model systems in cation transport through cellular membrane (57-60) They have found use in organic chemistry to study certain chemical reaction including the catalysis of ionic organic reactions by solvolizing cationic species (61-64).

The stability and thermodynamic studies for most macrocyclic crown ethers in water or methanol have been reported. Several excellent reviews of the crown and hetero-crown compounds and their interaction with metal cations have recently been published (65-71).

The stability of crown ether complex was reported (71) to be dependent on the several important parameters discussed below.

(i) Relative sizes of cation and ligand cavity

In general, these ligands complex most strongly those metal ions whose ionic crystal radius best matches the radius of the cavity formed by the ring upon complexation (55). The ionic diameters and the sizes of cavities of crown ethers are listed in Table 2.

Frensdoff (72) reported that the optimum polyether ring size being such that the cation just fits into "hole" was benzo-15-crown-5 for  $\text{Na}^+$ , benzo-18-crown-6

for  $K^+$  and 21-crown-7 for  $Cs^+$ . However, the relative size of cation to ligand cavity have been found to be not the only parameter which influence the stability of crown ether. For example, Izatt, et al (73) reported almost no cation selectivity was seen for 15-crown-5 in water.

Table 2. Diameters of Selected Cations and Macrocyclic Polyether Cavities(a)

Cation	Ionic diameter Å	Polyether	Diameter of cavity Å
Lithium	1.20	All 14-crown-4	1.2-1.5
Sodium	1.90	All 15-crown-5	1.7-2.2
Potassium	2.66	All 18-crown-6	2.6-3.2
Ammonium	2.84	All 21-crown-7	3.4-4.3
Rubidium	2.96		
Cesium	3.34		
Silver	2.52		
Barium	2.70		

(a) Reference 72

(ii) Type and charge of cation

In solution, for alkali and alkali earth metals, the selectivities of crown ethers for  $K^+$  and  $Ba^{2+}$  are generally higher than those for smaller and larger cations. Since smaller ions like  $Li^+$  are so strongly

solvated that considerably more energy must be expended in the desolvation step than for larger ions like  $\text{Cs}^+$ , on the other hand the larger cations are unable to attract and organize the ligand as well as smaller ones.

In general, large dipositive ions often have higher stability constants than monopositive ions of similar size. For example, potassium ion has about the same diameter as the barium ion, however, the stability constant ( $\log K$ ) of  $\text{Ba}^{2+}$ -dicyclohexyl 18-crown-6 ( $\text{Ba}^{2+}$ -DC18C6) complex is about 3.6, but it is about 2.0 (67) for the potassium complex. The result is an evidence that the binding of alkali and alkaline earth metal ions to macrocyclic ligands is electrostatic in nature.

(iii) Type of donor atom

The substitution of nitrogen or sulfur for oxygen in crown ether reduces the latter's affinity for alkali ions (72), the stability constants falling in the order of decreasing electronegativity  $\text{O} > \text{NR} > \text{NH} > \text{S}$ . However, the effects of N or S substitution of  $\text{Ag}^+$  (72) and  $\text{Hg}^{2+}$  (71) complexing were exactly the opposite. The results were explained in terms of the covalent bonding, not electrostatic force between donor atoms and metal ions in the  $\text{Ag}^+$  (74) and  $\text{Hg}^{2+}$  cases.

(iv) Number of donor atoms

The increasing in number of donor atoms without changing the size of the ring can enhance the stability

of the complexes. Cram (75) reported 18-crown-5 is a much poorer host for t-butyl ammonium ion than is 18-crown-6.

(v) Substitution on the macrocyclic ring

The addition of the benzo group to the 18-crown-6 caused decreasing in the stability of potassium-18-crown-6 complex in methanol was reported by Frensdoff (72). The result was explained in terms of decreasing in both cavity of ligand and electron density of oxygen. Meanwhile the addition of benzo group also alter the selectivity of the ligand. In methanol, the formation constant of the  $Ba^{2+}$  complex of 18-crown-6 is larger than that of the  $K^+$  complex by a factor of ten. Dibenzo 18-crown-6, on the other hand, displays the opposite preference, binding  $K^+$  better than  $Ba^{2+}$  (76).

(vi) Solvent effect

Popov, et al (77) investigated the complexation of 18-crown-6 with  $Cs^+$  in several nonaqueous solvents. They reported that both 1:1 and 2:1 ligand/ $Cs^+$  complexes are formed, previously only 1:1 complex was found in aqueous solution (73). The stability for 2:1 complexes increasing among the nonaqueous solvents in the order  $DMSO < DMF < PC < PY < AC$ . The authors concluded that, in general, the increase in the donor number of the solvents caused a decrease in the stability of complex. The solvent effect on the stabilities of complexes of alkali

metal ions with dibenzo-18-crown-6 (DB18C6) were also reported by several authors (78)(79). Matsura and Sasaki (78) reported that the solvent influence on the stabilities of the 1:1 DB18C6/ $M^+$  complex were in the order DMSO < DMF < PC. Evans and Cussler (79) found that alkali metal ions formed stronger complex with DB18C6 in acetonitrile than that in methanol.

The order of preference for alkali metal ions affected by the solvent was reported by Wong and coworkers (61). They reported that sodium in THF solution formed a stronger complex with dimethyldibenzo-18-crown-6 than potassium. Arnett and Moriarity (80) reported that stabilities of the complexes of large cations were less affected by solvent than those of smaller ones.

Several crystal structures of complexes of alkali metal ions with some crown ethers have been reported by several authors (81-85). The X ray studies of alkali metal 18-crown-6 complexes have shown that  $K^+$  sits exactly at the center of plane of the oxygen atoms while the  $Cs^+$  and  $Rb^+$  ions were displaced from the mean plane (81-83). The X ray studies (84) of sodium complexes of benzo-15-crown-5 have shown that the  $Na^+$  ion occupies the center of the plane of the oxygen atoms. A 2:1 sandwich 12-crown-4/ $Na^+$  complex have been found by X ray analysis (85). It was also found (84) that, for the potassium complex of dibenzo-30-crown-10 and apparently for other large ring cyclic polyethers, the complex consists of a wrap-around

structure where all the oxygen atoms are approximately equidistant from the potassium ion but not in the same plane.

( b ) MACROBICYCLIC CRYPTANDS

The diazopolyoxa macrobicyclics cryptands was synthesized by Lehn, et al (86). The cryptands are the strongest complexing agent presently known for alkali metal ions in aqueous solution (the stability constant up to  $10^5$  l mole<sup>-1</sup>). Several typical cryptands are shown in Figure 2. The optimum cryptand cavity size for cations was found to be cryptand C222 for K<sup>+</sup>, cryptand C221 for Na<sup>+</sup> and cryptand C211 for Li<sup>+</sup> (86). The crystal structure of several metal complexes of cryptand C222 have been determined by using X-ray crystallography (87)(88). In all cases, it was found that the metal ion was located in the cavity of the macromolecule and that the two nitrogen atoms participated in bonding to the metal atom. However, recently, Mei, et al (89) monitored the <sup>133</sup>Cs NMR of Cs cryptand C222 complex in various solvents. They suggested the presence of two types of 1:1 complexes in solution, an exclusive complex in which the ion may interact with the solvent, and an inclusive complex which has a solvent-independent chemical shift.

These cryptands can exist in the three configuration (90) exo-exo, endo-endo and endo-exo isomers which are shown in Figure 3. The endo configuration has the

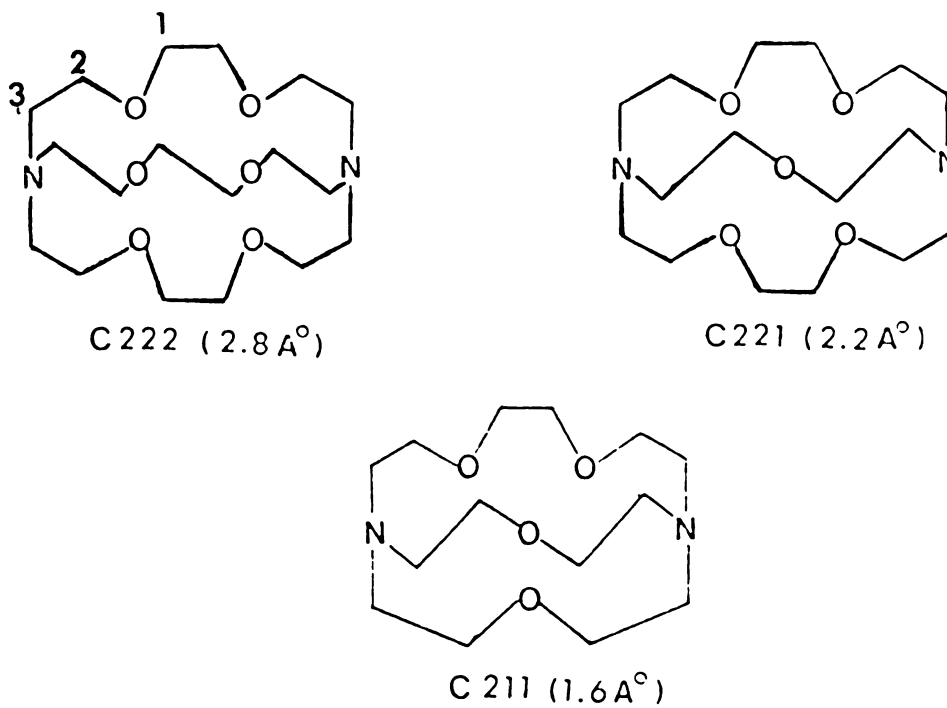


Figure 2. Cryptands C222, C221 and C211 (with internal diameters)

nitrogen lone pair electrons directed toward the interior of the cavity while the exo configuration has the nitrogen lone pair electrons turning outside. The endo-endo configurations for  $K^+$ -cryptate 222 and Rb-cryptate 222 were found by X ray crystallography (87).

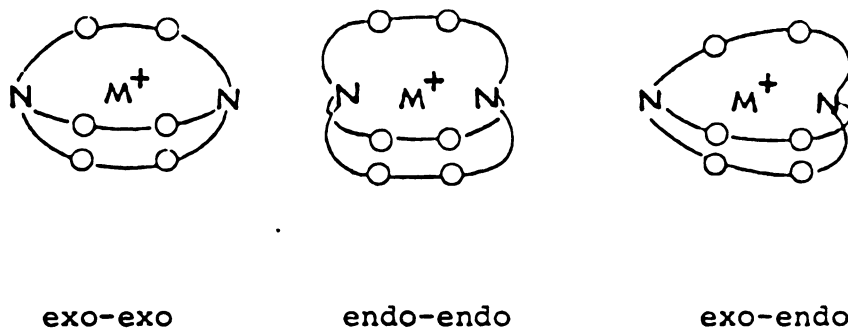


Figure 3. The Configurations of Cryptand C222

The stability constant of alkali cryptates in water and in methanol solution was reported by Lehn and coworkers (92). The cation selectivities of cryptands for alkali metal ions in water and methanol were found to be cryptand C222 for  $K^+$ , cryptand C221 for  $Na^+$  and cryptand C211 for  $Li^+$ . Popov and coworkers (89)(92)(93) extended this study to nonaqueous solvents by using alkali metal NMR methods such as  $^7Li$ ,  $^{23}Na$  and  $^{133}Cs$  NMR. They found that the formation constant of metal ion complex in nonaqueous solvents was always higher than that in water, and the stability constant of

complex was dependent on the donicity of the solvents. Dye and coworkers (94) isolated the alkali metal anions such as  $(\text{Na}^+\text{C222})\text{Na}^-$  which was investigated by  $^{23}\text{Na}$  NMR.

Recently, cyclindrical macrotricyclic cryptands have been synthesized (95) and shown in Figure 4.

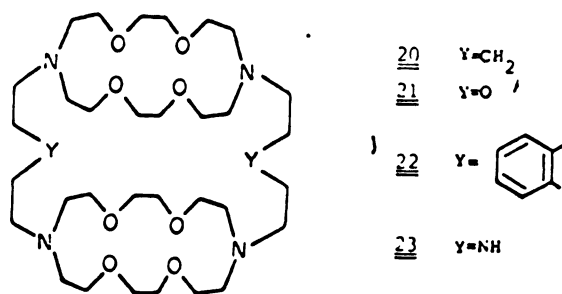


Figure 4. The Structures of Cyclindrical Macrotricyclic Cryptands

The formation of macrotricyclic cation inclusion complexes (96) have been reported. Cyclindrical macrotricyclic ligands are topologically well suited for the designed positioning of two metal cations in a binuclear inclusion complex.

CHAPTER II  
EXPERIMENTAL PROCEDURE

## EXPERIMENTAL

### (A) INSTRUMENTAL

#### (a) DA-60 Multinuclear NMR spectrometer

A modified DA-60 Fourier transform multinuclear NMR spectrometer was used to obtain the  $^{39}\text{K}$  chemical shifts in the studies of ionic association in neat nonaqueous solutions and the preferential solvation in mixed solvents. The spectrometer consists of modified NMR spectrometers MP-1000 spectrometer, a Nicolet 1083 computer, interface and the necessary accessories such as disk system, plotter etc.

The  $^{39}\text{K}$  chemical shift was measured at 2.8 MHz with the magnetic field 14 kilogauss (1.4 Tesla). The frequency source of the RF unit is a 56.4 MHz crystal controlled oscillator. The  $^{39}\text{K}$  nuclear magnetic resonance was operated with pulsed width  $\sim 300 \mu\text{sec}$ . External lock system ( $\text{H}_2\text{O}$ ) is used. A 25 ml NMR tube with 5 ml sample solution were used. The saturated  $\text{KNO}_2$  (31 M) in  $\text{D}_2\text{O}$  solution was used as the external reference. Using the DA-60 spectrometer, the signal for 0.01 M of  $\text{KPF}_6$  in acetonitrile can be observed.

#### (b) Bruker WH-180 NMR spectrometer

A Bruker WH-180 superconducting multinuclear NMR spectrometer was used to study the complexation of potassium and macrocyclic ligand such as crown ethers and cryptands. The spectrometer consists of a superconducting solenoid, a Nicolet 1180 computer disk system and temperature control units.

The quadrature detector system is used in WH-180. In conventional FT NMR, a single phase-sensitive detector (such as used on DA-60) can only determine the magnitude of the frequency difference between the signal and rf pulse, but not the sign of this difference, so the rf pulse is usually set at one end of the spectral region to avoid folding back of the resonance. This gives rise to two problems: (1) The power bandwidth of the rf pulse must be at least equal to twice of the total spectral width (ie,  $rH_1 \geq 2\pi(SN)$ ) and (2) Noise from the unused side of the decreasing S/N by a factor of  $\sqrt{2}$ . Quadrature detection can solve both of these problems directly. Since the rf power requirement varies as the square of the spectral width, quadrature techniques bring an effective gain of a factor 4.

The data memory available in the Nicolet 1180 computer in Bruker WH-180 is 16 K while 8 K in Nicolet 1083 in DA-60 spectrometer. The  $^{39}\text{K}$  resonance was operated at resonance frequency 8.403 MHz at the magnetic field of 42.3 kilogauss. A 20 mm NMR tube and 10 ml of sample solution were used in this work. A saturated (31 M)  $\text{KNO}_2$  in  $\text{D}_2\text{O}$  solution was again used as the reference sample. The signal of  $^{39}\text{K}$  resonance for 0.005 M of  $\text{KPF}_6$  in acetonitrile can be obtained in the short time (~15 minutes) and is shown in Figure 5.

(c) Varian CFT 20 spectrometer

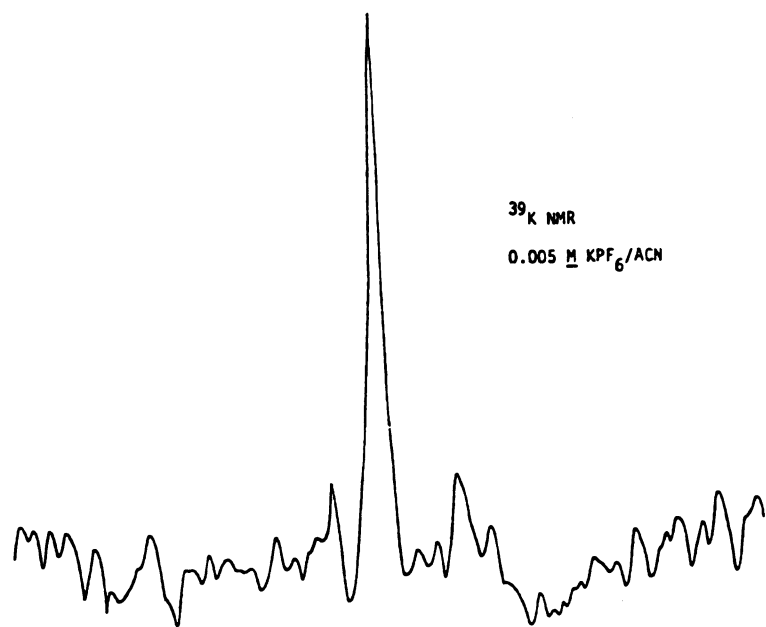


Figure 5. Potassium-39 NMR Resonance of 0.005 M  $\text{KPF}_6$  in Acetonitrile by Bruker 180 Spectrometer. (2000 scans, 15 minutes, line width  $\sim 10$  Hz)

All the carbon-13 NMR chemical shift measurement was performed on a varian CFT-20 high resolution NMR spectrometer with a constant field of 18.7 kilogauss. The  $^{13}\text{C}$  NMR was operated at resonance frequency 20 MHz. One ml of sample for measurement of the  $^{13}\text{C}$  chemical shift was placed in 5 mm inner tube of coaxial tube. While the mixture of lock and reference sample (vol 50% of acetone in  $\text{D}_2\text{O}$ ) in 8mm outer tube.

( B ) CHEMICAL SHIFT MEASUREMENTS

All the  $^{39}\text{K}$  chemical shifts reported are referred to the infinite dilution chemical shift of the potassium ion in water. The paramagnetic shift (down field), was designated as negative values.

The chemical shifts reported here are also corrected for differences in bulk diamagnetic susceptibility between sample and reference ( $\text{H}_2\text{O}$ ) according to the relationship of Live and Chan (97) for the spectrometer such as DA-60 where the applied polarizing magnetic field is transverse to the long axis of the cylindrical sample, the bulk susceptibility correction to the observed chemical shift is shown to be:

$$\delta_{\text{corr}} = \delta_{\text{obs}} + \frac{2}{3}(X_{\text{v}}^{\text{ref}} - X_{\text{v}}^{\text{sample}}) \quad (\text{II.1})$$

where  $X_{\text{v}}^{\text{ref}}$  and  $X_{\text{v}}^{\text{sample}}$  are the magnetic susceptibilities

for reference and sample respectively. For high field spectrometers such as Bruker WH-180 where the polarizing magnetic field is along the long axis of the sample.

The correction for the observed chemical shift is given by

$$\delta_{\text{corr}} = \delta_{\text{obs}} - \frac{4}{3} (\chi_{\text{v}}^{\text{ref}} - \chi_{\text{v}}^{\text{sample}}) \quad (\text{II.2})$$

Since Templeman and Van Geet (98) reported that the contribution of the salt to the susceptibility of the solution is very small (for 9.65 M Na<sup>+</sup> solution < 0.1 ppm), no correction for the contribution of the salt was applied. The respective susceptibility corrections for the solvents, for both DA-60 and WH-180 spectrometers are shown in Table 3.

For the mixed solvents, the volume diamagnetic susceptibility of a given mixtures was calculated by the Wiedemann's equation

$$\chi_{\text{v}}^{\text{mix}} = \frac{V_{\text{A}}}{V_{\text{A}} + V_{\text{B}}} \cdot \chi_{\text{v}}^{\text{A}} + \frac{V_{\text{B}}}{V_{\text{A}} + V_{\text{B}}} \cdot \chi_{\text{v}}^{\text{B}} \quad (\text{II.3})$$

where  $\chi_{\text{v}}^{\text{mix}}$  is the calculated volume susceptibility of the mixture.  $\chi_{\text{A}}$  and  $\chi_{\text{B}}$  are the volume susceptibilities of pure solvent A and B respectively,  $V_{\text{A}}$  and  $V_{\text{B}}$  are the volumes of solvents of A and B respectively.

All the C-13 NMR chemical shifts reported here are referred to TMS resonance. The paramagnetic shift (down field) was conventionly designated as positive values.

Table 3. Magnetic Susceptibility Corrections to the  $^{39}\text{K}$  Chemical Shifts

Solvent	Volumetric Susceptibility <sup>(a)</sup> ( $-X \times 10^6$ )	corr(ppm) (for DA-60)	corr(ppm) (for WH-180)
Nitromethane	0.391	-0.69	+1.38
Formic Acid	0.527	-0.40	+0.80
Propylene Carbonate	0.640	-0.18	+0.36
Acetone	0.460	-0.55	+1.01
Methanol	0.530	-0.43	+0.86
Formamide	0.551	-0.35	+0.70
Dimethylformamide	0.500	-0.31	+0.62
Acetonitrile	0.529	-0.39	+0.78
Water	0.720	0	0
Pyridine	0.610	-0.23	+0.46
Dimethylsulfoxide	0.630	-0.24	+0.48
Ethylenediamine	0.686	-0.07	+0.14

(a) Reference 99

(C) POTASSIUM SALTS

Potassium perchloride (Baker), thiocyanate, fluoride, chloride, bromide, iodide (Fisher) and acetate (Baker) were of reagent grade and were dried under vacuum at  $\sim 60^{\circ}\text{C}$  for at least 48 hours before use. Potassium hexafluorophosphate (Pfaltz & Banner) was purified by recrystallization from water and then dried under vacuum at  $\sim 110^{\circ}\text{C}$  for 72 hours. Potassium tetraperborate was prepared as the precipitate of the reaction of potassium nitrite and sodium tetraperborate in water. The precipitate was washed with conductance water and recrystallize from acetone and dried under vacuum at  $\sim 60^{\circ}\text{C}$  for 72 hours.

(D) SOLVENTS

Acetone (Mallinkrodt) was fractionally distilled over calcium sulfate and then dried over Linde 4A molecular sieves. Nitromethane, acetonitrile and pyridine (Fisher) were fractionally distilled over calcium hydride and dried over Linde 4A molecular sieves. Propylene carbonate, dimethylformamide, dimethylsulfoxide and ethylenediamine were vacuum distilled over calcium hydride and dried over 4A molecular sieves. Formamide and formic acid were purified by repeated fractional freezing and dried over Linde 4A molecular sieves. Metahnol was fractionally distilled over magnisum and iodine. The water content in the

solvent was analyzed with an automatic Karl Fischer Titrator and was always below 100 ppm.

(E) PURIFICATION OF CRYPTANDS AND CROWN ETHERS

Cryptand C222 was recrystallized from hexane and dried under vacuum at about 40°C for 48 hours. Both cryptand C221 and C211 were dried under vacuum before use.

Macrocyclic 18-crown-6 was purified by forming a complex with acetonitrile. When about 5 grams of 18-crown-6 was dissolved in 25 ml of acetonitrile, fine white crystals of the complex were formed. The flask was cooled in an ice-acetone bath (not dry ice) to precipitate as much of the complex as possible and the solid was then collected by rapid filtration. The weakly bound MeCN was removed from the complex by pumping under vacuum. The melting point of recrystallized 18-crown-6 was 39-40°C, identical to the literature value (100). Dibenzo-18-crown-6 was purified by recrystallization from benzene and dried under vacuum for at least 48 hours.

Both 15-crown-5 and 12-crown-4 were purified by vacuum distillation (pressure ~10 torr) at 80°C ~120°C. Carbon-13 and <sup>1</sup>H NMR were used to detect impurities and water contents.

Monobenzo-15-crown-5 was synthesized by M. Shamsipur in our laboratory. It was recrystallized from heptane

before use.

( F ) DATA HANDLING

The time averaging of NMR spectra and Fourier transformation of  $^{39}\text{K}$  data were done on the Nicolet computers (Nicolet 1180 on Bruker WH-180 and Nicolet 1083 on varian DA-60) using program FTNMRD and QFN for the WH-180 and DA-60 spectrometers respectively. Chemical shift readout was directly obtained from the spectra during the experiment. All the chemical shift data reported in this thesis are relative to the chemical shift of  $^{39}\text{K}^+$  in an infinitely dilute solution. The measurements were also corrected for the differences in bulk diamagnetic susceptibility between nonaqueous solutions and the reference ( $\text{H}_2\text{O}$ ).

Chemical shift data obtained from solvation and complexation studies were all fitted with appropriate equations on a CDC-6500 computer using the least squares program KINFIT (101) to obtain the respective formation constants of ion-pairs and complexes. The applications of the related subroutine equations and KINFIT program are described in the Appendices.

### CHAPTER III

POTASSIUM-39 NUCLEAR MAGNETIC RESONANCE STUDIES  
OF IONIC SOLVATION AND ASSOCIATION OF POTASSIUM  
SALTS IN VARIOUS SOLVENTS

CHAPTER III (A)

IONIC SOLVATION AND ASSOCIATION STUDIES OF  
THE POTASSIUM IONS IN NEAT SOLVENTS

## INTRODUCTION

Nuclear magnetic resonance of metallic nuclei is a very sensitive probe of the ionic environment. Therefore, nuclear magnetic resonance has become a powerful method for the investigation of electrolyte solutions. The measurement of chemical shift of metal nuclear resonance yield valuable quantitative and qualitative information about ion-solvent and ion-ion interactions.

In the past, the solvation and association of Lithium, sodium cesium salts have extensively studied by  $^7\text{Li}$ ,  $^{23}\text{Na}$  and  $^{133}\text{Cs}$  NMR respectively. However, since  $^{39}\text{K}$  nucleus resonates at very low frequency and, in addition, has low sensitivity, the studies on the  $^{39}\text{K}$  resonance have been much more sparse and, in most cases, confined to aqueous solution of fairly high concentration ( $>0.2 \text{ M}$ ). The recent development of Fourier transform NMR technique and of superconducting solenoids with high magnetic fields renders the study of  $^{39}\text{K}$  resonance a much easier task. In this study, the potassium-39 chemical shifts of potassium salts were studied in eleven solvents in the  $0.01\text{-}1.0 \text{ M}$  concentration range.

## RESULTS AND DISCUSSION

The  $^{39}\text{K}$  chemical shifts of potassium salts such as potassium hexafluorophosphate, perchlorate, tetraphenylborate, thiocyanate, chloride, fluoride, bromide and iodide were measured in various solvents. The data are

presented in Table 4. The  $^{39}\text{K}$  chemical shifts as function of  $\text{K}^+$  ion concentration are illustrated in Figure 6-10. As can be seen in most cases, the  $^{39}\text{K}$  chemical shift of potassium salts show concentration dependence. Since  $^{39}\text{K}$  chemical shift of  $\text{K}^+$  ion is only sensitive to the short range interaction, it seems reasonable to assume that the variation of the chemical shifts with concentration is an indication of cation-anion interaction, presumably the formation of contact ion pairs.

It is also seen that in general, increasing concentration of the potassium halides leads to a paramagnetic (downfield) chemical shift while potassium salts with polyatomic anions such as  $\text{PF}_6^-$ ,  $\text{ClO}_4^-$ , and  $\text{BPh}_4^-$  give the diamagnetic (upfield) shifts with increasing concentration. Since the potassium- $^{39}\text{K}$  chemical shift is dominated by the paramagnetic term in the chemical shift equation (Ramsey's equation) (51), according to Kondo-Yamashita theory (52), the increase in electron density around the  $\text{K}^+$  ion results in rise of a strong short-range repulsive force which induce the excitation of  $3p$  electron of the  $\text{K}^+$  ion to higher energy states, and decrease the shielding of the potassium nucleus. In other words, the increase in electron density around the  $\text{K}^+$  ion will result in a downfield shift. Replacement of solvent molecules in the potassium ions inner solvation sphere by anions may either increase or

Table 4.  $^{39}\text{K}$  Chemical Shifts of Potassium Salt Solutions  
KPF<sub>6</sub>

Solvent	Conc.(M)	$\Delta$ ppm	Solvent	Conc.(M)	$\Delta$ ppm	Solvent	Conc.(M)	$\Delta$ ppm
Acetone (30°C)	1.5	16.9	Acetone	1.5	13.0	Acetonitrile	0.5	5.5
	1.25	16.3	(-14°C)	1.25	13.6		0.2	4.3
	1.0	16.1		1.0	12.8		0.1	4.2
	0.8	15.8		0.8	13.2		0.05	3.8
	0.6	15.2		0.6	12.8		0.01	2.5
	0.4	14.9		0.4	12.8	Water	0.5	3.2
	0.2	13.9		0.2	12.1		0.4	2.6
	0.1	13.4		0.1	11.1		0.3	2.3
	0.01	12.8	Formamide	1.0	10.7		0.2	1.7
	1.0	-6.3		0.8	7.3		0.1	1.1
DMSO	0.75	-6.6		0.5	6.5		0.05	0.8
	0.5	-6.7		0.25	5.6		0.025	0.4
	0.4	-6.9		0.10	4.7	Formic Acid	0.7	15.9
	0.3	-6.9	DMF	0.75	5.6		0.5	14.2
	0.2	-7.0		0.5	4.7		0.25	13.4
	0.1	-7.1		0.25	3.9		0.10	12.7
	0.1	12.5		0.1	3.9		0.075	12.7
	0.075	12.0		0.05	3.5		0.05	12.7
	0.05	11.6		0.02	3.0			
	0.025	11.7						



Table 4. Continued

Solvent	KI			KSCN			KSCN		
	Conc.(M)	$\Delta$ ppm	Solvent	Conc.(M)	$\Delta$ ppm	Solvent	Conc.(M)	$\Delta$ ppm	$\Delta$ ppm
Formamide	1.0	0.5	PC	1.0	12.5	DMSO	1.0	12.5	-7.4
	0.8	1.2		0.75	12.5		0.8	12.5	-7.4
	0.5	2.1		0.5	12.5		0.65	12.5	-8.3
	0.25	3.8		0.4	12.5		0.5	12.5	-7.4
	0.1	4.7		0.3	12.5		0.35	12.5	-7.4
	0.05	5.1		0.2	12.5		0.2	12.5	-8.3
Formic Acid	1.0	7.3		0.1	12.5		0.1	12.5	-7.4
	0.8	8.1		0.075	12.5	Acetone	0.75	12.5	5.5
	0.5	9.9		0.025	12.5		0.5	12.5	6.3
	0.25	11.3	Acetonitrile	0.85	-2.2		0.4	12.5	6.9
	0.10	11.6		0.75	-3.2		0.3	12.5	7.7
	0.05	11.6		0.65	-2.2		0.2	12.5	8.4
			0.5	-2.2		0.1	12.5	8.8	
			0.25	-2.2		0.075	12.5	9.2	
			0.10	-0.6		0.05	12.5	9.8	
			0.05	+0.3		0.035	12.5	10.1	
		MeNO <sub>2</sub>	0.075	18.3		0.02	12.5	10.4	
			0.05	18.6		0.01	12.5	10.7	
			0.04	18.8					
			0.02	19.5					
			0.01	19.9					

Table 4. Continued

Solvent	KSCN			KSCN			KBPh <sub>4</sub>		
	Conc. (M)	$\Delta$ ppm	Solvent	Conc. (M)	$\Delta$ ppm	Solvent	Conc. (M)	$\Delta$ ppm	Appm
Water	1.0	-0.6	DMF	1.0	2.2	Acetone	0.1	11.4	11.4
	0.65	-0.4		0.85	2.2		0.075	11.4	11.4
	0.5	-0.2		0.65	2.2		0.05	10.6	10.6
	0.35	-0.2		0.5	2.2		0.025	11.4	11.4
	0.2	-0.2		0.2	2.2		0.01	11.4	11.4
Methanol	0.05	+0.3		0.1	2.2	DMF	0.4	2.6	2.6
	1.0	7.7		0.05	2.2		0.3	2.6	2.6
	0.75	8.1		0.025	2.2		0.2	2.6	2.6
	0.5	8.5	Formic Acid	0.85	11.6		0.1	2.6	2.6
	0.25	8.5		0.65	11.6		0.075	2.6	2.6
Ethylene-diamine	0.1	8.9		0.5	11.6		0.05	2.6	2.6
	0.05	9.8		0.25	12.0		0.025	2.6	2.6
	1.0	-23.8		0.05	11.6		0.01	2.6	2.6
	0.85	-23.8				DMSO	0.4	-7.1	-7.1
	0.65	-23.8					0.3	-7.1	-7.1
0.5	-23.8					0.2	-6.8	-6.8	
0.25	-23.8					0.1	-6.5	-6.5	
0.10	-22.9					0.075	-7.1	-7.1	
0.05	-23.8					0.05	-7.1	-7.1	



decrease the electron density at the cation. The symmetric polyanions apparently decrease the electron density resulting in the upfield shift. On the other hand, replacement of a solvent molecule by the halides increase the electron density around the  $K^+$  ion resulting in a downfield shift. This indicates that both the halides and thiocyanate anion are better electron donors than the solvent molecule they replace. On the other hand, these symmetric polyanions are poorer electron donors to the  $K^+$  ion than the solvent molecule.

The data obtained for solutions of potassium salts in formamide and water are illustrated in Figure 6. Both water and formamide have high dielectric constants (109.5 and 78.5 respectively) and high donor numbers of 24.7 and 33 respectively. The dielectric constants and Gutmann donor numbers of the solvents are shown in Table 5. As Figure 6 shows, in the formamide and aqueous solutions, potassium salts except  $KPF_6$  in  $H_2O$  give a linear chemical shift dependence on salt concentration. Similar linearity of chemical shift vs salt concentration plots in the case of halide NMR study for alkali halides have been reported by Deverell and Richards (13). This phenomenon was interpreted in terms of the formation of "collisional" ion pairs or very weak contact ion pairs. In the  $KPF_6$  aqueous solution, the slight curvature seems to indicate a slight amount of ionic association. The

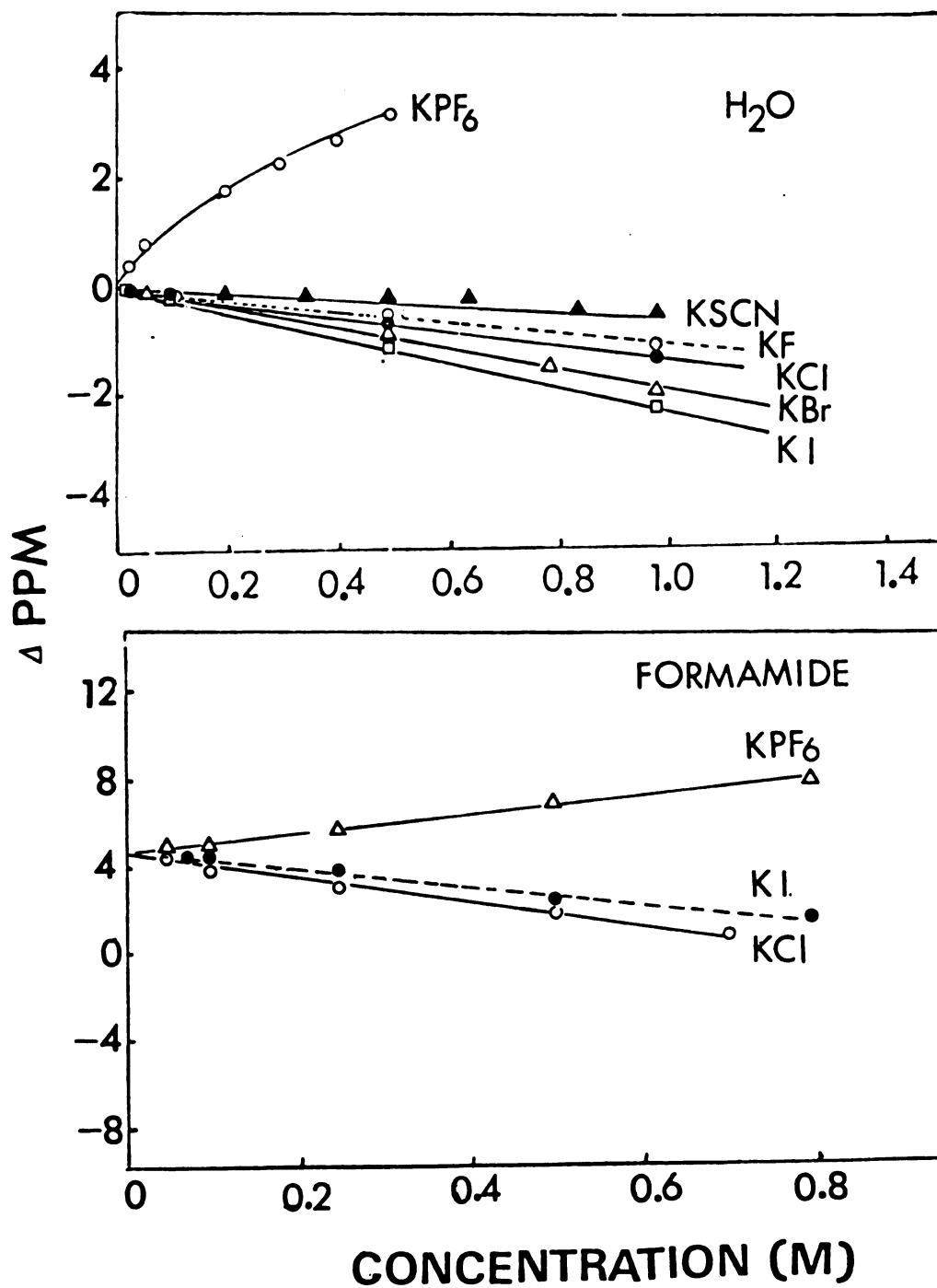


Figure 6. K-39 Chemical Shifts of Potassium Salts in Water and Formamide

Table 5. Key Solvent Properties

Solvent	Donor Number <sup>(a)</sup>	Dielectric Constant
Nitromethane	2.7	35.9
Acetonitrile	14.1	38.8
Propylene Carbonate	15.1	65.0
Acetone	17.0	20.7
Formic Acid	17.0	56.1
Tetrahydrofuran (THF)	20.0	7.6
Formamide	24.7	109.5
Methanol	25.7 <sup>(b)</sup>	32.7
Dimethylformamide (DMF)	26.6	36.7
Dimethylsulfoxide (DMSO)	28.9	46.7
Ethanol	31.5	24.6
Pyridine	33.1	12.3
Water	33	78.5
Ethylenediamine	55	12.9

(a) Reference 24

(b) Reference 29

(a)

Gutmann donor number scale. The scale is based on the enthalpy of the reaction  $S + SbCl_5 \rightarrow S \cdot SbCl_5$  in dilute 1,2-dichloroethane solution. The donor number of the Solvent S is defined as  $DN(S) = - \Delta H_{S \cdot SbCl_5}$ .

slight ionic association (for  $\text{KPF}_6$  in  $\text{H}_2\text{O}$ ) has also been reported from a conductance study by Robinson and Stokes (102). It can be seen that for the halides, the extent of the paramagnetic shift increase in the order  $\text{I}^- > \text{Br}^- > \text{F}^-$ , which is always observed for alkali metal NMR. The result was explained in terms of the increased collision probability with increasing the anion size (7)(13)(36). The smaller shifts for the thiocyanate than the halides is probably attributed to a greater basicity of the halides (32). The greater availability of the electrons on the more basic anions results in a proportionately greater perturbation of the spherical symmetry of the outer electron cloud of the potassium ion.

Potassium-39 NMR measurements were also made on potassium salt solutions in dimethylformamide and dimethylsulfoxide. Both dimethylformamide and dimethylsulfoxide have high donor ability (with donor number of 26.6 and 29.8 respectively) and average dielectric constants (36.1 and 45.0 respectively). The results are shown in Figure 7. In dimethylsulfoxide solutions, linear chemical shifts dependence on concentration were also observed in the  $\text{KClO}_4$  and  $\text{KPF}_6$  cases. However, the  $^{39}\text{K}$  chemical shifts is independent of salt concentration in the  $\text{KSCN}$  and  $\text{KBPh}_4$  cases which can be explained either by absence of contact ion pairing

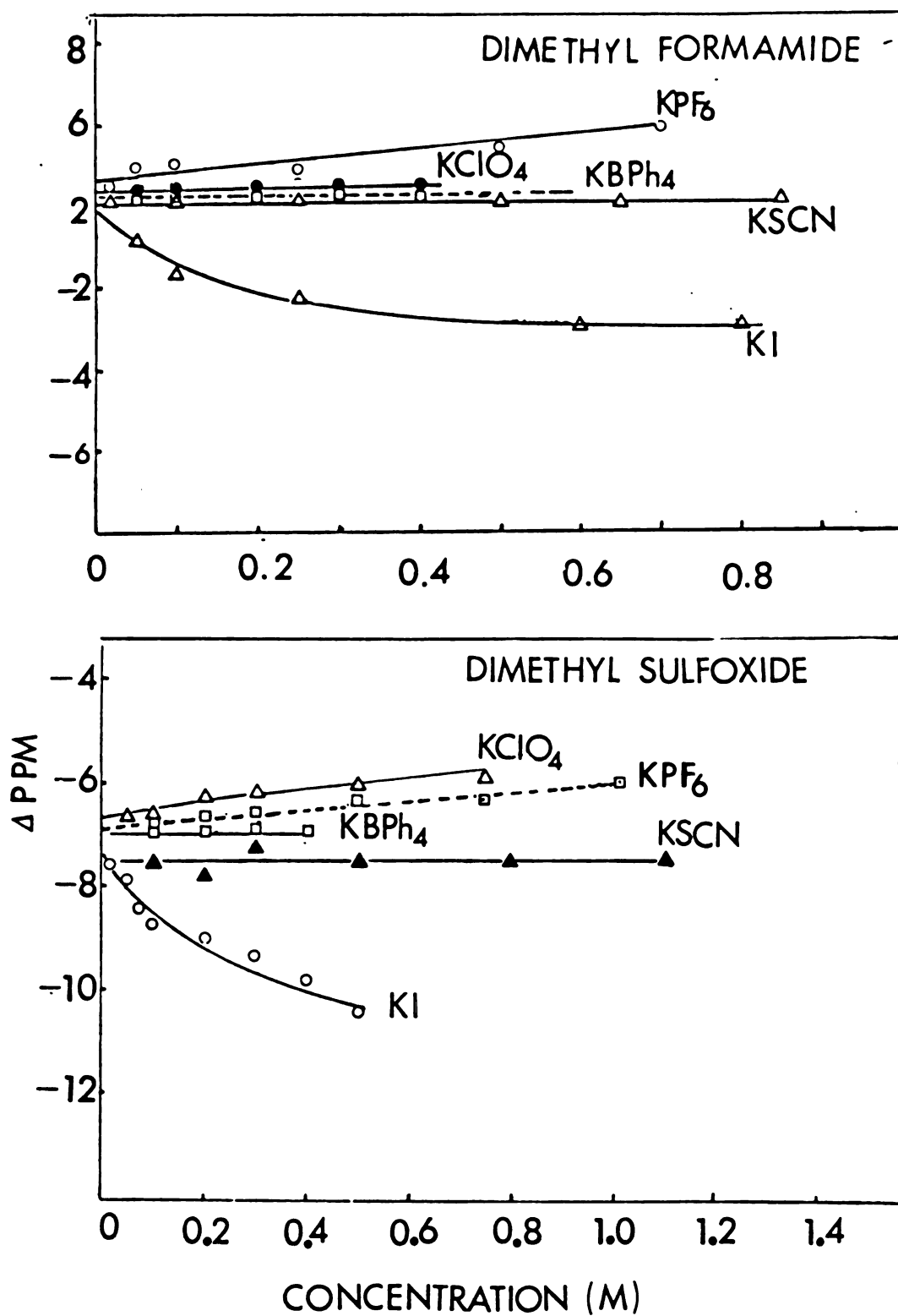


Figure 7. K-39 Chemical Shifts of Potassium Salts in Dimethylformamide and Dimethylsulfoxide

formation or by a coincidental equality of electron density at the  $K^+$  ion upon replacement of solvent molecules by the anions. In the KI case, a small concentration dependence of the chemical shift is indicative of the some amount of the ionic association. As can be seen, the results in dimethylformamide are similar to those obtained for the dimethylsulfoxide solutions.

The data obtained for solutions of potassium salts in formic acid and propylene carbonate are illustrated in Figure 8. Both formic acid and propylene carbonate also have high dielectric constants (55.0 and 69.0 respectively). The results in the formic acid case are similar to those obtained for the formamide solutions, in which the potassium salts used gave a linear chemical shift dependence on salt concentration. Once again the results are indicative of the formation of very weak contact ion pairs or the collisional ion pair. However, propylene carbonate (PC) shows a little different behavior. The small extent of ionic association of potassium salts in PC would be expected due to the high dielectric constant of the solvent. However for  $KPF_6$  solution in PC, the ionic association seems to be significant, as seen by the some degree of curvature in the plot of chemical shift vs concentration. Although propylene carbonate has a high dielectric constant of

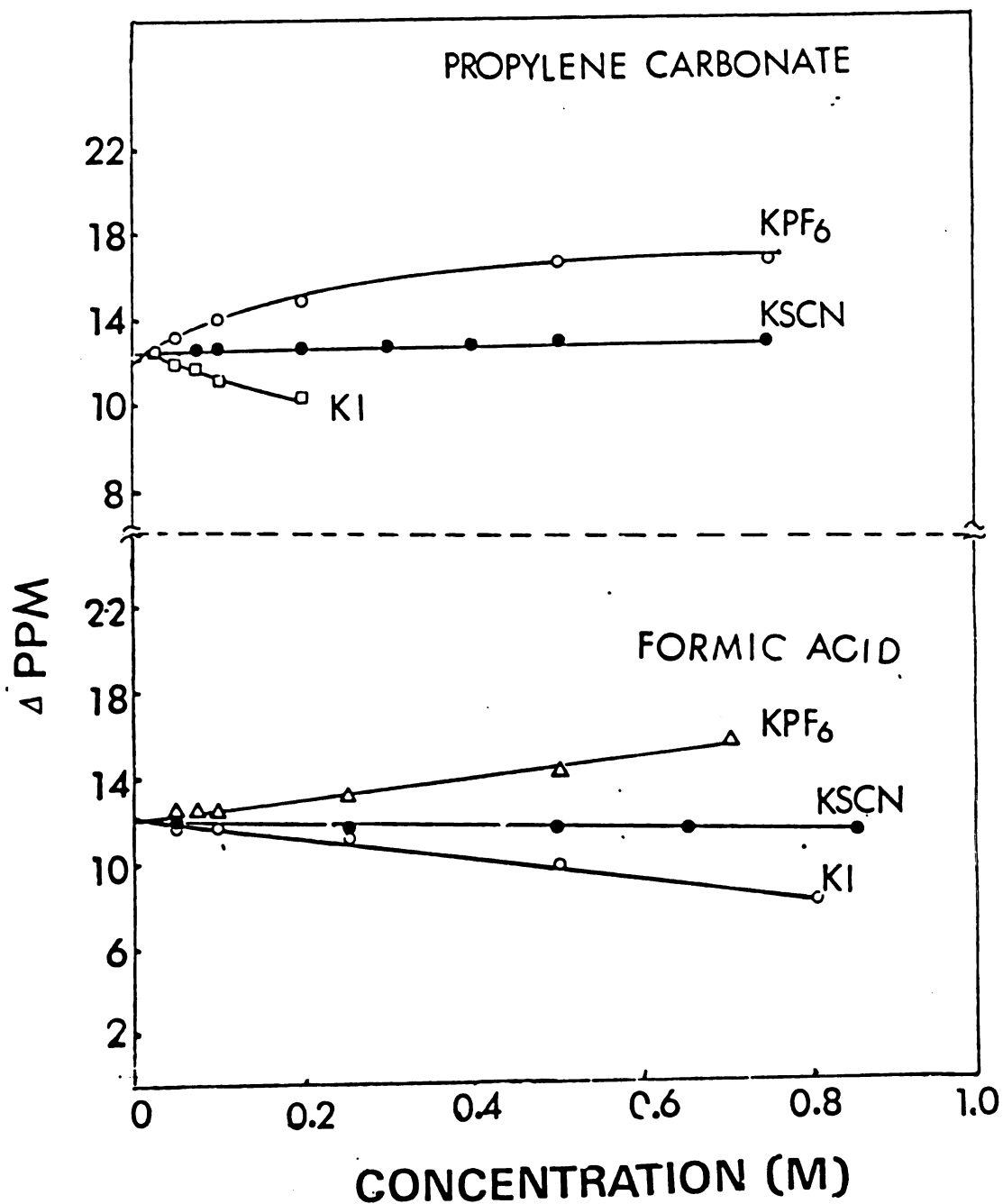


Figure 8. K-39 Chemical Shifts of Potassium Salts in Propylene Carbonate and Formic Acid

65, it has a low donor number of 15.0. The data suggest that the dielectric constants of the solvent is not the only parameter which influence the ionic association. It is evident that the donicity of the solvent is also an important parameter in the formation of ion-pairs.

Potassium salt solutions in solvents of low donicity and medium dielectric constant, such as methanol and acetonitrile (see Table 5), were also investigated by using the  $^{39}\text{K}$  NMR. The results are presented in Figure 9. As expected, all the potassium salts in acetonitrile and methanol undergo a significant extent of ionic association, as indicated by the significant degree of curvature of the plot of the chemical shift vs salt concentration. As can be seen from Figure 10, concentration dependent chemical shifts were also observed for  $\text{KPF}_6$  and  $\text{KSCN}$  in acetone which has a low donicity of 17.0 and a low dielectric constant of 20. However, the  $^{39}\text{K}$  chemical shift of potassium tetrphenylborate shows concentration independence. It is not surprising, since  $\text{BPh}_4^-$  is a large and relatively nonpolarizable ion which would only weakly interaction with a cation. Unfortunately, potassium tetrphenylborate is only slightly soluble in most solvents, which limits the study of the ionic association of this salt.

The concentration dependence chemical shift of the solutions in ethylenediamine were also measured and the

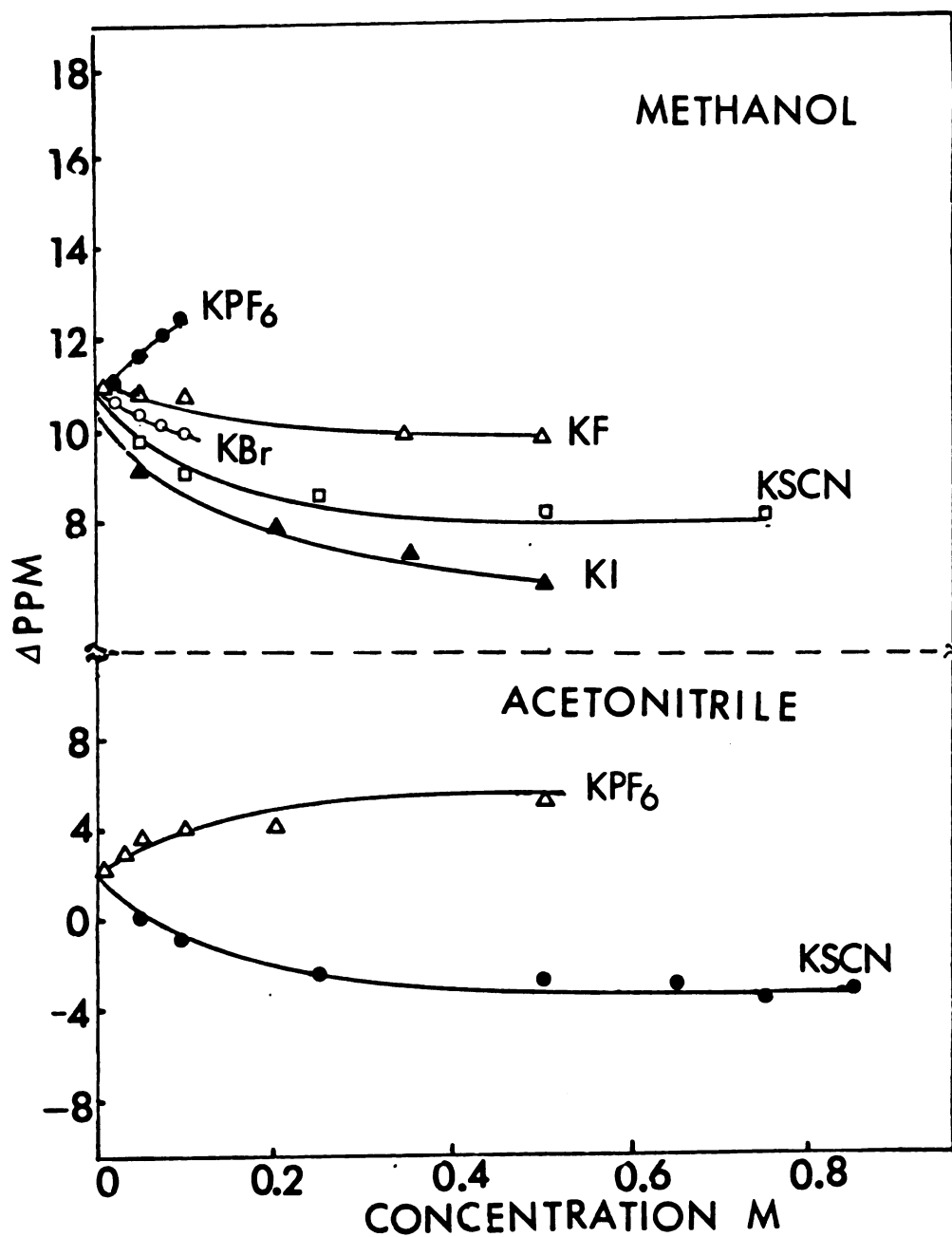


Figure 9. <sup>39</sup>K Chemical Shifts of Potassium Salts in Methanol and Acetonitrile

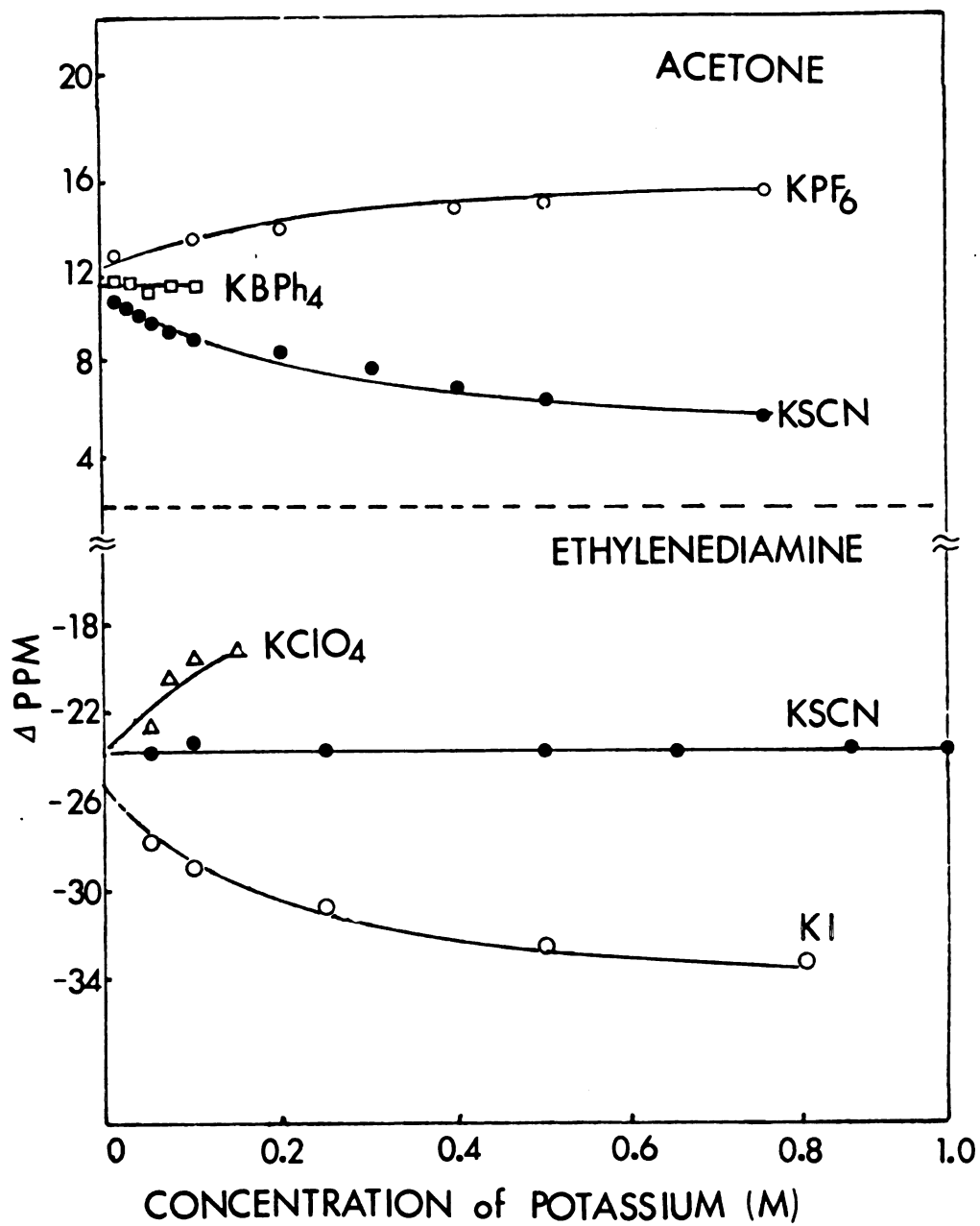


Figure 10.  $^{39}K$  Chemical Shifts of Potassium Salts in Acetone and Ethylenediamine

results are presented in Figure 10. Ethylenediamine has a very high donor number of 55, but a very low dielectric constant of 12. Unfortunately, most potassium salts are only sparingly soluble in this solvent. As Figure 10 shows, the high donicity of ethylenediamine does not prevent the ionic associations in KI and  $\text{KClO}_4$  solutions, as indicated in the plot of chemical shift vs concentration. However, a chemical shift that was independent of the salt concentration was observed in the KSCN case.

Nitromethane has very low donicity of 2.7 but a relatively large dielectric constant of 36. However, the solubilities of most potassium salts in nitromethane are low ( $< 0.1 \text{ M}$ ). Only the solutions of KSCN and  $\text{KPF}_6$  at low concentration ( $< 0.1 \text{ M}$ ) were studied, and the data are presented in Table 4. The slight change in chemical shift in low concentration range (from 0.02 to 0.1  $\text{M}$ ) does not provide much information about the ionic association, but it is qualitatively indicative of the ionic association in such low concentration range.

It was of interest to us to investigate the effect of the solvent on the ionic association of potassium salts with a same anion. As can be seen from Figure 11, in the case of the potassium iodide, in all solvents used, the chemical shifts of KI show concentration dependence, indicative of some extent of ionic association. Even in the solvents of high donicity, such as

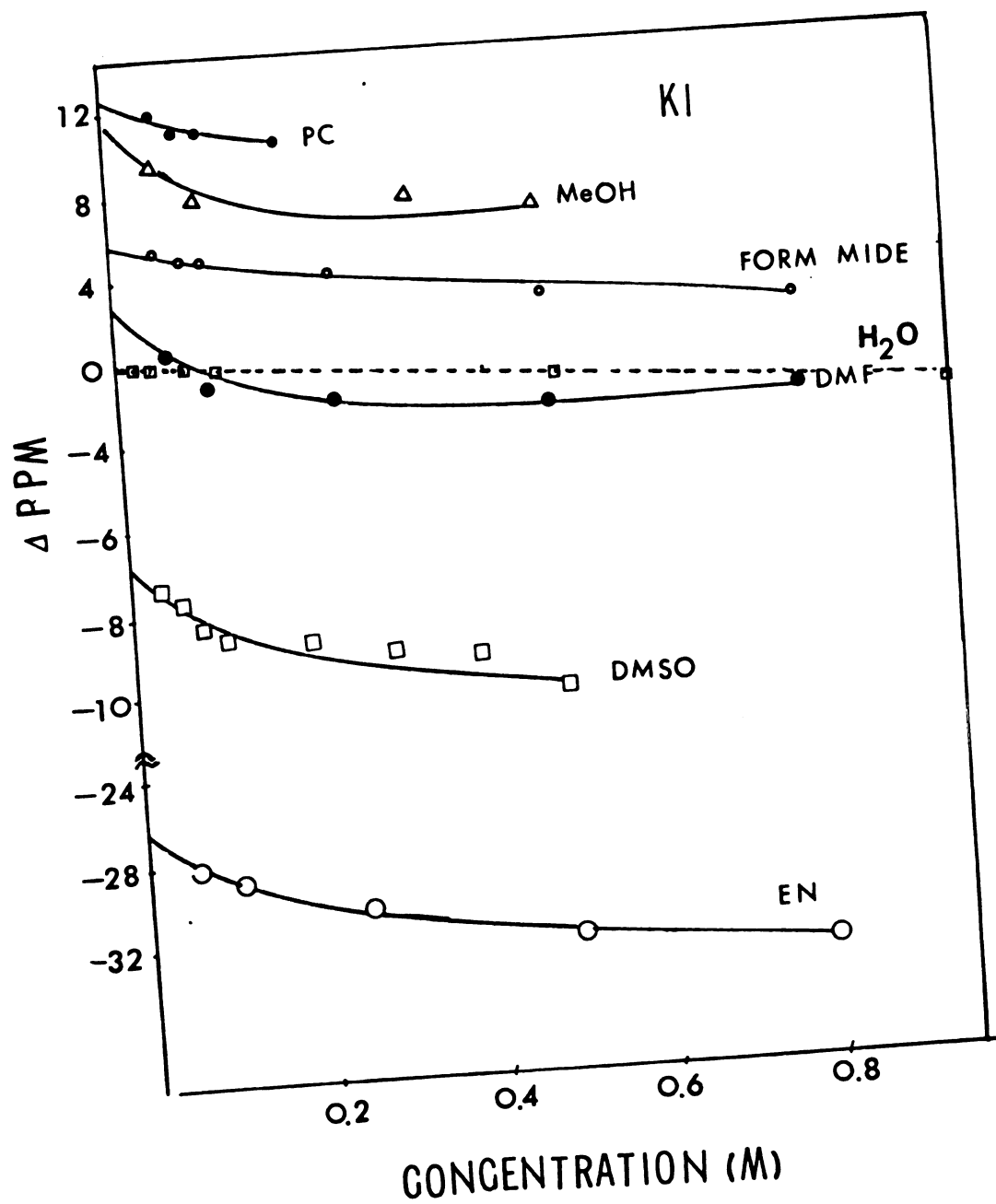


Figure 11. <sup>39</sup>K Chemical Shifts of Potassium Iodide in Various Solvents

ethylenediamine and dimethylsulfoxide, there is significant ionic association, which is indicated by curvatures of the plot. The results seem to suggest the donicity of the solvents seems not to be a predominant factor for the ionic association of KI. However, in the solvents of high dielectric constant such as formamide, water and formic acid, the linear concentration dependence of  $^{39}\text{K}$  chemical shift of KI were observed, which are indicative of very small extent of ionic association or only the "collisional" ion pairs. These results suggest that for potassium iodide, the dielectric constant of the solvent seems to be a more important factor than the donicity of the solvent for the contact ion-pairing formation. However, in the KSCN case, as shown in Figure 12, the chemical shifts of KSCN in the solvents with either high donicity, such as dimethylsulfoxide, ethylenediamine, dimethylformamide or in the solvents with high dielectric constant, such as propylene carbonate, formic acid (see Table 5) show concentration independence. As can be seen, the ionic association is only exhibited in the solvent of medium dielectric constant and low donicity, such as acetonitrile, acetone and methanol.

In the case of  $\text{KPF}_6$  (Figure 13), in all cases, the chemical shift show concentration dependence, indicative of the ionic association. Although propylene carbonate (PC) has a much higher dielectric constant than dimethylformamide (DMF), the larger degree of curvature of the

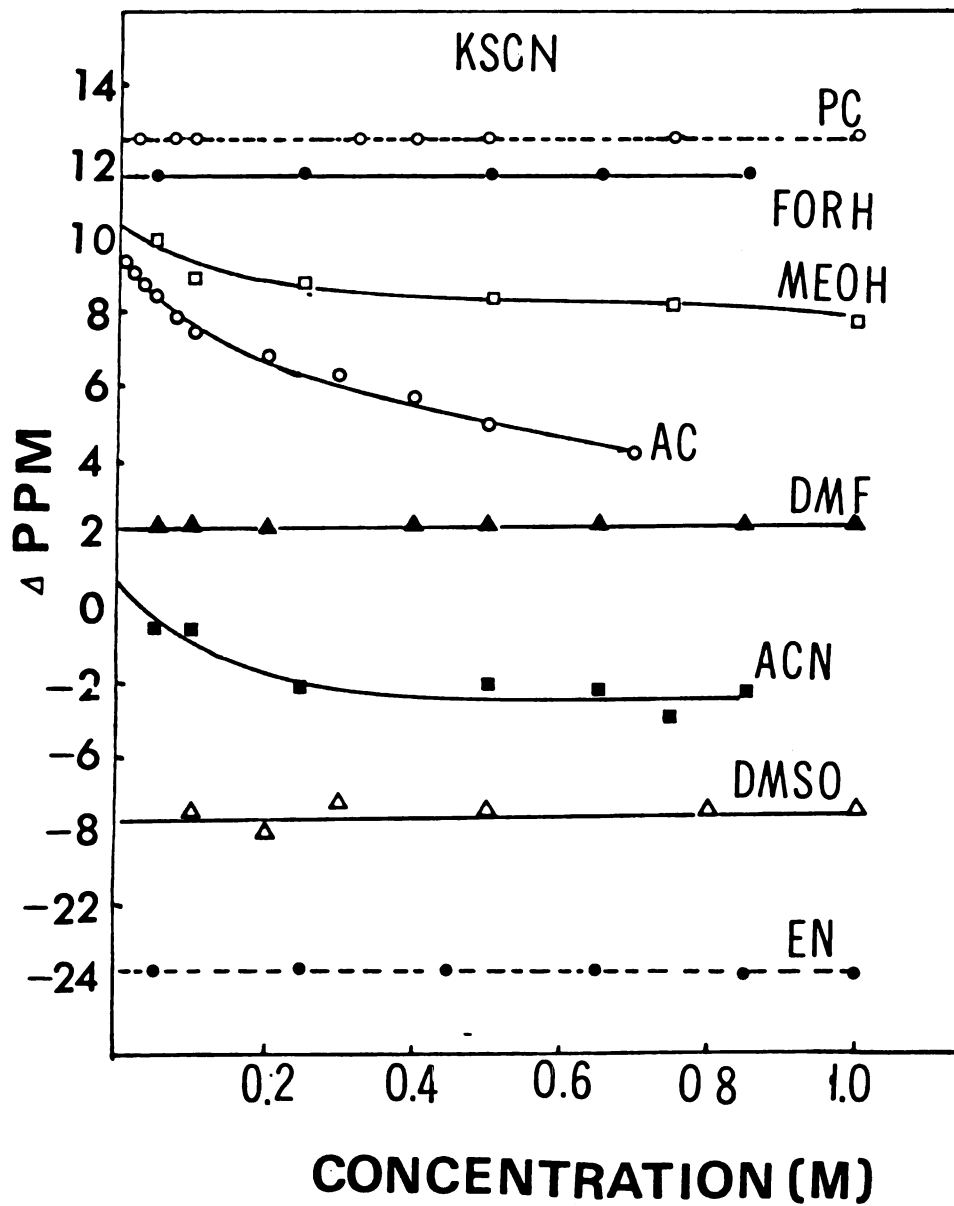


Figure 12.  $^{39}\text{K}$  Chemical Shifts of Potassium Thiocyanate in Various Solvents

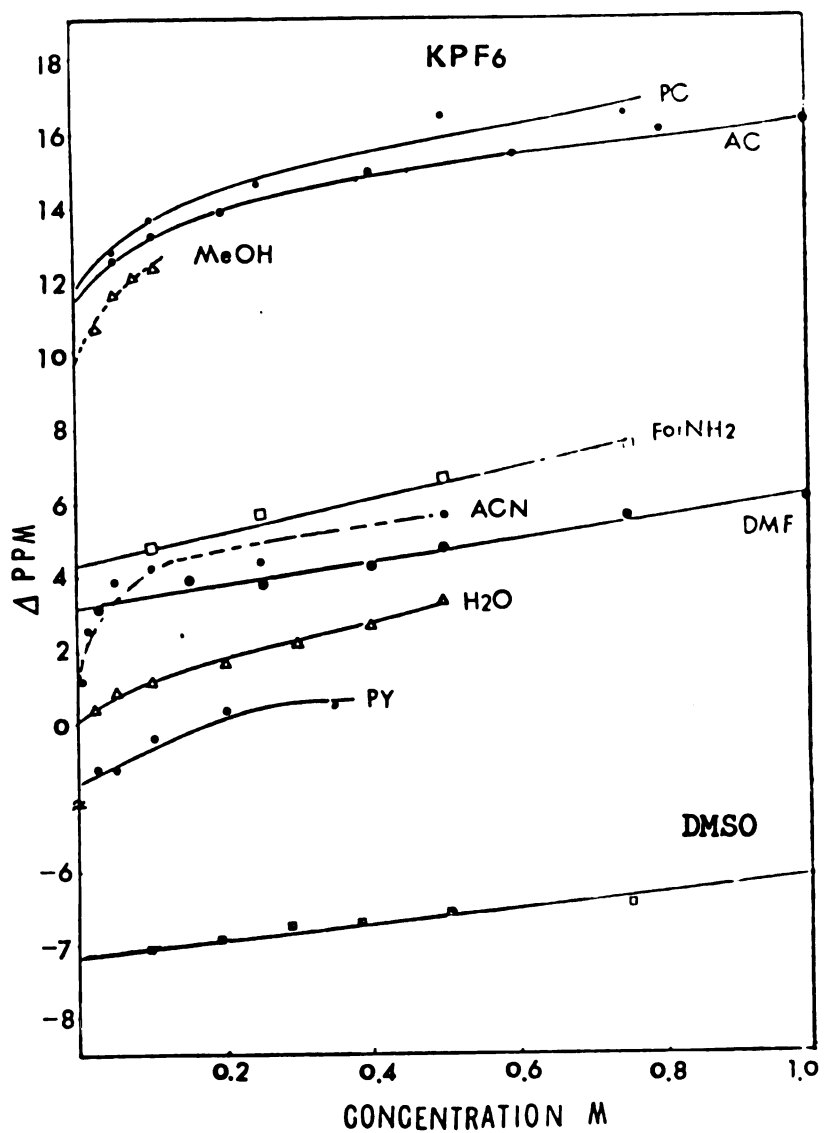


Figure 13.  $^{39}K$  Chemical Shifts of Potassium Hexafluorophosphate in Various Solvents

plot was found in PC and DMF, the result seems to be the evidence for the effect of donicity of solvent on the ionic association, since PC has lower donicity than DMF. However, compared to pyridine, DMF has a lower donicity but a higher dielectric constant. The smaller extent of ionic association of  $\text{KPF}_6$  was observed in DMF than that in pyrinine, as indicated by the degree of curvature of the plot. The results suggest that the dielectric constant is also an important factor for the ionic association of  $\text{KPF}_6$ .

The ion pairing formation also can be determined by the measurements of the chemical shifts as function of the salt concentration. The ion-pairing formation constants can be determined by the following equations (33)

$$\delta_{\text{obs}} = \frac{-1 + (1 + 4K_{\text{IP}}C_{\text{T}}^{\text{M}} \cdot \gamma_{\pm}^2)^{1/2}}{2K_{\text{IP}}C_{\text{T}}^{\text{M}} \cdot \gamma_{\pm}^2} (\delta_{\text{F}} - \delta_{\text{IP}}) + \delta_{\text{IP}}$$

$$\frac{(1.823 \times 10^6) I^{1/2}}{(DT)^{3/2}} \quad (\text{IIIA.1})$$

$$\text{and } -\log \gamma_{\pm} = \frac{(1.823 \times 10^6) I^{1/2}}{1 + \frac{5.029 \times 10^9}{(DT)^{1/2}} I^{1/2}}$$

(IIIA.2)

where  $\delta_{\text{obs}}$  is the observed chemical shift,  $\delta_{\text{F}}$  and  $\delta_{\text{IP}}$  are the chemical shifts of potassium ions in the free solvated state and in the ion pair respectively.  $K$  is the ion-pairing formation constant,  $C_{\text{T}}^{\text{M}}$  is the total concentration of the  $\text{K}^+$  ions in solution,  $\gamma_{\pm}$  is the activity coefficient,  $I$  is the ionic strength,  $D$  is the dielectric constant of the solvent,  $T$  is temperature in  $^{\circ}\text{K}$ ,  $a$  is the size parameter of potassium salt. The ion pairing formation constant was calculated by fitting the concentration dependent chemical shift data using the above equation by the KINFIT program (101). The application of KINFIT and subroutine equations to calculate the ion-pairing formation constant are described in Appendix I.

The ion pairing formation constants for potassium salts in various solvents are shown in Table 6. The equilibrium constant  $K_{\text{IP}}$  is thermodynamic constant where activity corrections are applied, and  $K_{\text{c}}$  is the concentration equilibrium constant. As can be seen in most cases, the values of  $K_{\text{IP}}$  are small. In the case of  $\text{KPF}_6$ , the very weak interactions between the potassium ions and  $\text{PF}_6^-$  anions in some solvents were also observed using  $^{19}\text{F}$  NMR by DeWitte and Popov (7). This result is not unexpected, since both  $\text{K}^+$  and  $\text{PF}_6^-$  are large and relatively nonpolarizable ions.

As seen from Figure 14, the degree of ionic association shows temperature dependence. In  $\text{H}_2\text{O}$  and acetone cases, the degree of curvature of the chemical shift—

Table 6. The Ion-Pairing Formation Constants and Limiting Chemical Shifts of Potassium in Various Solvents

Solvent	Salt	Kc (a)	K <sub>IP</sub> (b)	$\delta_{lim}$ (ppm)
Acetonitrile	KPF <sub>6</sub>	10.84 ± 0.8	19.29 ± 10.30	6.0
Propylene carbonate	KPF <sub>6</sub>	4.91 ± 2.09	6.45 ± 3.17	18.7
Water	KPF <sub>6</sub>	4.82 ± 1.78	5.40 ± 1.99	7.8
Dimethylformamide	KPF <sub>6</sub>	~0	0.65 ± 0.03	87.8
Acetone	KPF <sub>6</sub>	8.23 ± 0.17	~0	22.3
Formamide	KPF <sub>6</sub>	~0	~0	~200
Formic acid	KPF <sub>6</sub>	~0	~0	~200
Dimethylsulfoxide	KPF <sub>6</sub>	~0	~0	~40
Methanol	KI	5.43 ± 2.11	1.36 ± 0.93	0.6
Water	KI	~0	~0	~200
Ethylenediamine	KI	1.03 ± 0.48	~0	-59.4
Dimethylsulfoxide	KI	1.79 ± 1.11	4.82 ± 3.08	-14.9
Formamide	KI	~0	0.59 ± 0.15	-15.39
Acetonitrile	KSCN	0.59 ± 0.46	10.53 ± 1.11	-5.25
Acetone	KSCN	1.43 ± 0.27	9.28 ± 1.02	-2.46
Methanol	KSCN	2.39 ± 0.35	4.24 ± 3.57	2.9
Water	KSCN	~0	~0	~100

(a) Kc is the concentration equilibrium constant

(b) K<sub>IP</sub> is the thermodynamic equilibrium constant

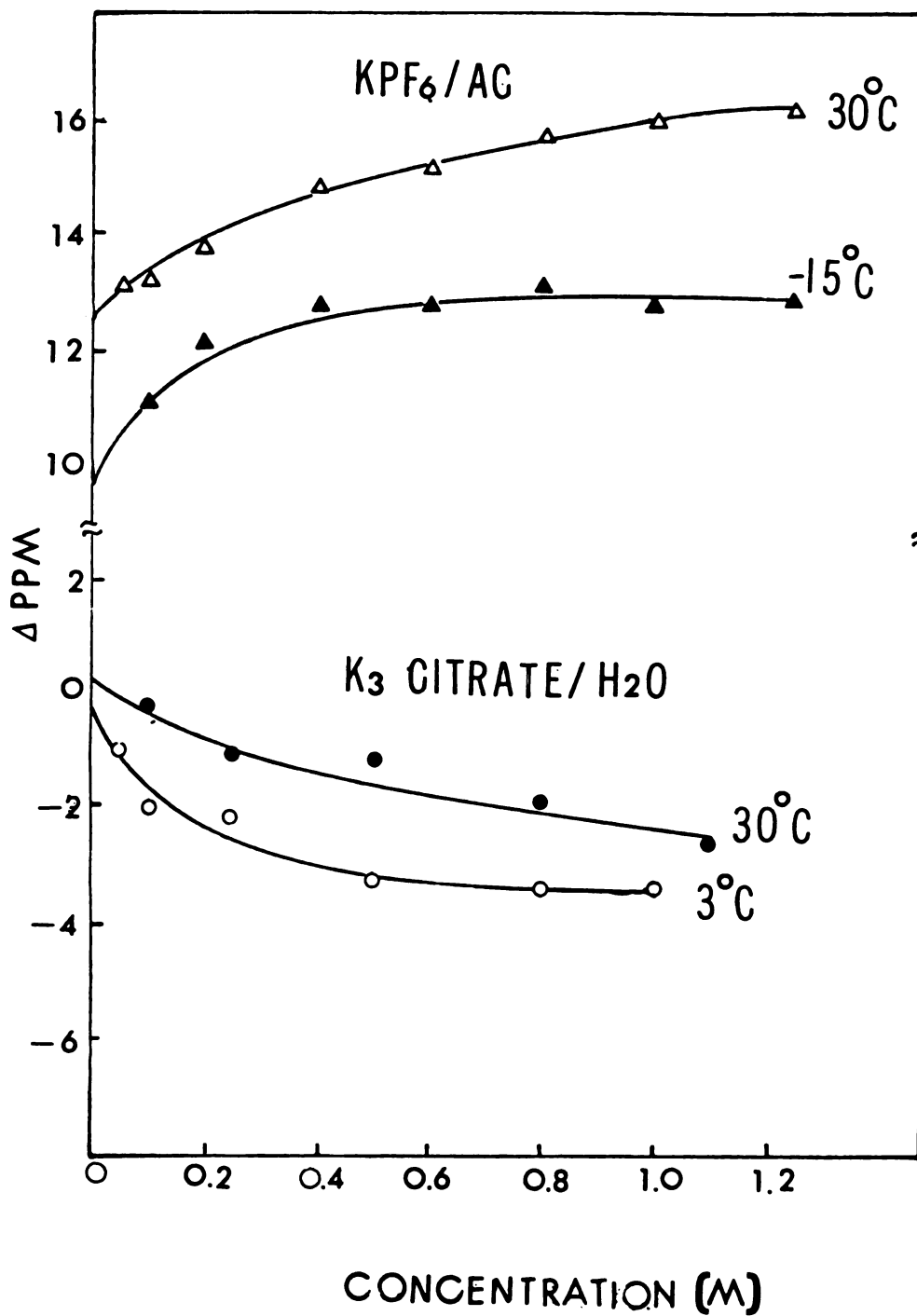


Figure 14. The Temperature Dependent Ionic Association of Potassium Salts in Water and Acetone

concentration plot increases with decreasing temperature, which is indicative of a stronger ion-ion interaction.

The concentration dependent chemical shift study also can provide the information about the ion-solvent interaction. At infinite dilution, it is reasonable to assume that only ion-solvent interaction exist. Therefore, the study of the infinite dilution chemical shift can give some information about the ion-solvent interaction. The "infinite dilution" chemical shift was obtained by extrapolation of the curve to zero concentration by using the computer program KINFIT, the application of KINFIT program and subroutine equation for this study are described in Appendix II.

The mean infinite dilution chemical shift of the  $K^+$  ion in various solvents are presented in Table 7. The plot of infinite dilution chemical shift vs the Gutmann donor number (24) is illustrated in Figure 15. It is readily seen that in general, there is a correlation between the magnitude of the downfield chemical shift and the donor number. Nine of the twelve solvents seem to fall on a respectable straight line but the correlation is not good for methanol, acetonitrile and dimethylsulfoxide solution. It is interesting to note that DeWitte and Popov (33) observed identical behavior in the case of cesium-133 resonance, where the same solvents show deviation from linearity in the chemical

Table 7. Potassium-39 Chemical Shifts at Infinite Dilution in Various Solvent

<u>Solvent</u>	<u><math>\delta_0</math>(ppm)</u>	<u>Donor Number</u> (b)
Nitromethane	21.1 $\pm$ 0.4	2.7
Formic Acid	11.6 $\pm$ 0.4	17.0
Propylene Carbonate	11.5 $\pm$ 0.4	15.0
Acetone	10.5 $\pm$ 0.9	17.0
Methanol	10.1 $\pm$ 0.7	25.7
Formamide	4.6 $\pm$ 0.6	24.7
Dimethylformamide	2.8 $\pm$ 0.8	26.6
Acetonitrile	0.4 $\pm$ 0.8	14.1
Water	0 <sup>(a)</sup>	33.0
Pyridine	-0.8 $\pm$ 0.4	33.1
Dimethylsulfoxide	-7.3 $\pm$ 0.6	29.8
Ethylenediamine	-23.6 $\pm$ 0.7	55.0 <sup>(c)</sup>

(a) Reference

(b) Gutmann donor number scale. The scale is based on the enthalpy of the reaction  $S + SbCl_5 \rightarrow S \cdot SbCl_5$  in dilute 1,2-dichloroethane solution. The donor number of the Solvent S is defined as  $DN(S) = -\Delta H_{S \cdot SbCl_5}^\circ$

(c) Estimated from  $^{23}Na$  chemical shifts. M. Herlem and A. I. Popov, J. Amer. Chem. Soc., 94, 1431 (1972)

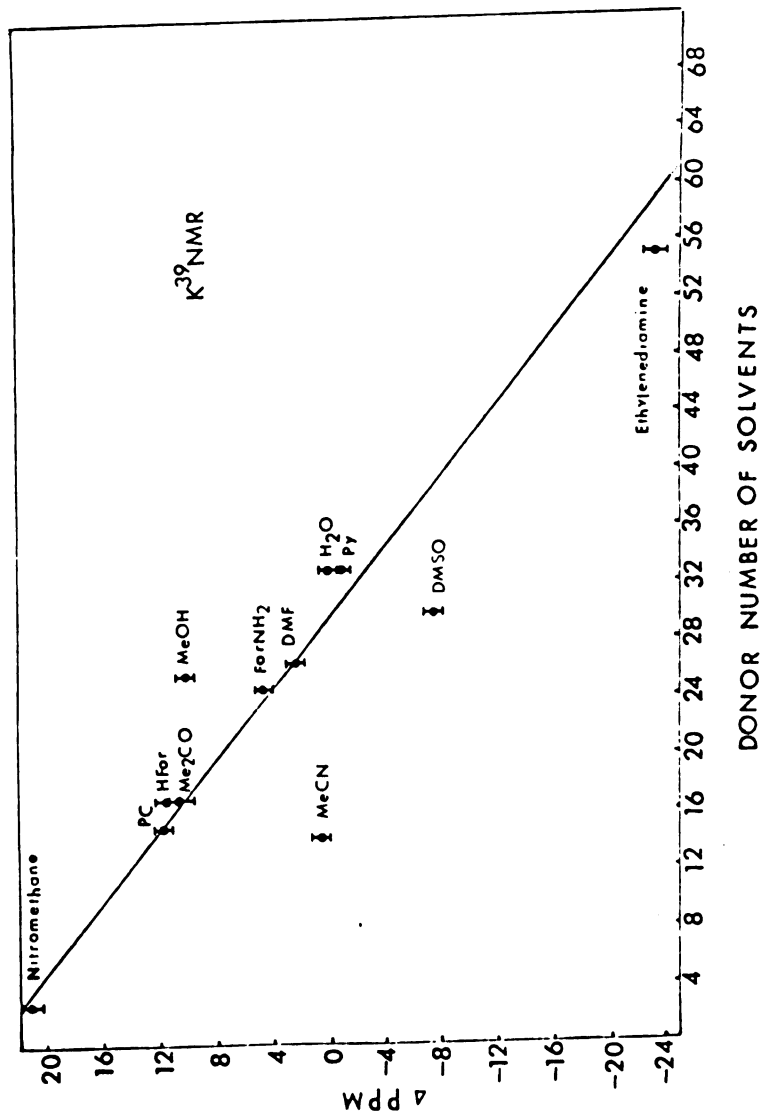


Figure 15. The Plot of the Infinite Dilution Chemical Shift vs the Gutmann Donor Number.

shift-donor number plot. The sign and the magnitude of the deviations were in the same direction and, approximately, of the same magnitude. However, a good linear correlation has been observed for Na infinite dilution chemical shift with solvent donicities without exception (29).

The correlation between the infinite dilution chemical shift ( $\delta_0$ ) of  $^{39}\text{K}$  resonance and donor number (DN) of the solvents can be expressed by the following equation:

$$\delta_0 = 24.1 - 0.82 \text{ DN}$$

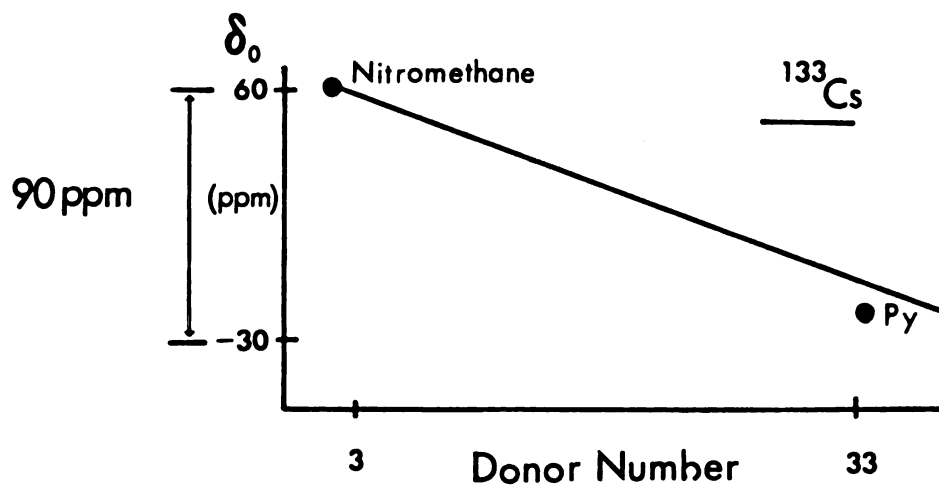
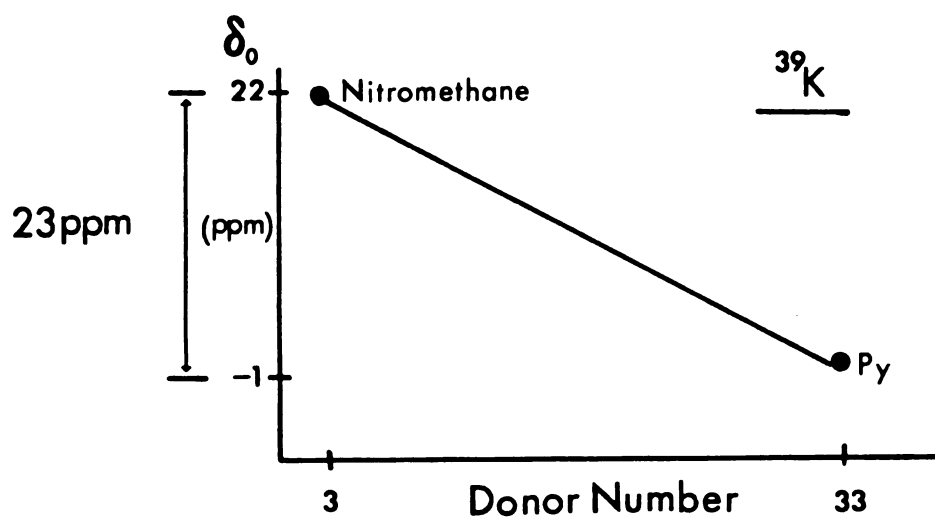
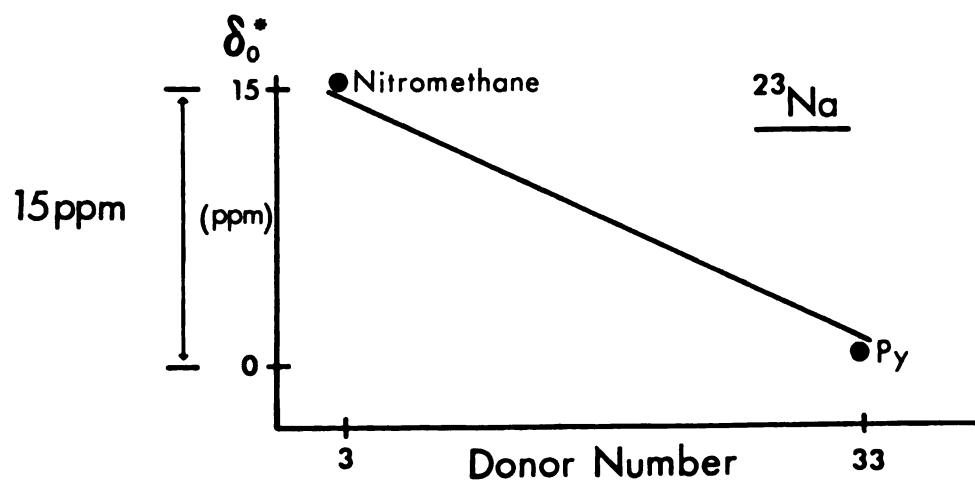
The donor number of methanol from this  $^{39}\text{K}$  chemical shift-donor plot can be predicted to be about 18.0, not 25.7. The value of 19.0 for methanol donicity was reported by Olofsson (31). The deviation of acetonitrile from linearity in the plot is probably due to some covalent interaction between the nitrogen on acetonitrile and the  $\text{K}^+$  ion (32). As can be seen from Table 7 with the exception of DMSO and  $\text{H}_2\text{O}$ , the infinite dilution chemical shifts of the  $\text{K}^+$  ion in the nitrogen donor solvents go more down field than that in oxygen donor solvents. Similar behaviors were reported in the Na and Cs cases (29)(32)(33). The phenomenon was interpreted (32) in terms of the small amount of covalent interaction between the cation and the solvent. Overlap between s and p orbitals of the solvent and p orbital of cation would permit the partial electron transfer from solvent to cation.

It is interesting to compare the magnitude and the "range" of the potassium-39 chemical shift to that of sodium-23 (29) and that of cesium-133 (33). As can be seen from Figure 16, the difference between chemical shifts of  $\text{Na}^+$ ,  $\text{K}^+$  and  $\text{Cs}^+$  in nitromethane and pyridine are 15, 23, and 90 ppm respectively. These results are not unexpected, since according to Ramsay's theory, one electron donated by the solvent to the cation induce the change in paramagnetic chemical shift by the following equation:

$$\begin{aligned} \Delta\delta_p &= \left(-\frac{e^2}{\Delta M^2 C^2}\right) \langle \psi_0 | \Sigma (\hat{L}_p \hat{L}_p / r_p^3) | \psi_0 \rangle \\ &= -\frac{e^2}{M^2 C^2} \frac{\langle r_p^{-3} \rangle}{\Delta} = (\text{constant}) \frac{\langle r_p^{-3} \rangle}{\Delta} \quad (\text{IIIA.3}) \end{aligned}$$

where  $\Delta$  is the average excitation energy of one electron from  $np$  to  $(n+1)p$  orbital.  $e$  and  $M$  are charge and mass of electron respectively.  $C$  is the velocity of light.  $L_p$  is angular momentum of the  $p$  orbital electron and  $r_p$  is the radial distance of the  $p$  orbital electron from the origin at the nucleus. According to this equation, the change in chemical shift of solvation is function of the quantity  $\frac{\langle r_p^{-3} \rangle}{\Delta}$ . The values of  $\frac{\langle r_p^{-3} \rangle}{\Delta}$  for  $\text{Na}^+$ ,  $\text{K}^+$ ,  $\text{Rb}^+$  and  $\text{Cs}^+$  reported (13) to be 5.9, 7.9, 13.8 and 18.7 (a.u./Rydberg) respectively. Therefore change in chemical

Figure 16. The Range of Infinite Dilution Chemical Shifts between Nitromethane and Pyridine for  $^{23}\text{Na}$ ,  $^{39}\text{K}$  and  $^{133}\text{Cs}$  Resonance



$\delta_0^*$ . Infinite dilute chemical shift

shift ( $\delta_p$ ) due to the solvation of alkali metal ions should increase in the order;  $\text{Na}^+ < \text{K}^+ < \text{Rb}^+ < \text{Cs}^+$ .

As can be seen from Figure 17, in the cases of nitromethane, dimethylsulfoxide and acetonitrile, there are the nearly linear correlations between the infinite dilution chemical shifts of the  $^{39}\text{K}$  resonances and the atomic numbers of alkali metals.

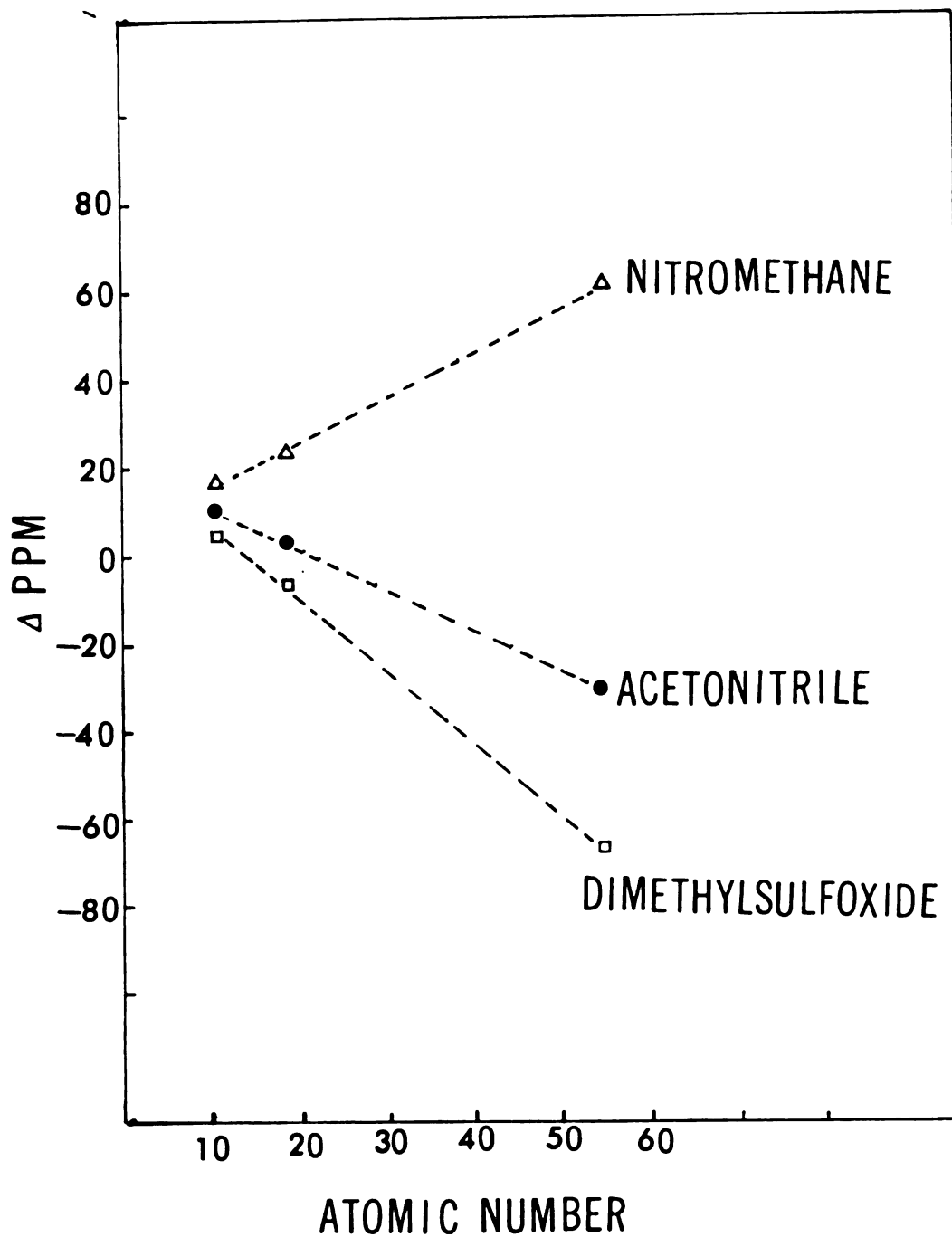


Figure 17. The Plot of Infinite Dilution Chemical Shift vs Atomic Number of Alkali Metal Ions

CHAPTER III (B)

IONIC SOLVATION OF THE POTASSIUM ION IN MIXED  
SOLVENTS

## (B) IONIC SOLVATION OF THE POTASSIUM ION IN MIXED SOLVENTS

It is well known that when a solute is dissolved in binary solvent mixtures, the primary solvation shell of the solute need not maintain the composition of the bulk solvent. It is likely that it may prefer one solvent over the other. Thermodynamic methods has usually been applied to study the preferential solvation. However, they often can not differentiate between short and long range effects. Since the chemical shift of nuclear magnetic resonance is only sensitive to contact solvation. NMR technique has become a powerful tool for the study of preferential solvation.

The study of preferential solvation of ions by metal nuclei resonance have been reported by several authors (11) (29)(103). The variation of the NMR chemical shift with solvent composition was explained in terms of preferential solvation of the metal ion by one of the solvents in the mixture as indicated by isosolvation point (equisolvation point). This isosolvation point is the composition at which the chemical shift lie halfway between the two pure solvent values. It has been postulated that it corresponds to the composition at which both solvents participate equal in the contact solvation shell. In addition, it is assumed that constant solvation number in solution at various solvent composition, and no solvent-solvent interaction in the mixtures.

## RESULTS AND DISCUSSION

The potassium-39 chemical shifts of potassium salts were measured as function of the solvent composition in twelve binary mixtures and the data are presented in Table 8. The results for the mixtures of acetone with nitromethane, acetonitrile, water and pyridine are illustrated in Figure 18 and Table 9. It can be seen, that in all cases there are the smooth transition as a function of solvent composition from the chemical shift characteristic of acetone to other solvents. The isosolvation points in the mixtures of acetone with nitromethane, acetonitrile, pyridine and water are at 0.20, 0.34, 0.38 and 0.75 mole fraction of acetone respectively. The data seem to suggest that the relative order of solvating ability is nitromethane < acetonitrile < pyridine < acetone < water.

The results for the mixtures of acetonitrile with nitromethane, propylene carbonate, acetone and water are presented in Figure 19 and 20 and Table 9 and the isosolvation points are at 0.41, 0.47, 0.66 and 0.92 mole fraction of acetonitrile. Again the solvating abilities for  $K^+$  ions among these solvents increase in the order: nitromethane < propylene carbonate < acetonitrile < acetone < water.

The results from the studies of the acetone mixtures and acetonitrile mixtures suggest that for  $KPF_6$  the solvating abilities of these solvents increase in the following

Table 8.  $^{39}\text{K}$  Chemical of Potassium Salt Solutions in Mixed Solvents

Mixture	MF of AC	$\Delta$ ppm	Mixture	MF of AC	$\Delta$ ppm	Mixture	MF of DMSO	$\Delta$ ppm
AC-NM	0	23.6	AC-ACN	0	3.4	DMSO-EN	0	-23.6
(0.1 M $\text{KPF}_6$ )	0.12	20.5	(0.2 M $\text{KPF}_6$ )	0.11	5.5	(0.5 M KSCN)	0.14	-20.2
	0.24	18.4		0.23	7.2		0.29	-18.5
	0.42	16.2		0.42	8.9		0.48	-15.9
	0.58	15.6		0.57	10.7		0.63	-12.5
	0.81	14.9		0.74	13.7		0.79	-10.6
	1.0	13.7		1.0	13.8		1.0	-8.0
Mixture	MF of AC	$\Delta$ ppm	Mixture	MF of AC	$\Delta$ ppm	Mixture	MF of AC	$\Delta$ ppm
AC-PY	0	0.5	AC-ACN	0	-1.4	DMSO-AC	1.0	4.1
(0.2 M $\text{KPF}_6$ )	0.16	3.3	(0.2 M KSCN)	0.11	-0.6	(0.5 M KSCN)	0.9	-1.9
	0.32	6.5		0.23	+0.1		0.8	-3.7
	0.52	8.6		0.31	+2.4		0.7	-6.3
	0.67	10.3		0.42	+2.8		0.49	-7.2
	0.86	12.2		0.57	+4.1		0.29	-8.0
	1.0	13.7		0.74	+5.9		0.20	-8.0
				0	+7.9		0.10	-8.0
							0	-8.0



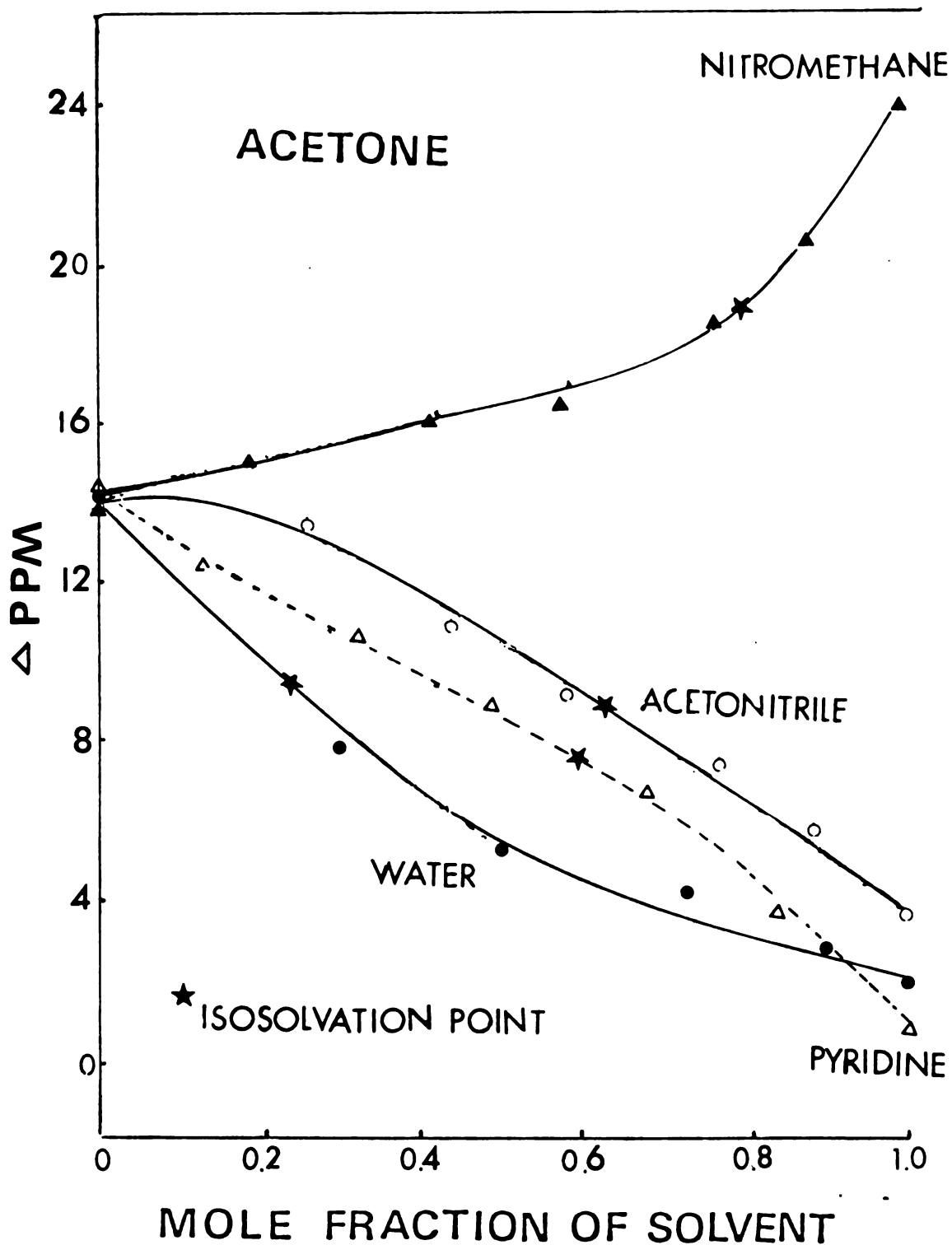


Figure 18.  $^{39}\text{K}$  Chemical Shifts of  $\text{KPF}_6$  in the Binary Mixtures of Acetone with Nitromethane, Acetonitrile, Water and Pyridine.

Table 9. Summary of Isosolvation Point Data for Potassium Salts in the Binary Solvent Mixtures

Mixture	Isosolvation Point
Acetone (a)-Nitromethane	0.20 Mole fraction of acetone
Acetone-Acetonitrile (KPF <sub>6</sub> )	0.34 "
Acetone-Pyridine	0.38 "
Acetone-water	0.75 "
Acetone-Acetonitrile (KSCN)	0.47 "
Acetonitrile (a)-Nitromethane	0.41 Mole fraction of acetonitrile
Acetonitrile-Propylene Carbonate	0.47 "
Acetonitrile-Acetone	0.66 "
Acetonitrile-Water	0.92 "
Dimethylsulfoxide (b)-Acetone	0.15 Mole fraction of DMSO
Dimethylsulfoxide-Water	0.35 "
Dimethylsulfoxide-Ethylenediamine	0.48 "
Water (c)-Methanol	0.51 Mole fraction of MeOH
Ethylenediamine-Methanol	0.53 "

- (a) In the acetone and acetonitrile mixtures, 0.2 M of KPF<sub>6</sub> were used as solute, except in the mixtures of nitromethane were 0.1 M of KPF<sub>6</sub> were used.
- (b) In all the mixtures of dimethylsulfoxide, 0.5 M KSCN were used as solute
- (c) In methanol mixtures case, 0.2 M KI was used as solute.

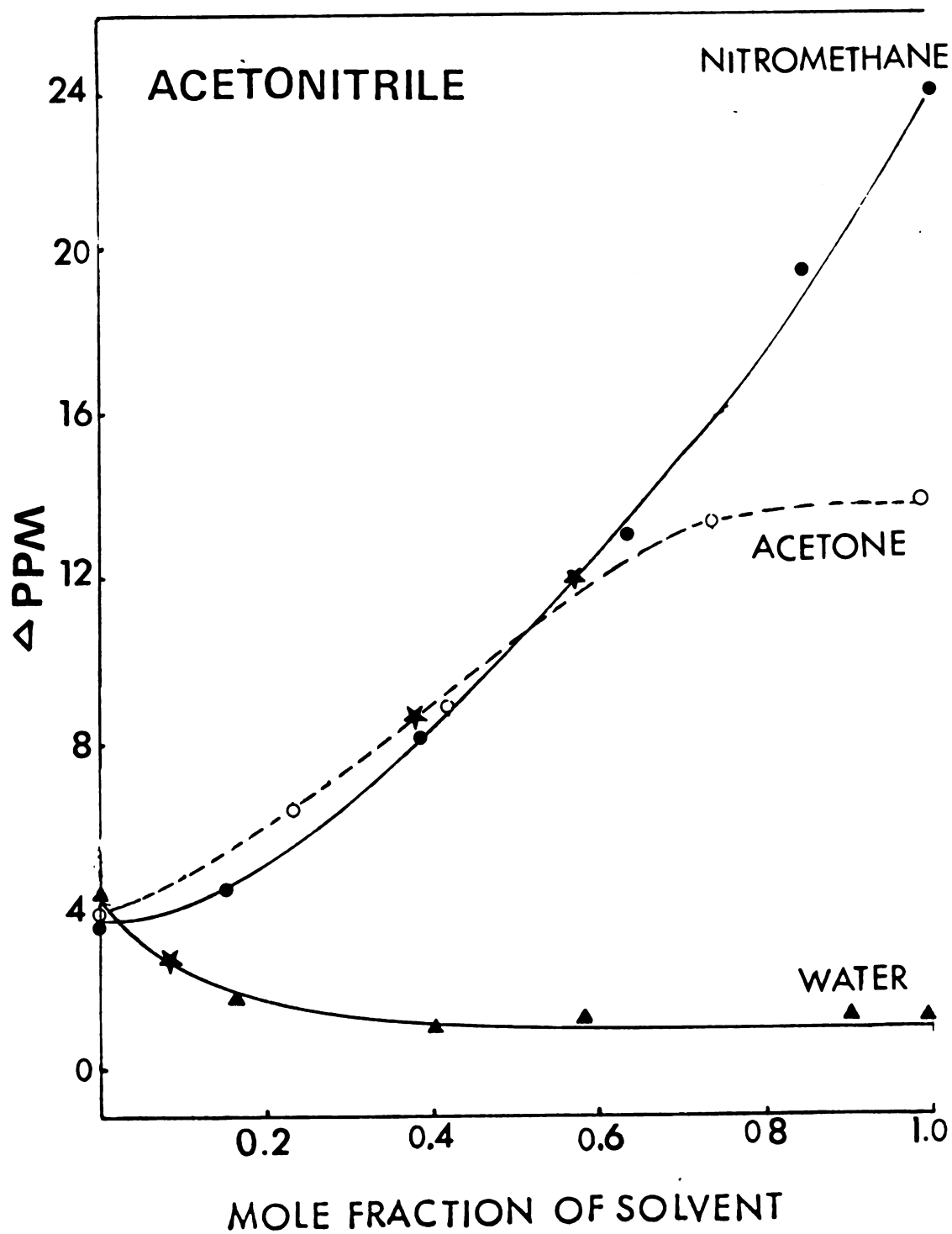


Figure 19.  $^{39}\text{K}$  Chemical Shifts of  $\text{KPF}_6$  in the Mixtures of Acetonitrile with Nitromethane, Acetone and Water.

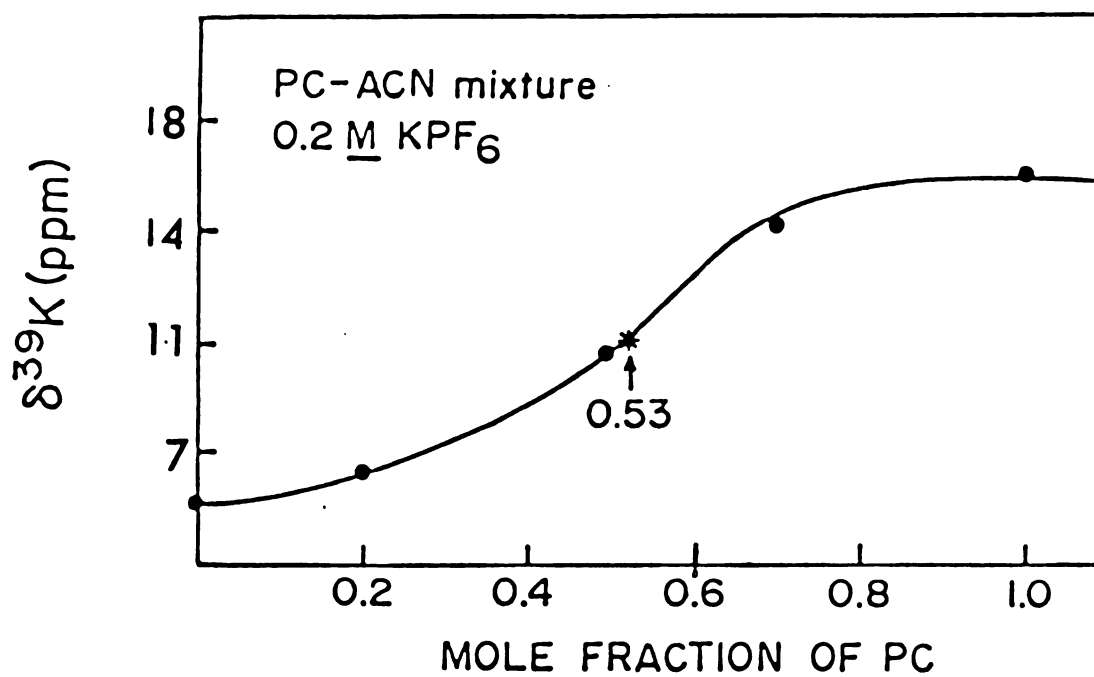


Figure 20.  $^{39}\text{K}$  Chemical Shifts of  $\text{KPF}_6$  in the Acetonitrile-Propylene Carbonate Mixtures.

orders, nitromethane < propylene carbonate  $\leq$  acetonitrile < pyridine < acetone < water.

The  $^{39}\text{K}$  chemical shifts of KSCN as function of the composition of the mixtures of dimethylsulfoxide with acetone, water and ethylenediamine are presented in Figure 21 and Table 9 and the isosolvation points are exhibited at 0.15, 0.35 and 0.48 mole fraction of DMSO. It seems to indicate that the relative order of solvating ability is  $\text{DMSO} \geq \text{ethylenediamine} > \text{water} > \text{acetone}$ . Despite the very high donicity of ethylenediamine, it does not appear to be a better solvating agent than dimethylsulfoxide. The enhancement of donicity of DMSO by introduction of even small amount of another solvent into neat DMSO was reported (29) previously. It was explained in terms of the break up of the polymeric structure of DMSO by addition of the other solvent. Therefore, it seems reasonable to assume that the high solvating ability of DMSO in the DMSO-ethylenediamine mixtures results from the same causes.

Finally, the preferential solvation of KI in the mixture of methanol with water and ethylenediamine were investigated. The results are shown in Figure 22 and Table 9. The isosolvation points for the mixtures of methanol with water and ethylenediamine are exhibited at 0.51 and 0.53 respectively, which indicates that the relative solvating ability in ethylenediamine > water >

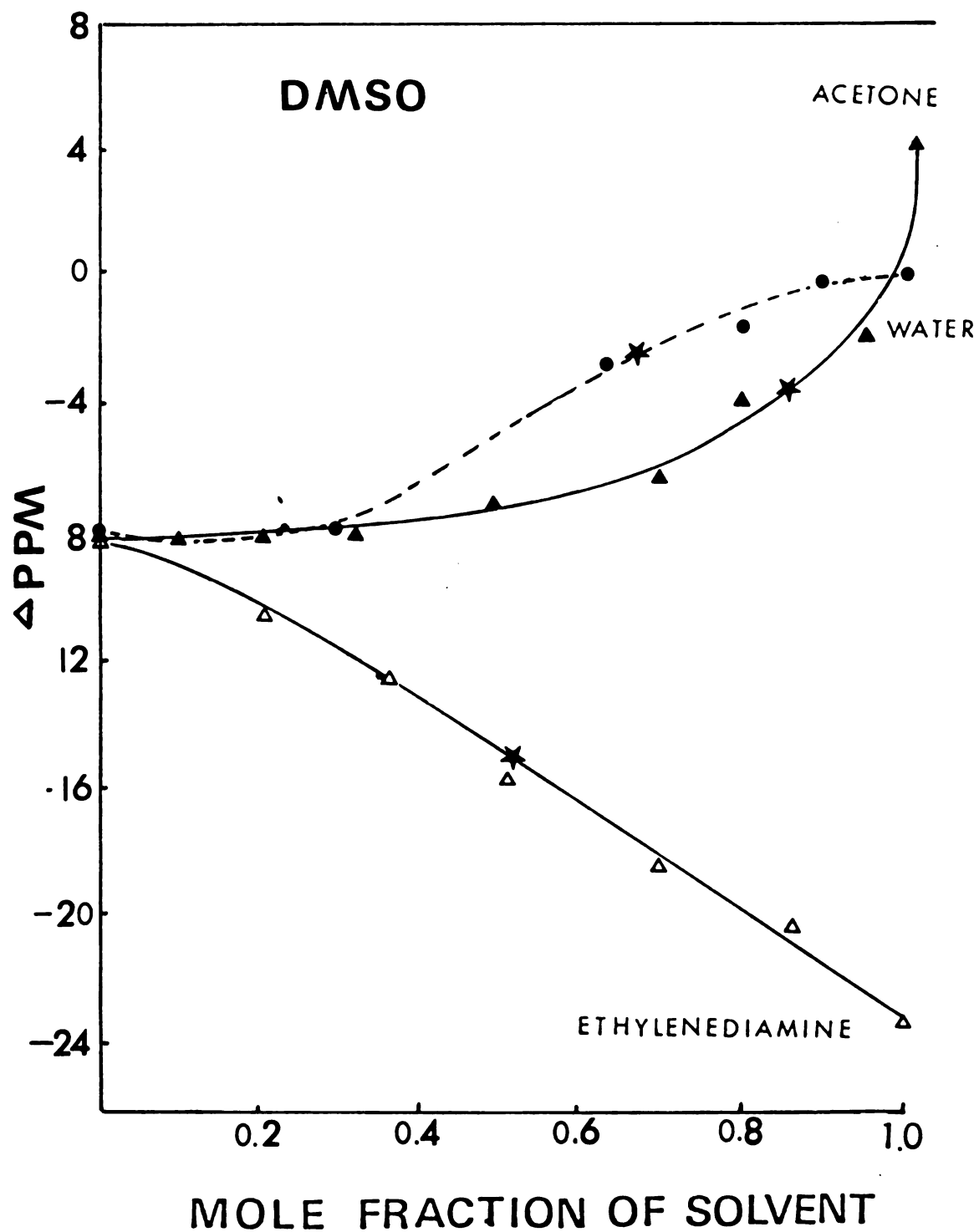


Figure 21.  $^{39}\text{K}$  Chemical Shifts of KSCN in the Mixtures of DMSO with Acetone, Water and Ethylenediamine.

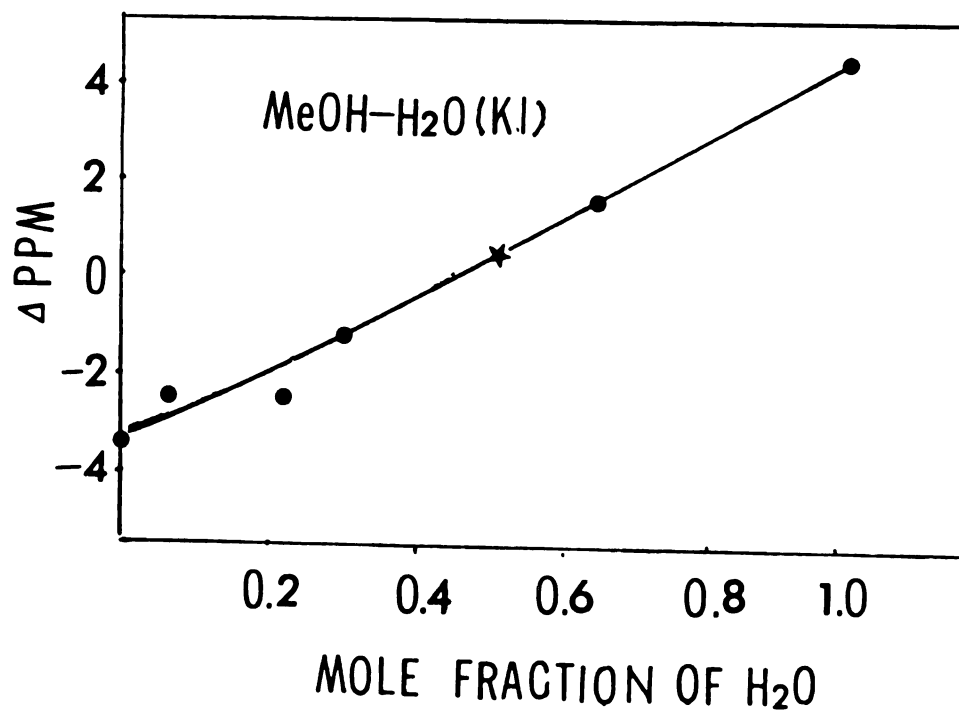
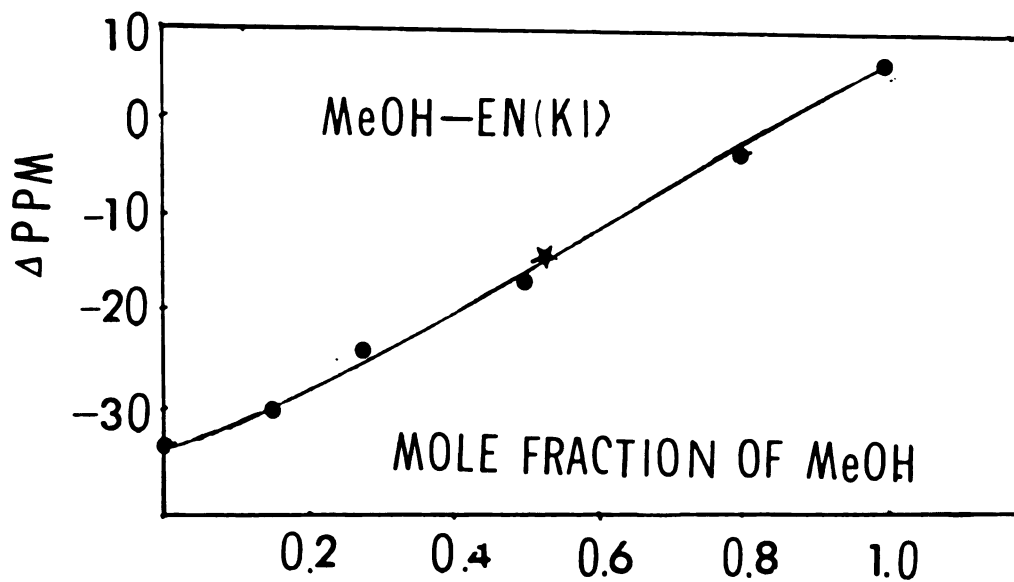


Figure 22.  $^{39}\text{K}$  Chemical Shifts of KI in Mixtures of Methanol with Water and Ethylenediamine.

methanol.

Recently, Covington, et al (28) developed a quantitative model for preferential solvation of ions in binary solvent mixtures. They presented a equation that allows the calculation of equilibrium constants and the changes in free energy of preferential solvation. The equation is

$$\frac{1}{\delta} = \frac{1}{\delta_p} \left( 1 + \frac{1}{K^{1/n} \frac{X_B}{X_A}} \right) \quad (\text{IIIB.1})$$

where:  $\delta$  = observed chemical shift relative to  
the resonance of  $M^+$  in pure A (solvent)

$\delta_p$  = total range of the chemical shift  
(ie:  $\delta_A^0 - \delta_B^0$ )

$K^{1/n}$  = the geometric equilibrium constant

$n$  = the solvation number

$X_A, X_B$  = the mole fraction of A and B (solvents)  
respectively

The  $K^{1/n}$  and  $1/\delta_p$  can be calculated from the slope and intercept of the plot of  $1/\delta$  vs  $X_B/X_A$  respectively, and finally the free energy of preferential solvation,  $\Delta G/n$  can be obtained as following:

$$\Delta G^0/n = -RT \ln K^{1/n} \quad (\text{IIIB.2})$$

The two typical plots of  $1/\delta$  vs  $X_B/X_A$  are shown

in Figure 23 and 24, and the values of  $K^{1/n}$  and  $\Delta G$  for each system were obtained by linear least squares procedure by KINFIT program and summarized in Table 10. The computer subroutine equations used to calculate  $K^{1/n}$  is described in Appendix II. In spite of a number of idealized assumption, in all cases shown in Table 10, the plot of  $1/\delta$  vs  $X_B/X_A$  yield straight lines. The Covington's quantitative approach seems to be successful in the  $^{39}\text{K}$  NMR preferential solvation studies.

Table 10. The Equilibrium Constants and Free Energy Change in the Mixed Solvents

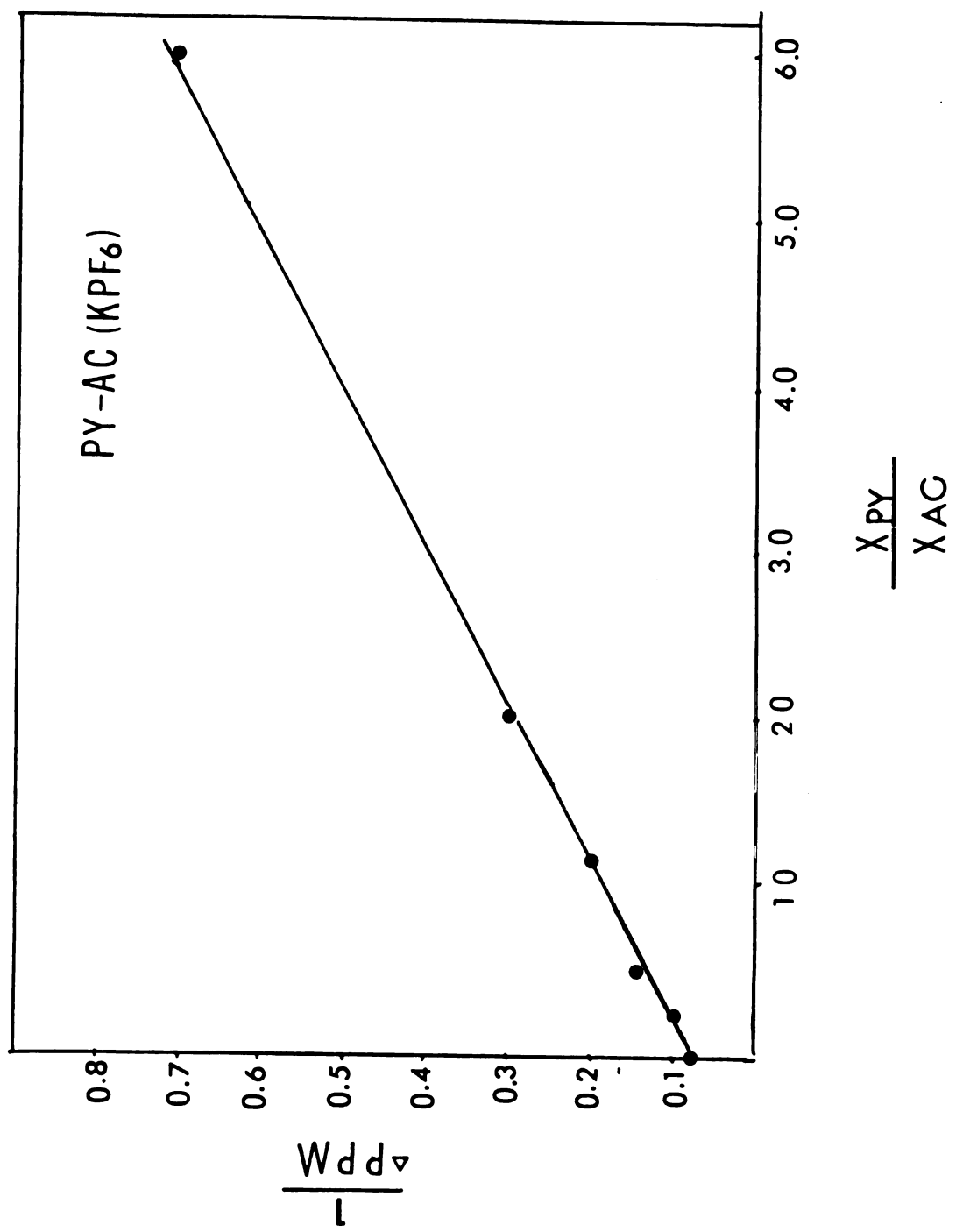
Mixtures (A-B)	Salt	Is Pt (a)	K <sup>1/n</sup> (c)	ΔG/n (KJ/mole) (c)
AC-NM(d)	KPF <sub>6</sub>	AC 0.2 MR (b)	4.08	3.568
AC-ACN	KPF <sub>6</sub>	AC 0.34 MR	2.16	1.954
AC-ACN	KSCN	AC 0.47 MR	1.19	0.448
AC-PY	KPF <sub>6</sub>	AC 0.38 MR	1.21	0.485
AC-H <sub>2</sub> O	KPF <sub>6</sub>	AC 0.75 MR	0.63	-1.160
DMSO-PY	KPF <sub>6</sub>	DMSO 0.35 MR	1.81	1.498
DMSO-EN	KSCN	DMSO 0.48 MR	1.33	0.726
DMSO-H <sub>2</sub> O	KSCN	DMSO 0.35 MR	0.93	0.184
ACN-NM	KPF <sub>6</sub>	ACN 0.2 MR	1.47	0.977
MeOH-EN	KI	MeOH 0.53 MR	0.85	-0.392

(a) Isosolvation point (b) Isosolvation point at mole fraction 0.2 of acetone.  
(c) ΔG and K are the free energy and the equilibrium constant in the equation



(d) AC: Acetone, ACN: Acetonitrile, NM: Nitromethane, PY: Pyridine, EN: Ethylenediamine, MeOH: methanol, DMSO: Dimethylsulfoxide.

Figure 23. Convington Plot for Pyridine-Acetone Mixtures



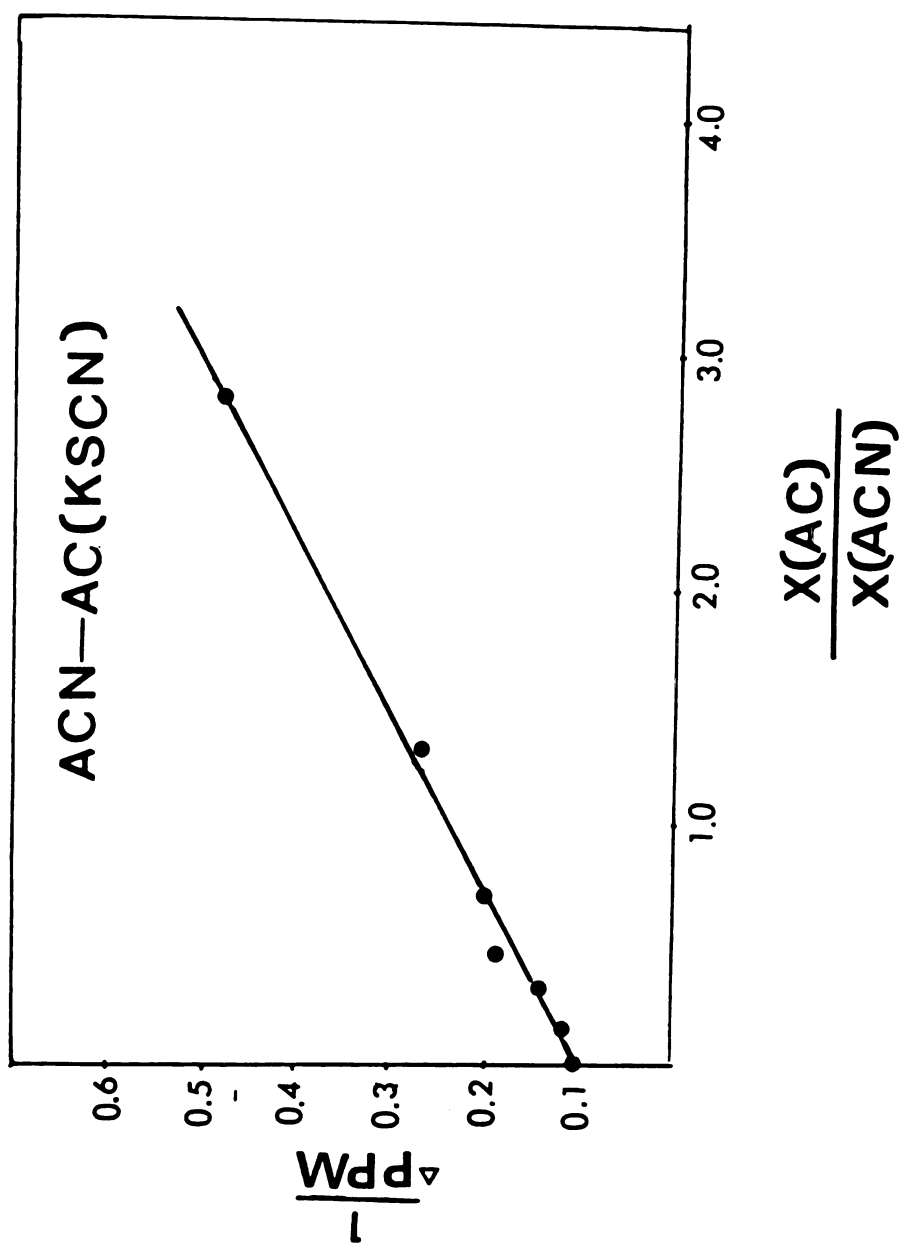


Figure 24. Convington Plot for the Acetonitrile-Acetone Mixtures

CHAPTER IV

POTASSIUM-39 AND CARBON-13 NMR STUDIES OF POTASSIUM  
SALT COMPLEXATION IN VARIOUS SOLVENTS

CHAPTER IV (A)

COMPLEXATION OF THE  $K^+$  IONS BY CRYPTANDS

## INTRODUCTION

Since the advent of macrocyclic crown ethers and cryptands (55)(66), the complexation of crown ethers with alkali metals in water and methanol have been studied extensively. However, the complexation of crown ether with metal ion in nonaqueous solvents (except methanol) have received much less attention.

Potassium-39 and carbon-13 NMR can be applied as sensitive and useful probes for the quantitative and qualitative studies of the complexation reactions of potassium salt with macrocyclic crown ethers and cryptands in various solvents.

### (A) COMPLEXATION OF THE $K^+$ IONS BY CRYPTANDS

The complexation studies of potassium ions with cryptand C222, C221 and C211 have been carried out in various solvents. In the  $^{39}K$  NMR mole ratio study, the concentration of  $KPF_6$  was held constant (0.02 M) and the ligand concentration varied. On the other hand, in the carbon-13 NMR study, the ligand concentration was kept constant (0.05 M) and  $KPF_6$  concentration varied. The cavity size of cryptand C222 was reported to be 2.6<sup>0</sup>Å (66) which matches the diameter of the potassium ( $\sim 2.7$ Å). Therefore, the C222- $K^+$  complexes should be stable. In acetone, methanol and nitromethane solution cases, at mole ratio of 0.5 of C222/ $K^+$ , two  $^{39}K$  signals

are observed corresponding to the free  $K^+$  and complexed  $K^+$  ions respectively (Figure 25). Therefore, the exchange between free  $K^+$  ions and complexed  $K^+$  is slow on the  $^{39}K$  NMR time scale. In general, if  $\nu_{\text{free}}$  and  $\nu_{\text{complex}}$  are the resonance frequencies of free and complexed  $K^+$  respectively and

$$\text{exchange rate} < \left(\frac{1}{\sqrt{2}}\pi\right) (\nu_{\text{free}} - \nu_{\text{complex}}) \quad (\text{IVA.1})$$

than the two NMR signals corresponding to the two  $K^+$  sites will be observed. On the other hand when

$$\text{exchange rate} \geq \left(\frac{1}{\sqrt{2}}\pi\right) (\nu_{\text{free}} - \nu_{\text{complex}}) \quad (\text{IVA.2})$$

than, only one population averaged NMR signal will be observed. The  $^{39}K$  chemical shifts for free  $K^+$  and complexed  $K^+$  are listed in Table 11. As can be seen, the chemical shifts for complexed  $K^+$  ion in various solvents are about the same, which is indicative of the formation of inclusive  $K^+$ -C222 complexes. In an inclusive complex, the potassium ion is inside the ligand cavity and is completely enclosed by the macrocyclic ligand, it is essentially isolated from the solvent. In order to obtain further information about the strength and structure of the  $K^+$  C222 complexes in various solvents, carbon-13 NMR of ligand was also used to study the system.

Figure 25.  $^{39}\text{K}$  NMR Spectra of  $\text{KPF}_6$ -Cryptand C222 Solution

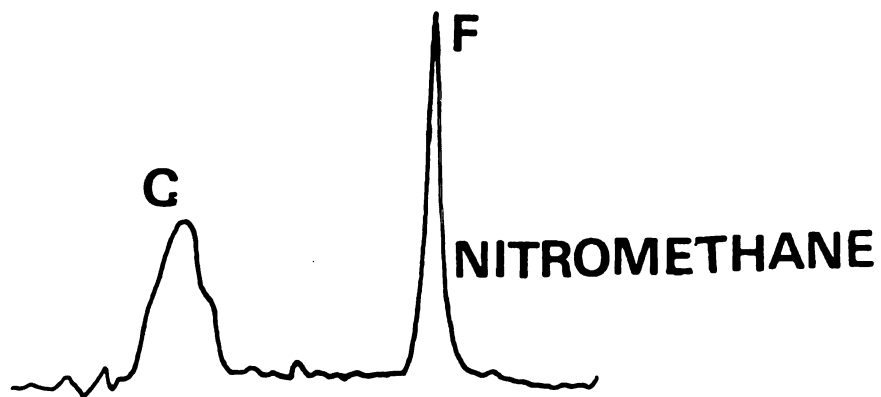
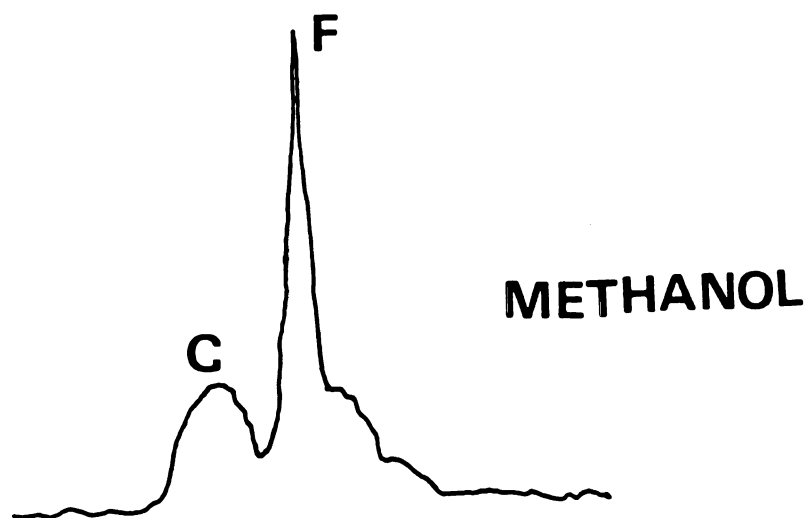
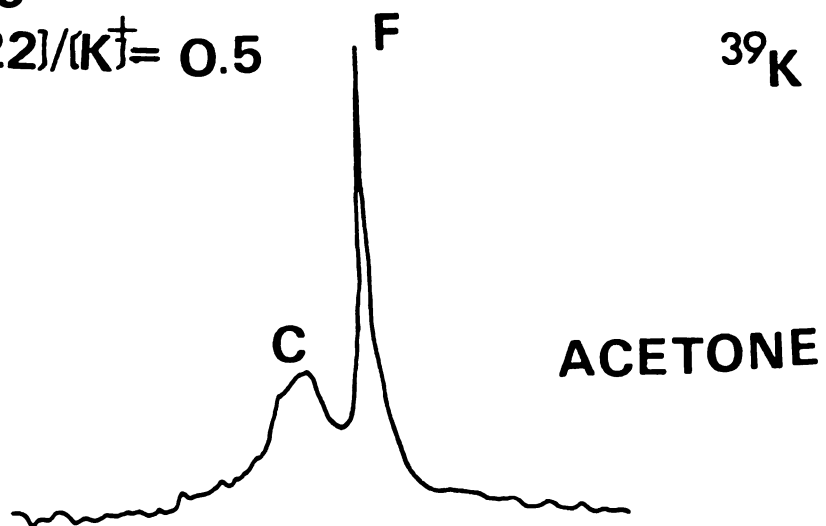
**KPF<sub>6</sub> - CRYPTAND 222****[C222]/[K<sup>+</sup>] = 0.5****<sup>39</sup>K NMR****COMPLEX    FREE K<sup>+</sup>**

Table 11. The Chemical Shifts and Line Widths of Potassium-39 of  $K^+C222$  Complexes at 0.5 Mole Ratio ( $C222/K^+$ )

Solvent	Chemical Shift (ppm)	Line Width (Hz)
Nitromethane	22.27 (F) <sup>(a)</sup>	44.0
	-2.48 (C)	92.8
Methanol	11.51 (F)	24.5
	-2.35 (C)	73.3
Acetone	12.01 (F)	19.3
	-2.78 (C)	87.9
Dimethylformamide <sup>(b)</sup>	6.28 (F)	25.2
	-2.04 (C)	90.2
Acetonitrile <sup>(b)</sup>	1.96 (F)	17.1
	-2.41 (C)	87.9

(a) F = Free  $K^+$ , C = Complexed  $K^+$  ion

(b) The signals for free  $K^+$  and complexed  $K^+$  are overlaped in dimethylformamide and acetonitrile.

The resulting C-13 chemical shifts are presented in Table 12 and Figure 26. The three observed C-13 NMR signals of free cryptands correspond to three kind of carbons in C222. The assignments of peaks for the three carbons are shown in Figure 26. Carbon(1) and carbon(2) are the  $\text{O}\underline{\text{C}}\text{H}_2$  carbons and carbon(3) is  $\text{N}\underline{\text{C}}\text{H}_2$  carbon. As Figure 26 shows, at mole ratio 0.5 of  $\text{K}^+/\text{C222}$ , the two signals for each carbon were observed for carbons of the free ligand and complexed ligand respectively. Again we have a slow exchange between the free ligand and the complexed ligand. As seen in Table 12 a slow exchange occurs even in solvents of high donor number and high dielectric constant, such as dimethylsulfoxide and dimethylformamide. At a mole ratio of 1.0, only one peak for each carbon was observed which corresponds to the complex. It is interesting to see that chemical shifts of both free ligand and complexed ligand are about the same in various solvents except  $\text{H}_2\text{O}$ . It appears, therefore, that the structures of either free cryptands or complexed cryptands in these solvents are about the same. However, in the water case, the chemical shifts for free cryptand show large difference from that in another solvents. For example, for the  $\text{N}\underline{\text{C}}\text{H}_2$  carbon, the  $^{13}\text{C}$  chemical shift is 54.76 ppm in the  $\text{H}_2\text{O}$  case, but it is about 58.10 ppm in another solvents. The different behavior in aqueous solutions

Table 12. Carbon-13 Chemical Shift of Potassium Cryptates C222

Solvent	Salt	Peak #	$\Delta$ ppm	Mole Ratio ( $K^+/C222$ )				
				0	1.0	2.0	3.0	
Acetone	KPF <sub>6</sub>	(1)	72.54 (OCH <sub>2</sub> )	72.55	72.14 (C)	72.07 (C)	-	
		(2)	71.75 (OCH <sub>2</sub> )	71.76	69.32 (C)	69.21 (C)	-	
		(3)	58.28 (NCH <sub>2</sub> )	58.37	55.61 (C)	55.61 (C)	-	
	DMF	KPF <sub>6</sub>	(1)	72.29 (OCH <sub>2</sub> )	72.36	71.97 (C)*	71.97 (C)	-
			(2)	71.51 (OCH <sub>2</sub> )	71.57	69.22 (C)	69.21 (C)	-
			(3)	58.03 (NCH <sub>2</sub> )	58.09	55.61 (C)	55.54 (C)	-
	DMSO	KPF <sub>6</sub>	(1)	72.37 (OCH <sub>2</sub> )	72.29	72.08 (C)	72.07 (C)	-
			(2)	71.68 (OCH <sub>2</sub> )	71.59	69.31 (C)	69.31 (C)	-
			(3)	58.09 (NCH <sub>2</sub> )	58.00	55.53 (C)	55.54 (C)	-

\* (C) Signal for complexes ligand

Table 12. Continued

Solvent	Salt	Peak #	0	Mole Ratio (K <sup>+</sup> /C222)				
				0.5	1.0	2.0	3.0	
DMSO	KSCN	(1)	72.37 (OCH <sub>2</sub> )	72.25	-	-	-	
		(2)	71.68 (OCH <sub>2</sub> )	72.04 (C)	-	-	-	
		(3)	58.09 (NCH <sub>2</sub> )	71.56	69.21 (C)	-	-	
H <sub>2</sub> O	KSCN	(1)	71.80 (OCH <sub>2</sub> )	57.90	-	-	-	
		(2)	70.71 (OCH <sub>2</sub> )	55.43 (C)	-	-	71.96	
		(3)	54.76 (NCH <sub>2</sub> )	71.88	69.53	-	69.59	
				55.16	-	-	55.33	

\* (C) Signal for complexed ligand

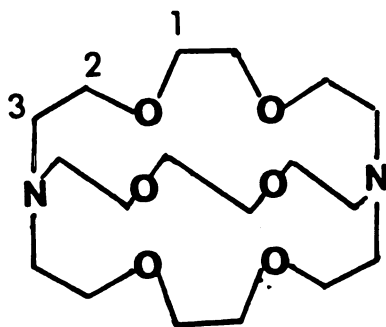
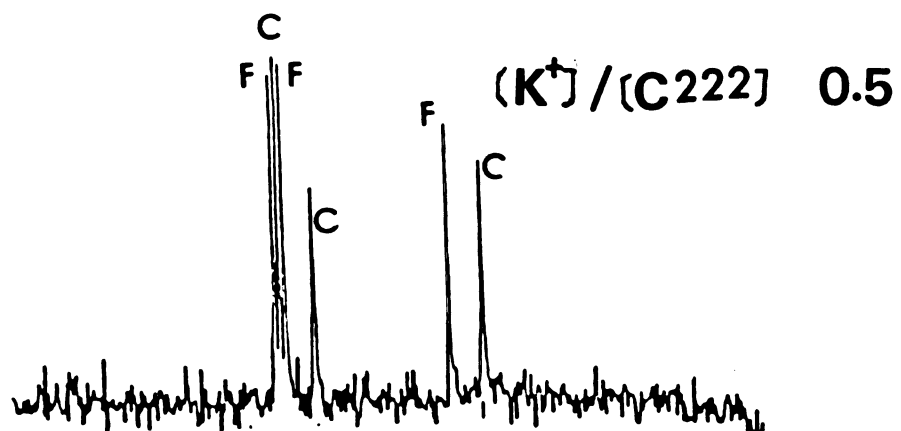
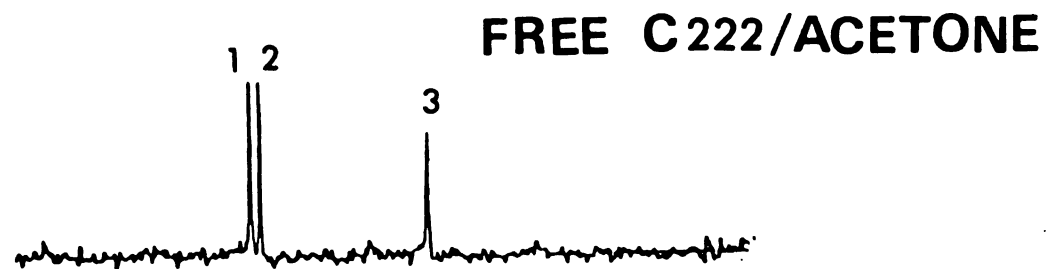


Figure 26.  $^{13}\text{C}$  NMR Spectra of  $\text{K}^+$ -Cryptand C222 in Acetone

may indicate some interaction between the free C222 and water, such as hydrogen bonding between the oxygen of the cryptand and the water molecule.

As can be seen from Table 13, in all cases there is a large change in chemical shifts for  $\text{NCH}_2$  carbon and one of  $\text{OCH}_2$  carbons (carbon 2 in Table 13) upon complexation, but a small change in the other  $\text{OCH}_2$  carbon (carbon 1 in Table 13). If the potassium ion is located in the center of cavity and the structure of cryptand does not change upon complexation, the changes in chemical shifts for two  $\text{OCH}_2$  carbons should be about the same and larger than that for  $\text{NCH}_2$  carbon since usually ion-dipole interaction for  $\text{O-M}^+$  is stronger than for  $\text{N-M}^+$ . However, actually, as can be seen from Table 13, the change in chemical shift for  $\text{NCH}_2$  carbon is larger than that of either  $\text{OCH}_2$  carbons. The most probable explanation is that there is the strong interaction between  $\text{K}^+$  and nitrogen atom which makes the change in structure of cryptand from the exo-exo (90) to the endo-endo conformation upon complexation, which makes a extremely change in the environment of  $\text{NCH}_2$  carbon.

The complexation of cryptand C221 and potassium ion was monitored by  $^{39}\text{K}$  NMR. As Figure 27 shows, at mole ratio 0.5 of  $\text{C221/K}^+$ , in acetone, methanol, diethylformamide and acetonitrile, the two  $^{39}\text{K}$  signals which correspond to the free  $\text{K}^+$  ion and complexed  $\text{K}^+$  ion were

Table 13. The Change in  $^{13}\text{C}$  Chemical Shift of  
Cryptand C222 upon Complexation

Solvent	Acetone	Dimethyl- sulfoxide	Dimethyl- formamide
$\Delta\delta_1(\text{OCH}_2)$	0.21 ppm	0.51 ppm	0.39 ppm
$\Delta\delta_2(\text{OCH}_2)$	2.28	2.45	2.35
$\Delta\delta_3(\text{NCH}_2)$	2.47	2.76	2.48

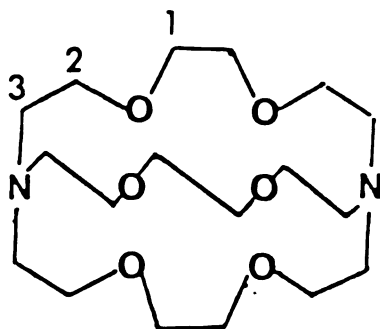
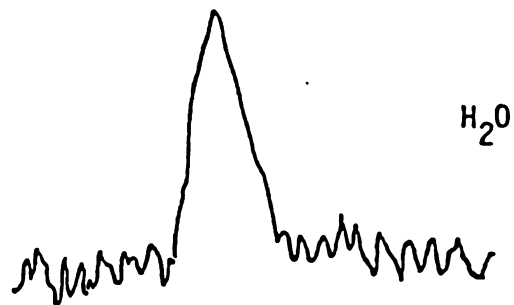
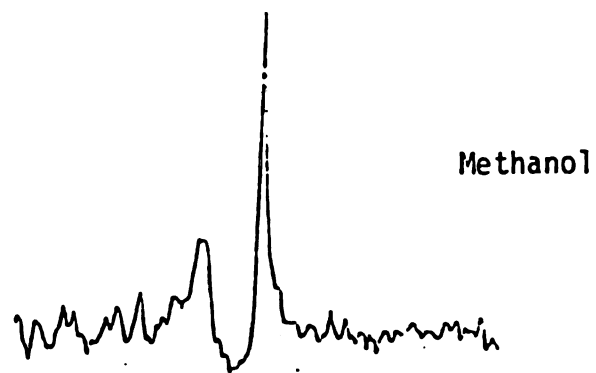
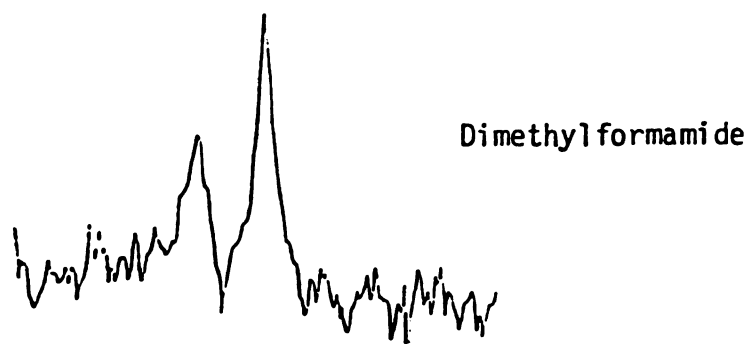
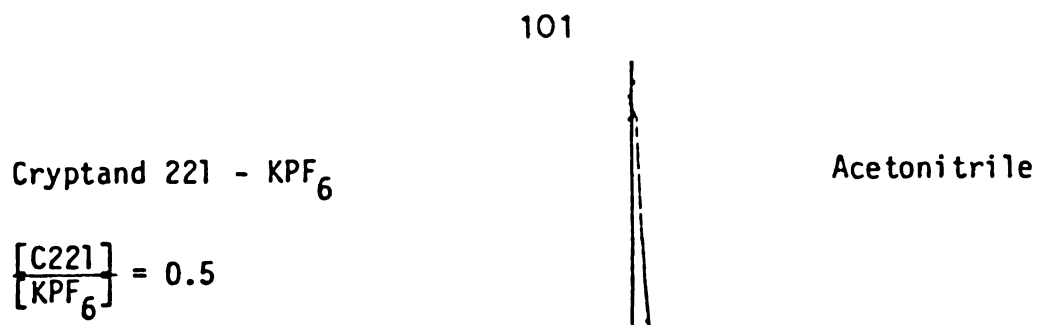


Figure 27. Potassium-39 Spectra of Potassium-C221 Cryptate  
in Various Solvents;  $[C221] = 0.01 \text{ M}$  ,  
 $[KPF_6] = 0.02 \text{ M}$ .



observed. It indicates the slow exchange between the free  $K^+$  and complexed  $K^+$  ion on the  $^{39}K$  NMR time scale. However, in the water case, the only one broad peak observed at mole ratio 0.5 indicates the fast exchange between free  $K^+$  and complexed  $K^+$ . The chemical shifts and line widths for the free  $K^+$  and complexed  $K^+$  in various solvents are shown in Table 14. The chemical shifts of  $K^+$ -C221 cryptate seem to be dependent on the solvent, which is indicative of some contact interaction between  $K^+$  ion and the solvent. It is reasonable to assume the formation of exclusive  $K^+$ -C221 complexes in these solvents.

The carbon-13 NMR was also applied for the investigation of complexation of  $K^+$  and cryptand C221. The  $^{13}C$  chemical shift as function of the  $K^+/C221$  mole ratio in acetone, dimethylsulfoxide and water are presented in Table 15. In the acetone case,  $^{13}C$  chemical shift for each carbon on cryptand seems to reach a limiting value after the mole ratio of 1.0 (the experimental error is about  $\pm 0.05$  ppm) which is indicative of the formation of a stable complex. However, at mole ratio 0.5 of  $K^+/C221$ , only one averaging peak for each carbon was observed, which is indicative of the fast exchange reaction between free and complexed cryptand C221 while the slow exchange reaction in the  $K^+$ -C222 case was observed as mentioned previously. Therefore, the  $K^+$ -C222 cryptate in nonaqueous solvents is a relatively inert complex

Table 14. Chemical Shifts and Line Widths of K-39  
of  $K^+$ -C221 Complexes at 0.5 Mole Ratio  
(C221/ $K^+$ )

Solvent	$\delta_{lim}$ (ppm)	$\nu_{1/2}$ (Hz)
Acetone	(1) +12.31 (F)	31.7
	(2) -10.94 (C)	53.8
Methanol	(1) +10.86 (F)	24.4
	(2) -14.13 (C)	78.1
Dimethylformamide	(1) +5.05 (F)	39.0
	(2) -14.13 (C)	68.0
Pyridine	(1) -0.18 (F)	30.3
	(2) -17.60 (C)	82.4
Acetonitrile	(1) +1.56 (F)*	19.5
	(2) -13.54 (C)*	68.3
H <sub>2</sub> O	(1) -4.83	102.5

(F)\* = Chemical shift for free potassium ion.

(C)\* = Chemical shift for complexed  $K^+$  in  $K^+$ -C221  
complex  $KPF_6 = 0.02$  M.

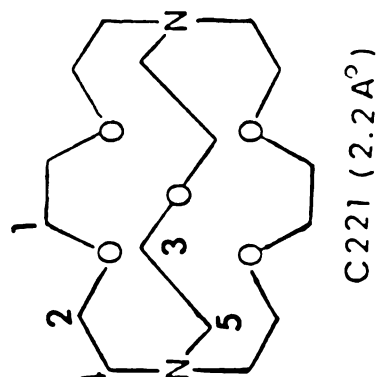


Table 15. Carbon-13 Chemical Shifts of Potassium Cryptate 221

Solvent	Salt	Peak #	Mole ratio (K <sup>+</sup> /C221)				
			0	0.5	1.0	2.0	
Acetone	KPF <sub>6</sub>	(1)	72.77 ppm	(OCH <sub>2</sub> ) <sub>c1</sub>	72.18	71.88	71.77
		(2)	72.29	(OCH <sub>2</sub> ) <sub>c2</sub>	71.97	71.40	71.28
		(3)	71.61	(OCH <sub>2</sub> ) <sub>c3</sub>	70.88	69.99	69.80
		(4)	59.09	(NCH <sub>2</sub> ) <sub>c4</sub>	59.49	59.88	59.87
		(5)		(NCH <sub>2</sub> ) <sub>c5</sub>		55.18	55.23
DMSO	KPF <sub>6</sub>	(1)	72.86	(OCH <sub>2</sub> ) <sub>c1</sub>	-	71.76	71.58
		(2)	72.37	(OCH <sub>2</sub> ) <sub>c2</sub>	-	71.30	71.09
		(3)	71.88	(OCH <sub>2</sub> ) <sub>c3</sub>	-	69.99	69.62
		(4)	58.78	(NCH <sub>2</sub> ) <sub>c4</sub>	-	59.85	59.77
		(5)		(NCH <sub>2</sub> ) <sub>c5</sub>			55.14
H <sub>2</sub> O	KI	(1)	71.79	(OCH <sub>2</sub> ) <sub>c1</sub>	-	-	72.36
		(2)	71.09	(OCH <sub>2</sub> ) <sub>c2</sub>	-	-	71.38
		(3)			-	-	70.20
		(4)	57.90	(NCH <sub>2</sub> ) <sub>c4</sub>	-	-	59.61
		(5)	56.03	(NCH <sub>2</sub> ) <sub>c5</sub>	-	-	55.34

while  $K^+$ -C221 cryptate is a relative labile complex.

The  $^{13}C$  chemical shifts for each carbon on free C221 in aqueous solution can be seen to show some difference from that in another solvents. For example, the chemical shift for carbon 5 ( $NCH_2$  carbon) is  $\sim 56$  ppm in the water case, but it is  $\sim 59$  ppm in acetone and DMSO cases. Again, this result may be due to the interaction between the cryptand C221 and the water.

The data of potassium- $^{39}K$  NMR chemical shifts for  $K^+$ -C211 cryptates are tabulated in Table 16. The mole ratio studies of the complexation in various solvents are illustrated in Figure 28. Since the exchange between free  $K^+$  and complexed  $K^+$  was fast on  $^{39}K$  NMR time scale, only one  $^{39}K$  signal was observed at various mole ratio of C211/ $K^+$ . In the cases of acetone, pyridine and acetonitrile solutions, the chemical shifts reach the limiting value at a low mole ratio of ligand/ $K^+$  ( $\sim 2.5$ ), which is indicative of the formation of relatively strong complexes. The formation constants for these complexes are listed in Table 16. In the dimethylformamide case, the chemical shift tends to change continually even after mole ratio 4.0, which indicates the formation of weak complexes. However, in the DMSO case the chemical shift of  $^{39}K$  seems not change with increasing ligand concentration. The formation constants of  $K^+$ -C211 complex was obtained by fitting the curve using KINFIT program, (the application

Table 16. Mole Ratio Study of Cryptand C211 Complexes with KPF<sub>6</sub> in Various Solvents

Solvent	C211/K <sup>+</sup>	$\Delta$ ppm	Solvent	C211/K <sup>+</sup>	$\Delta$ ppm	Solvent	C211/K <sup>+</sup>	$\Delta$ ppm
AC*	0	12.6	ACN	0	+1.6	DMF	0	5.6
	0.5	5.6		0.5	-3.1		0.5	4.5
	1.0	1.6		1.0	-6.6		1.0	3.3
	1.5	-0.2		1.5	-7.7		1.5	1.9
	2.0	-4.8		2.0	-11.2		2.0	0.9
	2.5	-5.4		2.5	-11.2		2.5	-0.1
	3.0	-5.4		3.0	-11.2		3.0	-0.8
	0	-6.0	PY	0	-2.4		4.0	-1.9
	0.5	-6.6		0.5	-4.8			
	1.0	-6.6		1.0	-6.6			
DMSO	2.0	-6.6		1.5	-7.7			
	3.0	-		2.0	-8.3			
	4.0	-6.4		3.0	-8.6			

\* Salt: 0.02 M KPF<sub>6</sub>

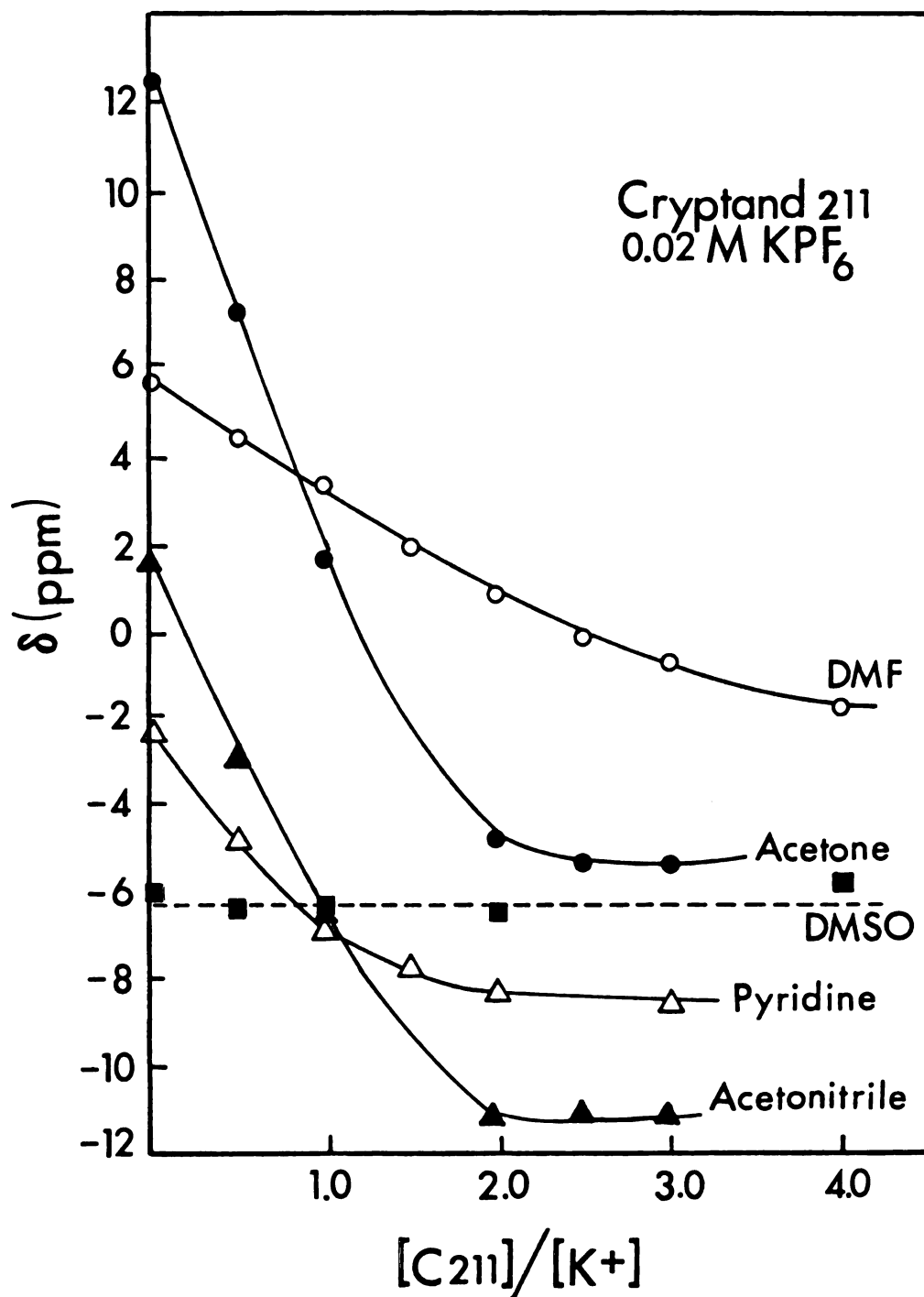


Figure 28.  $^{39}K$  Chemical Shift vs Mole Ratio of  $C_{211}/K^+$  in Various Solvents

of KINFIT and subroutine equation are described in Appendix IV). As Table 17 shows, the formation constants of  $K^+$ -C211 complexes among these solvents decrease in the order; acetone > acetonitrile > pyridine > dimethylformamide. It is not surprising that the most stable complex in acetone solution, since acetone has a low donicity and a low dielectric constant. Acetonitrile and dimethylformamide have about same dielectric constant ( $\sim 38$ ), but the difference in stabilities of complexes in both solvents was observed, which may be due to the lower donicity of acetonitrile than that of dimethylformamide. Pyridine has higher donicity than dimethylformamide and it would be expected that the complex in pyridine should be weaker than that in dimethylformamide. However the reverse experimental result was obtained. It should be noted that according to the Pearson's Hard-soft-acid-base (HSAB) theory (104), pyridine is a relatively soft solvent (base) and  $K^+$  is a hard ion (acid), the  $K^+$  ion should be expected undergo weak interaction with pyridine, and then the  $K^+$ -cryptand interaction would be expected to be strong.

The carbon-13 NMR chemical shift measurements were also made at mole ratio ( $M^+$ /cryptand) of 0.5 in alkali metal salt ( $Na^+$ ,  $K^+$  and  $Cs^+$ ) nonaqueous solutions. The data are presented in Table 18. The results seem to indicate that inert complexes are formed in the cases of

Table 17. Formation Constants and Limiting Chemical Shift for Complexation of  $\text{KPF}_6$  by C211

Solvent	Log Kf	$\delta_{\text{lim}}$ (ppm)
Acetone	> 4	-5.44 $\pm$ 0.05
Acetonitrile	2.80 $\pm$ 0.21	-11.78 $\pm$ 0.37
Pyridine	2.47 $\pm$ 0.06	-9.13 $\pm$ 0.08
Dimethylformamide	0.99 $\pm$ 0.06	-12.98 $\pm$ 0.20
Dimethylsulfoxide <sup>(a)</sup>	-	-

(a) The ligand concentration show no effect on the chemical shift of  $\text{KPF}_6$  in dimethylsulfoxide.

Table 18. Carbon-13 Chemical Shift ( $\Delta$  ppm) of Li, Na, K and Cs Cryptates

Cryptand	Solvent	$(K^+/L)$	Mole Ratio					Free Cryptand
			Li <sup>+</sup>	Na <sup>+</sup>	K <sup>+</sup>	Cs <sup>+</sup>		
C222	DMSO	0.5	peak					
			(1)	72.30	(a)	72.25(F)(b)	72.25	72.37(1)
			(2)	71.59	(a)	72.04(C)(c)	71.09	71.68(2)
C221	Acetone	0.5	(3)	58.01	(a)	71.56(F)	57.70	58.09(3)
			(1)	71.57	72.75(F)	72.18	Free C221	
			(2)	71.19	70.88(C)	71.97	72.77	72.29
			(3)	70.66	71.97	70.88	-	71.61
			(4)	57.99	59.08	59.49	-	59.09
					55.92(C) <sub>c4</sub>			
				55.23(C) <sub>c5</sub>				

(a) Broad signals (b) Signals for free ligand (c) Signals for complexed ligand

Table 18. Continued

Cryptand	Solvent	(K <sup>+</sup> /L) Mole Ratio	Li	Na <sup>+</sup>	K <sup>+</sup>	Cs <sup>+</sup>	Free Cryptand
C211	DMSO	0.5	(1) 72.27(F) 68.72(C)	71.47	72.08	72.07	72.36
			(2) 71.38 67.34(C)	71.17	71.39	71.28	71.46
			(3) 59.08 53.06(C)	59.76	59.48	59.47	59.07
			(4) 57.20 52.18(C)	57.58	57.51	57.10	57.28

$\text{Li}^+$  for cryptand C211,  $\text{Na}^+$  for cryptand C221 and  $\text{K}^+$  for cryptand C222, as indicated by two  $^{13}\text{C}$  signals observed for each carbon on cryptands which are corresponding to free ligand and complexed ligand respectively. It indicates that in nonaqueous solvents, cryptands still have very sharp cation selectivities; cryptand C222 for  $\text{K}^+$ , cryptand C221 for  $\text{Na}^+$ , and cryptand C211 for  $\text{Li}^+$ .

CHAPTER IV (B)

COMPLEXATION OF THE  $K^+$  IONS BY CROWN ETHERS

## (B) COMPLEXATION OF THE K<sup>+</sup> IONS BY CROWN ETHERS

In this work, the complexation reactions of potassium hexafluorophosphate with crown ethers, such as 18-crown-6, dibenzo-18-crown-6, 15-crown-5, monobenzo-15-crown-5 and 12-crown-4 were investigated in various solvents by <sup>39</sup>K NMR and <sup>13</sup>C NMR.

### RESULTS AND DISCUSSION

The chemical shifts of <sup>39</sup>K as function of mole ratio of ligand/K<sup>+</sup> were measured and the data in various cases are presented in Table 19. In the <sup>39</sup>K NMR complexation study, the concentration of KPF<sub>6</sub> was held constant (0.04 M) and the ligand concentration varied.

In the 18-crown-6 case, the plots of the <sup>39</sup>K chemical shift vs mole ratio of 18C6/K<sup>+</sup> in acetone, dimethylformamide, water and dimethylsulfoxide are illustrated in Figure 29. In the case of acetone, the chemical shift reaches the limiting value after mole ratio 1.0, which is indicative of the formation of very strong K<sup>+</sup>-18C6 complex. It is not surprising, since the diameter of potassium ion is 2.7Å, which is very close to the cavity size of 18-crown-6 (2.6Å) (72). The potassium ion would be expected to form a stable complex with 18-crown-6. However, in the solvents of high donicity and dielectric constant, such as dimethylsulfoxide, water and dimethylformamide, as can be seen from Figure 29, the curves level off at higher mole ratio (> 3.0),

Table 19. Mole Ratio Studies of Crown Ethers Complexes with  $\text{KPF}_6$  in Various Solvents

Solvent	$18\text{C6}/\text{K}^+$	$\Delta\text{ppm}$	Solvent	$18\text{C6}/\text{K}^+$	$\Delta\text{ppm}$	Solvent	$18\text{C6}/\text{K}^+$	$\Delta\text{ppm}$
AC	0	12.6	$\text{H}_2\text{O}^*$	0	-0.5	DMF	0	5.9
	0.5	7.9		0.5	+0.5		0.5	5.2
	1.0	4.5		1.0	+0.8		1.0	4.7
	1.5	4.5		1.5	+0.9		1.5	4.4
	2.0	4.5		2.0	+1.3		2.0	3.8
	3.0	4.5		2.5	1.6		2.5	3.8
DMSO	0	-6.7		3.0	1.6		3.0	3.8
	0.5	-3.1						
	1.0	-1.8						
	2.0	-0.2						
	2.5	+0.8						
	3.0	+0.6						

\* KI was used

Table 19. Continued

DBC 18C6 Solvent	ACN		Py		AC	
	DBC/K <sup>+</sup>	$\Delta$ ppm	DBC/K <sup>+</sup>	$\Delta$ ppm	DBC/K <sup>+</sup>	$\Delta$ ppm
	0	2.24	0	0.8	0	12.6
	0.25	-1.1	0.25	-0.4	0.25	8.6
	0.5	-3.6	0.5	-3.8	0.5	4.5
	0.75	-5.0	1.0	-8.6	0.75	-0.5
	1.0	-7.1	1.5	-9.7	1.0	-4.2
	1.5	-8.2	2.0	-10.9	1.25	-5.9
	2.0	-8.2	2.5	-12.0	1.5	ppt
			3.0	-12.0		
MB 15C5 Solvent	NM		ACN			
	MB 15C5/K <sup>+</sup>	$\Delta$ ppm	MB15C5/K <sup>+</sup>	$\Delta$ ppm		
	0	23.8	0	1.9		
	0.25	20.3	0.5	3.9		
	0.5	18.1	0.75	4.9		
	0.75	16.8	1.0	5.7		
	1.0	14.5	1.5	7.2		
	1.25	12.2	1.75	8.1		
	1.5	11.6	2.0	8.6		
	2.0	10.9	2.5	9.2		
	2.5	9.8	3.0	9.5		
	3.0	9.8	4.0	9.5		
	4.0	9.8				

Table 19. Continued

Solvent	DMSO		NM		PY		AC	
	$^{15}\text{C5/K}^+$	$\Delta\text{ppm}$	$^{15}\text{C5/K}^+$	$\Delta\text{ppm}$	$^{15}\text{C5/K}^+$	$\Delta\text{ppm}$	$^{15}\text{C5/K}^+$	$\Delta\text{ppm}$
	0	-7.7	0	22.2	0	0.4	0	12.0
	0.25	-6.3	0.5	16.7	0.5	2.2	0.25	11.7
	0.5	-5.3	0.75	14.6	0.8	3.4	0.5	10.9
	0.75	-4.3	1.0	12.9	1.0	3.9	1.0	10.3
	1.0	-3.0	1.5	12.3	1.25	4.8	1.5	10.9
	1.25	-1.9	2.0	12.0	1.5	7.4	2.0	11.7
	1.5	-1.1	3.0	11.7	2.0	10.3	3.0	11.7
	1.75	-0.2	4.0	11.7	2.5	11.2	4.0	11.4
	2.0	+0.9			3.0	11.8		
	2.5	+2.7			4.0	12.4		
	3.0	+5.0						
	3.5	+6.2						
	4.0	+6.9						
	5.25	+7.5						

Table 19. Continued

Solvent	DMF		PC		MeOH*		ACN	
	$^{15}\text{C5/K}^+$	$\Delta$ ppm						
	0	6.1	0	12.8	0	8.9	0	1.9
	0.25	6.4	0.25	11.6	0.5	8.1	0.25	2.4
	0.5	6.7	0.5	10.8	0.75	7.6	0.5	3.0
	0.75	6.7	0.75	9.3	1.0	6.9	0.65	3.3
	1.0	7.0	1.0	8.2	1.25	8.4	0.8	3.9
	1.25	7.6	1.5	9.0	1.5	9.3	1.0	4.5
	1.5	8.2	2.0	10.1	2.0	9.9	1.25	5.3
	1.75	8.8	2.5	10.8	2.5	11.3	1.5	6.2
	2.0	9.1	3.0	11.1	3.0	11.6	1.75	7.9
	2.5	9.9	4.0	11.1	3.5	11.9	2.00	9.7
	3.0	10.2			4.0	11.9	2.50	11.2
	4.0	11.1					3.00	11.4
	5.0	11.1					3.50	12.0
							4.0	12.0

\* KI was used

Table 19. Continued

Solvent	$^{12}\text{C}_4/\text{K}^+$	$\Delta\text{ppm}$	Solvent	$^{12}\text{C}_4/\text{K}^+$	$\Delta\text{ppm}$	Solvent	$^{12}\text{C}_4/\text{K}^+$	$\Delta\text{ppm}$
AC	0	13.2	$\text{H}_2\text{O}^*$	0	-0.4	MeOH	0	11.6
	0.5	12.0		0.25	-0.4		0.25	11.3
	1.0	10.9		0.5	-0.4		0.5	11.3
	1.5	10.3		0.75	-0.4		0.75	10.8
	2.0	8.5		1.0	-0.4		1.0	10.5
	2.5	8.5		1.5	-0.7		1.5	9.9
	3.0	8.5		2.0	-0.7		2.0	9.6
ACN	0	1.9		2.5	-0.7		2.5	9.3
	0.25	2.4		3.0	-0.7		3.0	8.9
	0.5	2.8		3.5	-0.7		3.5	8.7
	0.75	4.2		4.0	-0.7		4.0	8.4
	1.0	4.5	NM	0	23.8		5.0	8.4
	1.5	5.1		0.25	22.0	DMSO	0	-8.5
	2.0	5.2		0.5	20.3		0.5	-7.4
	2.5	5.3		0.75	18.6		1.0	-7.1
				1.0	16.8		1.5	-6.4
				1.5	13.3		2.0	-5.5
				1.75	12.1		3.0	-3.3
				2.0	10.9		4.0	-1.7
				2.5	9.8		5.0	-0.9
				3.0	8.7			
				4.0	8.7			

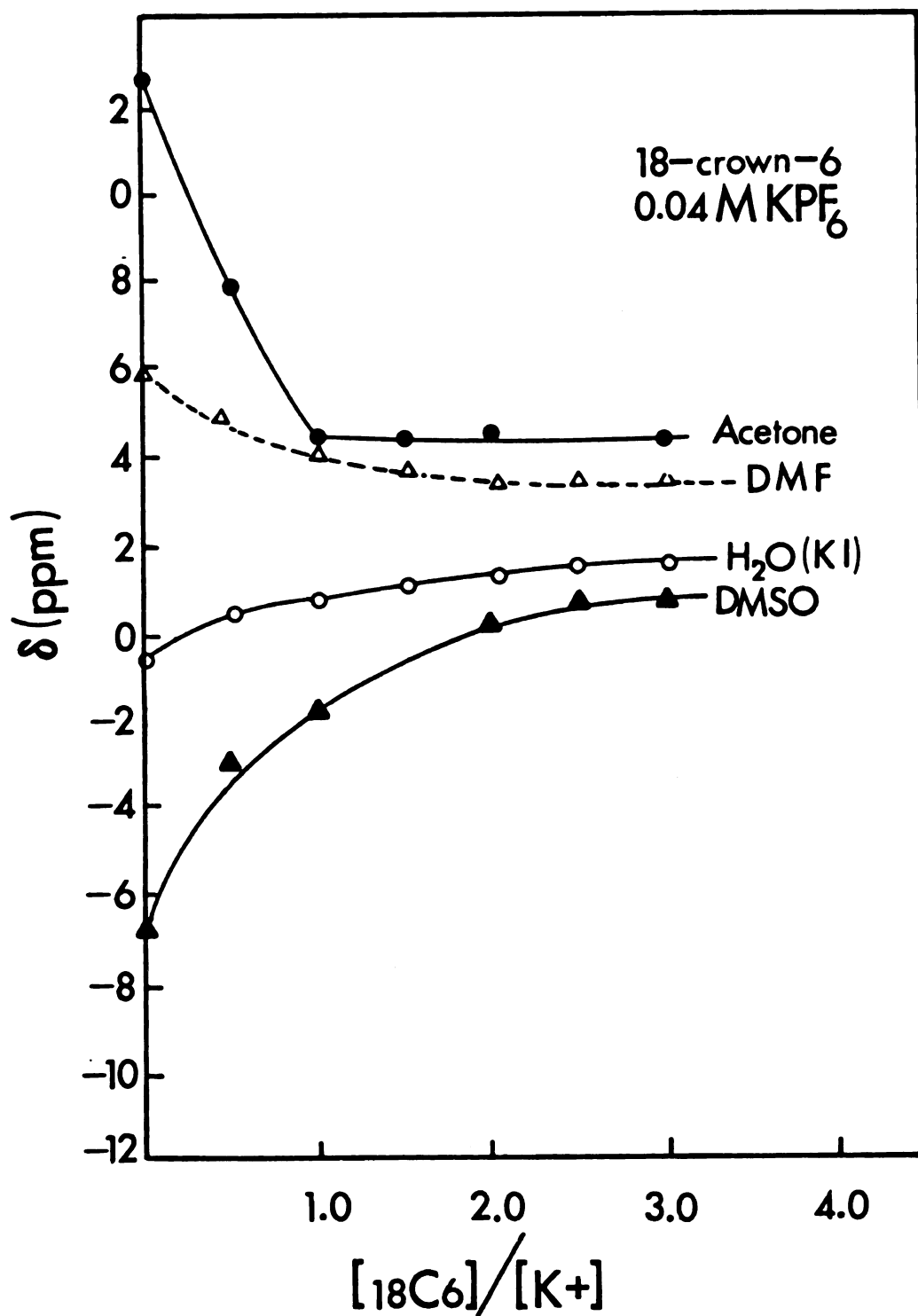


Figure 29. <sup>39</sup>K Chemical Shift vs Mole Ratio of 18C6/K<sup>+</sup> in Various Solvents

which is indicative of the formation of weaker complexes than that in acetone.

The formation constants of complexes in these solvents were calculated by use of the KINFIT program (101). The computer subroutine equations are described in Appendix IV. The formation constants of  $K^+$ -18C6 complexes in various solvents are presented in Table 20. The formation constants among these solvents are in the order; acetone > dimethylformamide > dimethylsulfoxide > water, which follows the inverse order of donicity of these solvents. These results are not surprising, since, as mentioned in Chapter III, the  $K^+$ -solvent interaction is a function of the donicity of the solvent. A strong  $K^+$ -solvent interaction would be expected in a solvent of high donicity and consequently a strong  $K^+$ -solvent interaction will prevent the interaction between  $K^+$  ions and 18-crown-6. The logarithm formation constant of  $K^+$ -18-crown-6 in  $H_2O$  obtained in this work is in good agreement with the value 2.06 reported from a calorimetric titration study (73).

As can be seen from Figure 30, the chemical shift of the 18-crown-6- $K^+$  complex is concentration independent, which is indicative of an absence of ion pairing between 18-crown-6- $K^+$  and the  $PF_6^-$  anion. The salt solution however, shows some  $K^+$   $PF_6^-$  ion pair formation.

The complexation reactions of the potassium ion with dibenzo-18-crown-6 (DB18C6) were also studied by

Table 20. Formation Constants and Limiting Chemical Shift for the Complexation of  $\text{KPF}_6$  by 18-crown-6 in Various Solvents

Solvent	Log Kf	$\delta_{\text{lim.}}$ (ppm)
Acetone	> 4	4.46
Dimethylformamide	$2.70 \pm 0.04$	3.85
Dimethylsulfoxide	$2.19 \pm 0.23$	1.43
Water*	$2.17 \pm 0.13$	1.56

\* KI was used instead of  $\text{KPF}_6$

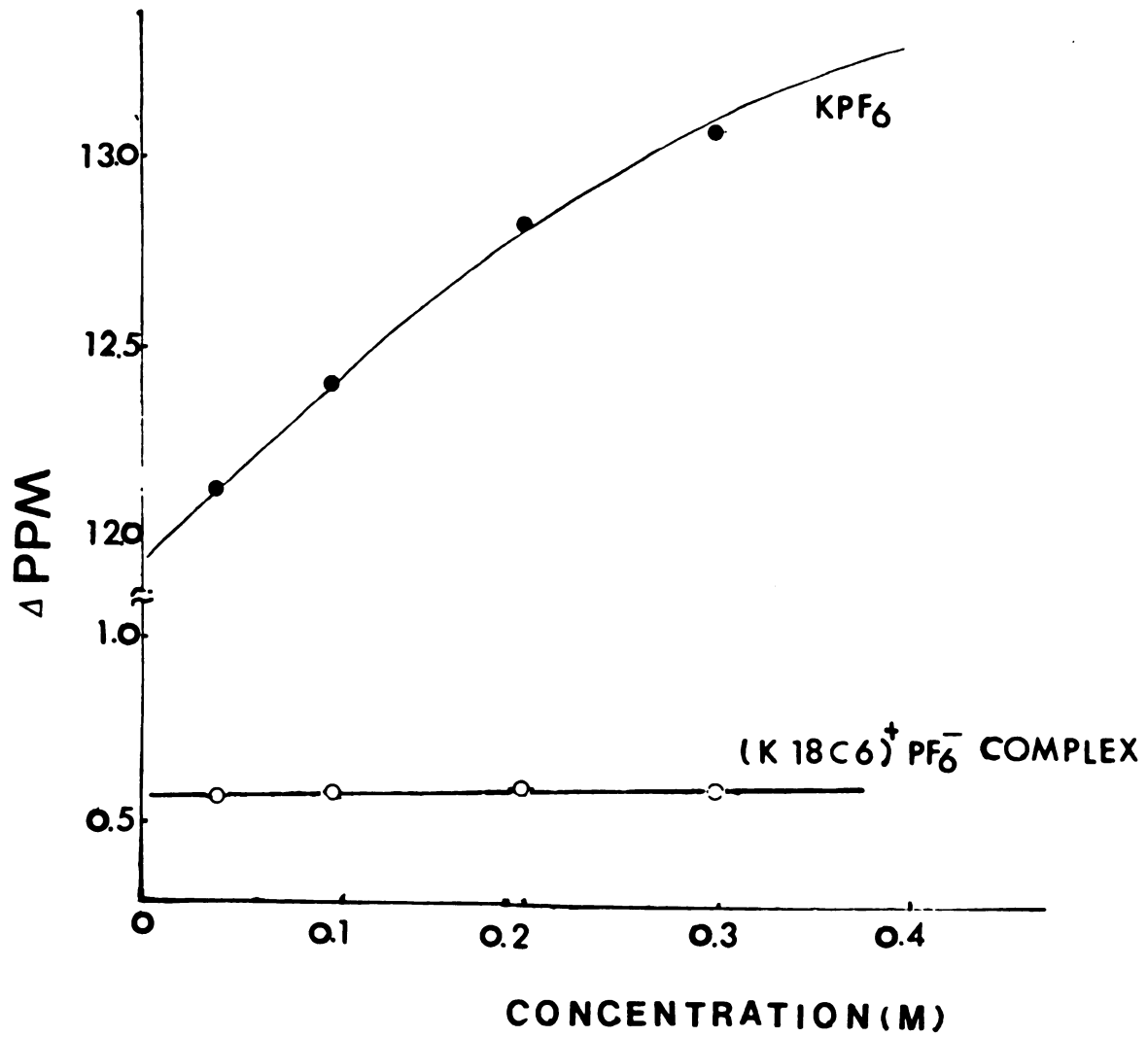


Figure 30. Chemical Shifts of 18 C 6  $K^+$  Complexes as Function of Concentration

$^{39}\text{K}$  NMR. Unfortunately, this study is limited by the low solubilities of dibenzo-18-crown-6 in most nonaqueous solvents. In this study, the  $\text{K}^+$  concentration was held constant at 0.02 M, instead of 0.04 M, which was used in the previous study.

The results are presented in Figure 31. As can be seen in the case of acetonitrile and pyridine, the curves level off at a mole ratio of ligand/ $\text{K}^+$   $\sim 1.5$  and 2.5 respectively, which indicates that the complex of dibenzo-18-crown-6- $\text{K}^+$  in acetonitrile is stronger than that in pyridine. This may be due to the much higher donicity of pyridine which weakens the ion-ligand interaction. Unfortunately, in the case of acetone, the low solubility of dibenzo-18-crown-6 limited the study after mole ratio 1.25, however, obviously, the curve for acetone solutions does not level off at mole ratio of 1.0 which indicates that the  $\text{K}^+$ -DB18C6 complex is weaker than  $\text{K}^+$ -18C6 complex which the curve levels off exactly mole ratio of 1.0 (see Figure 29 at page 119 ). The formation constants of  $\text{K}^+$ DB18C6 complexes in these solvents are presented in Table 21.

The value of the formation constant of  $\text{K}^+$ -dibenzo 18 C 6 complex in acetone must be suspect since not enough data were obtained after mole ratio of 1.0.

The complexation of the potassium ion with 15-crown-5 has been investigated the same technique. Since the

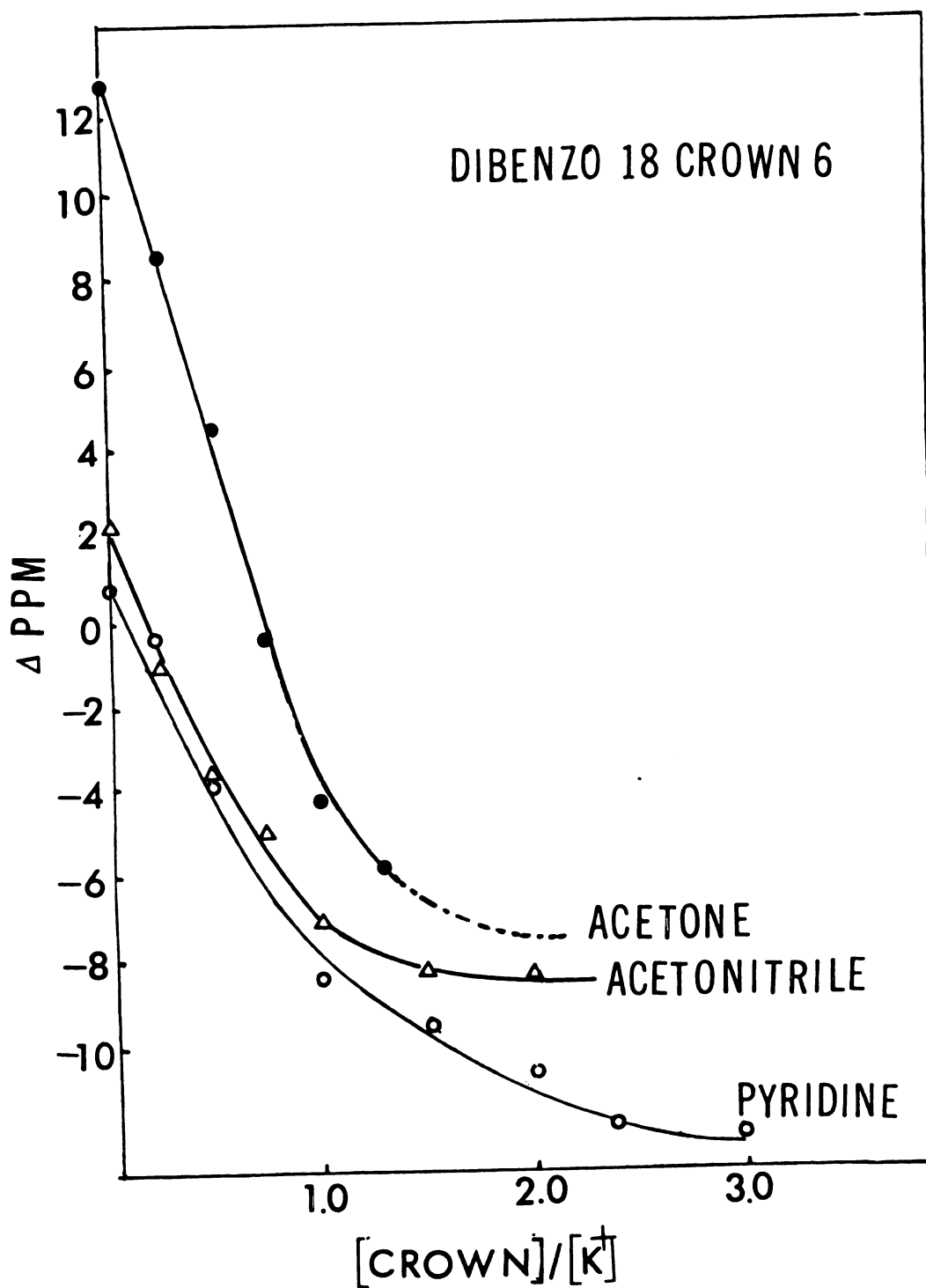


Figure 31.  $^{39}K$  Chemical Shifts vs Mole Ratio of Dibenzo 18C6/ $K^+$  in Various Solvents

Table 21. Formation Constants of Complexes of  $KPF_6$   
with Dibenzo-18-crown-6 in Various Solvents

Solvent	Log $K_1$	$\delta_1$ (ppm)
Acetonitrile	>4	-7.32
Pyridine	$3.42 \pm 0.11$	-13.65
Acetone	>3	-8.26

diameter of potassium ion and the cavity size of 15-crown-5 are  $2.6\overset{\circ}{\text{A}}$  and  $1.7\overset{\circ}{\text{A}}$  (72) respectively, the potassium ion is too large to fit into the cavity of the ligand. The variation of the chemical shifts as a function of the mole ratio of 15-crown-5/ $\text{K}^+$  is presented in Figure 32. In acetone and methanol solutions, the chemical shift goes down field until mole ratio of 1.0. Further addition of the ligand reverses the direction of the shift. It is reasonable to assume that the results indicate that formation of a stable 1:1 ( $15\text{C5}/\text{K}^+$ ) complex followed by the addition of a second 15-crown-5 molecule to form a 2:1 ( $15\text{C5}/\text{K}^+$ ) sandwich complex (81).

The formation of 2:1 ( $15\text{C5}/\text{K}^+$ ) sandwich complex at the  $15\text{C5}/\text{K}^+$  mole ratio 1.0 in acetone was also suggested by a carbon-13 NMR study. Since 15-crown-5 is a symmetric ligand, it shows only one  $^{13}\text{C}$  NMR signal. However, as Figure 33 shows, at mole ratio of 0.75 of  $\text{K}^+$ /ligand, two carbon-13 NMR signals were observed, which correspond to the 1:1 and 2:1 complexes respectively. The solid  $(15\text{-crown-5})_2\text{KPF}_6$  complex was precipitated from methanol solution of 0.1 M  $\text{KPF}_6$  and an excess of 15-crown-5 ( $> 0.2$  M). The elemental analysis data are shown in Table 22. The solid decomposed at  $255^\circ\text{C}$ .

As Figure 32 shows, there seems to be a weak break in the curve at mole ratio 1.0 in nitromethane and acetonitrile solutions, which is also indicative of a

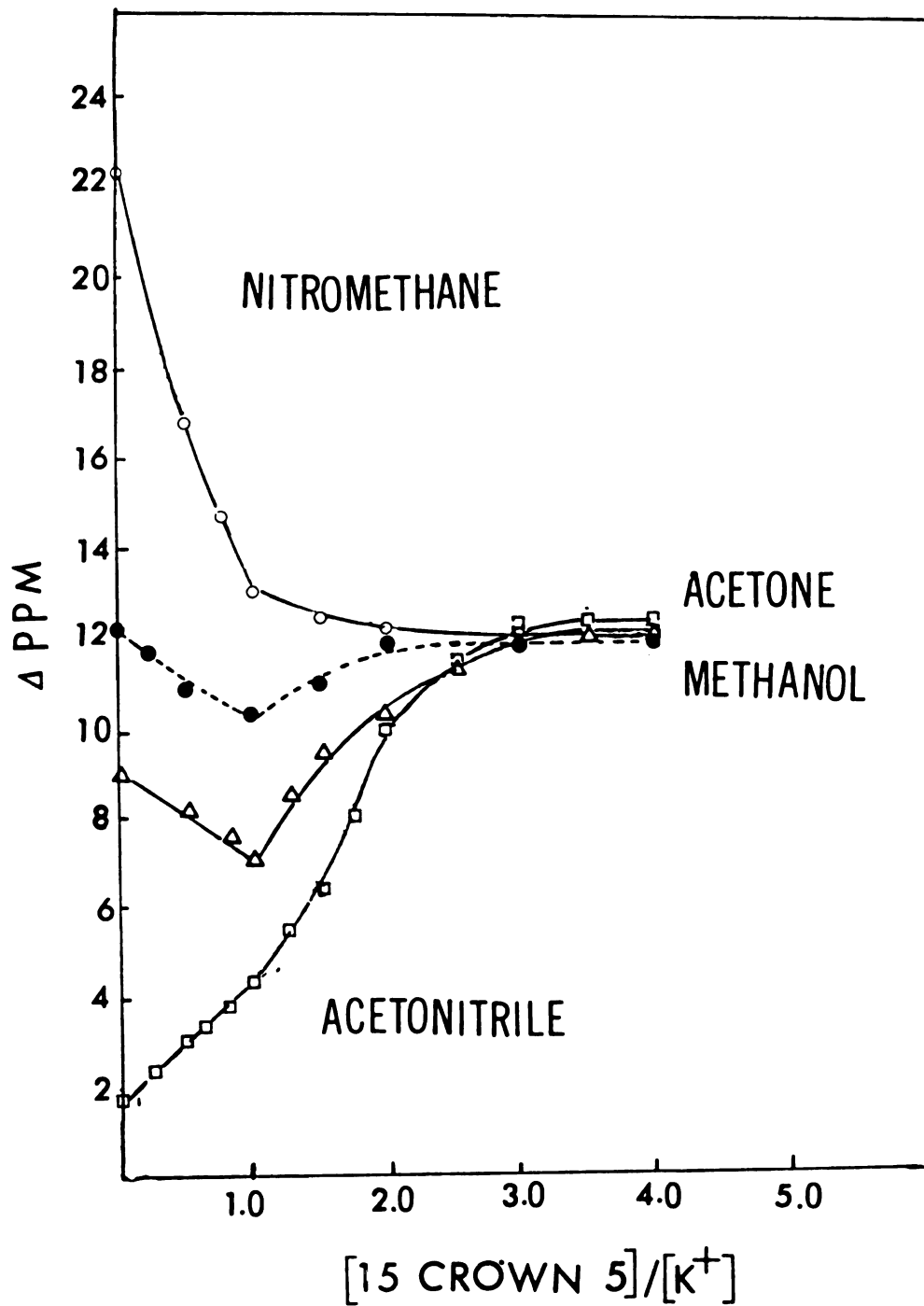


Figure 32. <sup>39</sup>K Chemical Shift vs Mole Ratio of 15C5/ $K^+$  in Nitromethane, Acetone, Methanol and Acetonitrile.

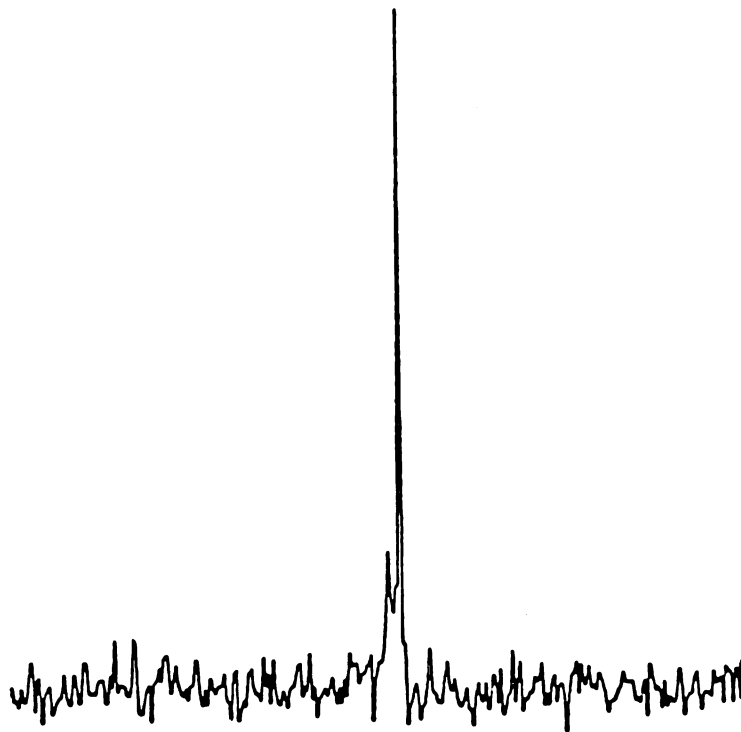


Figure 33.  $^{13}\text{C}$  Spectrum of 15-Crown-5 at Mole Ratio  
0.75 of  $\text{K}^+$ /15C5 in Acetone

Table 22. The elemental analysis for (15-crown-5)<sub>2</sub> KPF<sub>6</sub> sandwich complex

	C%	H%	P%
Observation:	38.48	6.36	4.97
Calculation:	38.46	6.41	4.96

probable formation of 2:1 complexes. Also, it is interesting to note that in all of these solvents, the limiting chemical shifts of the curves seem to approach the same value, which is another evidence for the 2:1 sandwich complex in these solvents. It is reasonable to assume that in all the nonaqueous solvents used including nitromethane and acetonitrile, the 2:1 sandwich (15-crown-5)<sub>2</sub>K<sup>+</sup> complex can be formed with excess ligand, whereas in water only the 1:1 complex has been reported (73).

The complexation reaction of K<sup>+</sup> with 15-crown-5 in pyridine, propylene carbonate, dimethylformamide and dimethylsulfoxide were also investigated, and the results are illustrated in Figure 34. In propylene carbonate another V shaped curve is obtained. In pyridine, dimethylformamide and dimethylsulfoxide solutions. There are also very weak breaks at mole ratio of 1.0. These results seem to indicate the formation of 1:1 and 2:1 complexes in these solvents. The formation constants for 1:1 and 2:1 complexes can be obtained by fitting these chemical shift data by using KINFIT computer program. One typical fitting is shown in Figure 35. The computer subroutine equations are described in Appendix V. The formation constants for 1:1 and 2:1 complexes in various solvents are shown in Table 23. As can be seen, the formation constants of 2:1 complexes seem to decrease in the order; nitromethane > acetone > propylene carbonate > pyridine >

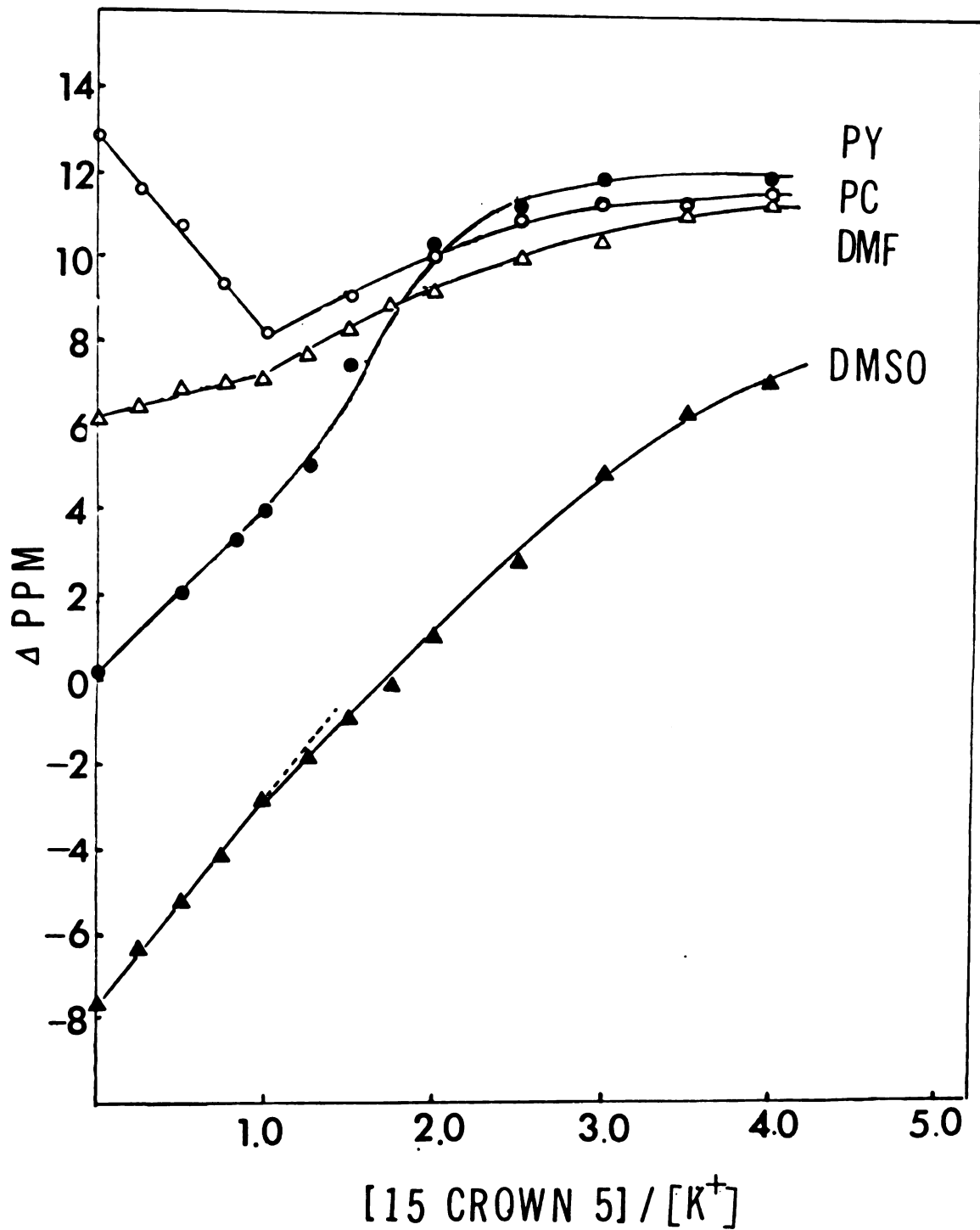


Figure 34.  $^{39}\text{K}$  Chemical Shift vs Mole Ratio of 15C5/ $\text{K}^+$  in Pyridine, Propylene Carbonate, Dimethylformamide and Dimethylsulfoxide.

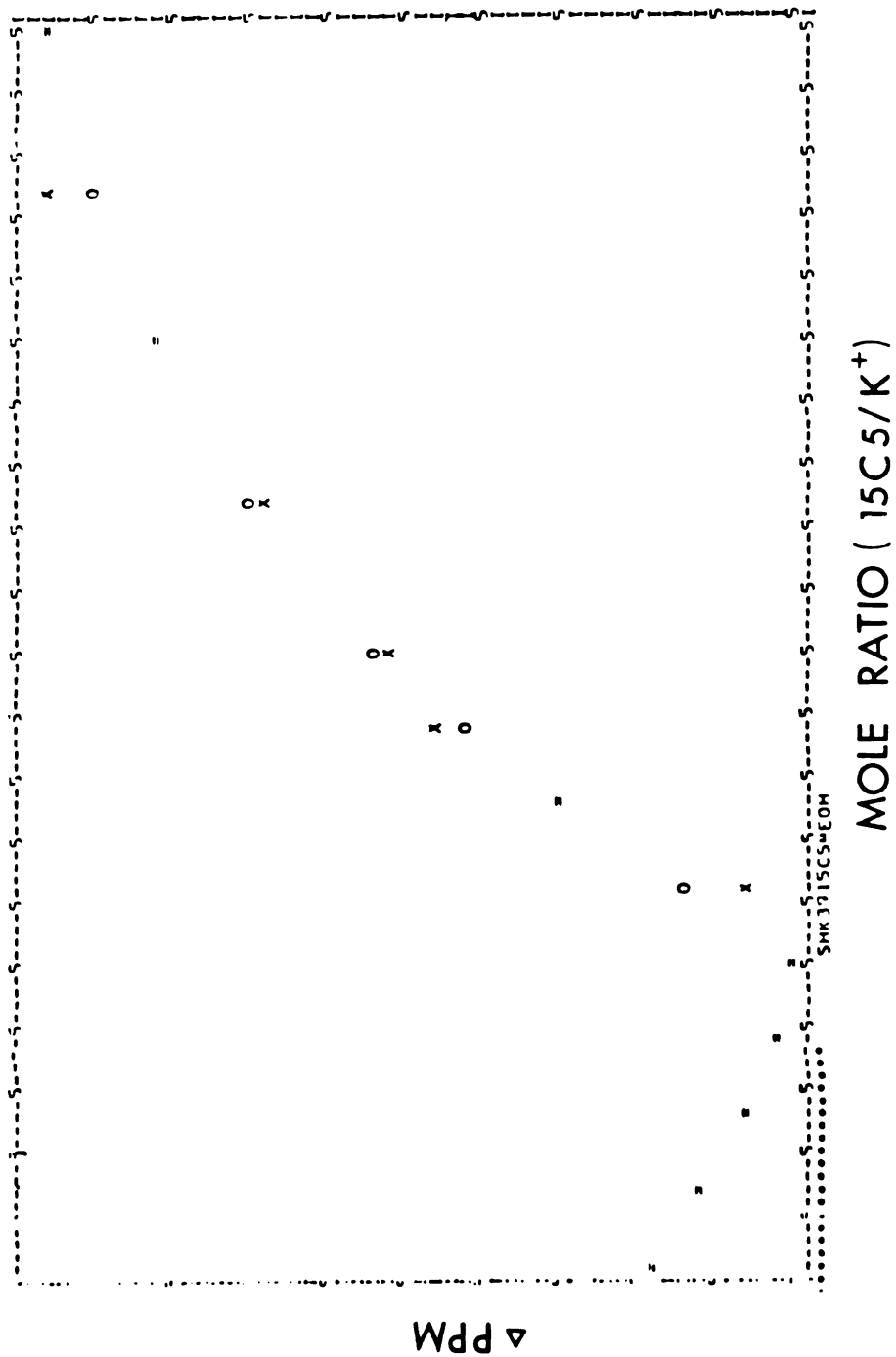


Figure 35. Computer Fitting for the Chemical Shifts vs Mole Ratio of 15C5/K<sup>+</sup> in Methanol.

Table 23. Formation Constants and Limiting Chemical Shifts for 1:1 and 2:1  
15-crown-5-K<sup>+</sup> Complexes in Various Solvents

Solvent	Log K <sub>1</sub> (a)	Log K <sub>2</sub>	$\delta_1$ (ppm)	$\delta_2$ (ppm)
Nitromethane	> 4	4.17 ± 0.06	16.89	11.79
Acetone	> 5	3.12 ± 0.16	9.95	11.58
Propylene Carbonate	> 4	2.38 ± 0.19	6.95	12.48
Pyridine	> 5	2.15 ± 0.06	1.95	12.69
Acetonitrile	> 5	2.04 ± 0.11	4.15	12.95
Methanol	> 4	2.03 ± 0.13	6.95	12.48
Dimethylformamide	4.11 ± 0.09	1.57 ± 0.13	6.99	12.05
Dimethylsulfoxide	2.91 ± 0.10	1.33 ± 0.03	-3.01	11.74

(a) K<sub>1</sub> and K<sub>2</sub> are the formation constants for 1:1 and 2:1 complexes respectively  
 $\delta_1$  and  $\delta_2$  are the limiting chemical shift for 1:1 and 2:1 complexes respectively

acetonitrile > methanol > dimethylformamide > dimethylsulfoxide. The order observed is the inverse order of donicity for these solvents except for pyridine, but does not correlate with the dielectric constants of these solvents. For example, although propylene carbonate (PC) has the highest dielectric constant of all the solvents used, the formation constant of the complex in PC is larger than that in most solvents. Therefore the donicity of the solvent seems to be a very important parameter in the complexation reaction.

Pyridine has the very low dielectric constant of 12.0 which may have some effect on the complexation, however, it is also a "soft" base and despite its high donicity, it may not solvate strongly the alkali ions which are "hard" acid.

It is seen in Table 23 that the chemical shifts for the 1:1 complexes ( $\delta_1$ ) seem to be solvent dependent. This is reasonable, since, in the 1:1 complex, the solvent molecules have a ready access to the cation. However, for the sandwich complexes, the cation should be insulated from the solvent, the chemical shifts are largely solvent independent.

It is surprising that the formation constants for 1:1 complexes in various solvents are always very large. Even in solvents of high donicity such as dimethylformamide and dimethylsulfoxide, the values of  $\log K_1$  are

4.11 and 2.91 respectively. The results were checked by carbon-13 NMR. The results are illustrated in Figure 36. As can be seen in the acetone case, the C-13 chemical shifts reach a limiting value after mole ratio 1.0 of  $K^+/^{15}C_5$ , which indicates the formation of a very strong complex. Even in dimethylsulfoxide, in which the chemical shifts reach a limiting value after mole ratio 2.0, the formation constant ( $\log K$ ) for the 1:1 complex obtained by fitting the curve is 2.78. The results are in good agreement with the K-39 NMR result.

The influence of the anion on the formation of the sandwich complexes was investigated in these solvents. The results shown in Table 24 clearly show that as expected, the nature of the anion has no influence on the  $^{39}K$  limiting chemical shift and therefore, there is no evidence for the complexed cation-anion interaction. Even for the 1:1 complex the data in Figure 37 shows only a very small degree of ion pairing between  $(^{15}C_5K)^+$  and  $PF_6^-$ , there is only a very small change in  $^{39}K$  chemical shift with complex concentration.

The complexation study of the potassium ion with monobenzo-15-crown-5 in various solvents was also performed by potassium-39 NMR. Since the attachment of the benzo group on crown ethers has been reported to diminish the basicity of the oxygens and to reduce the cavity size of the ligand (55), weaker complexes of potassium with

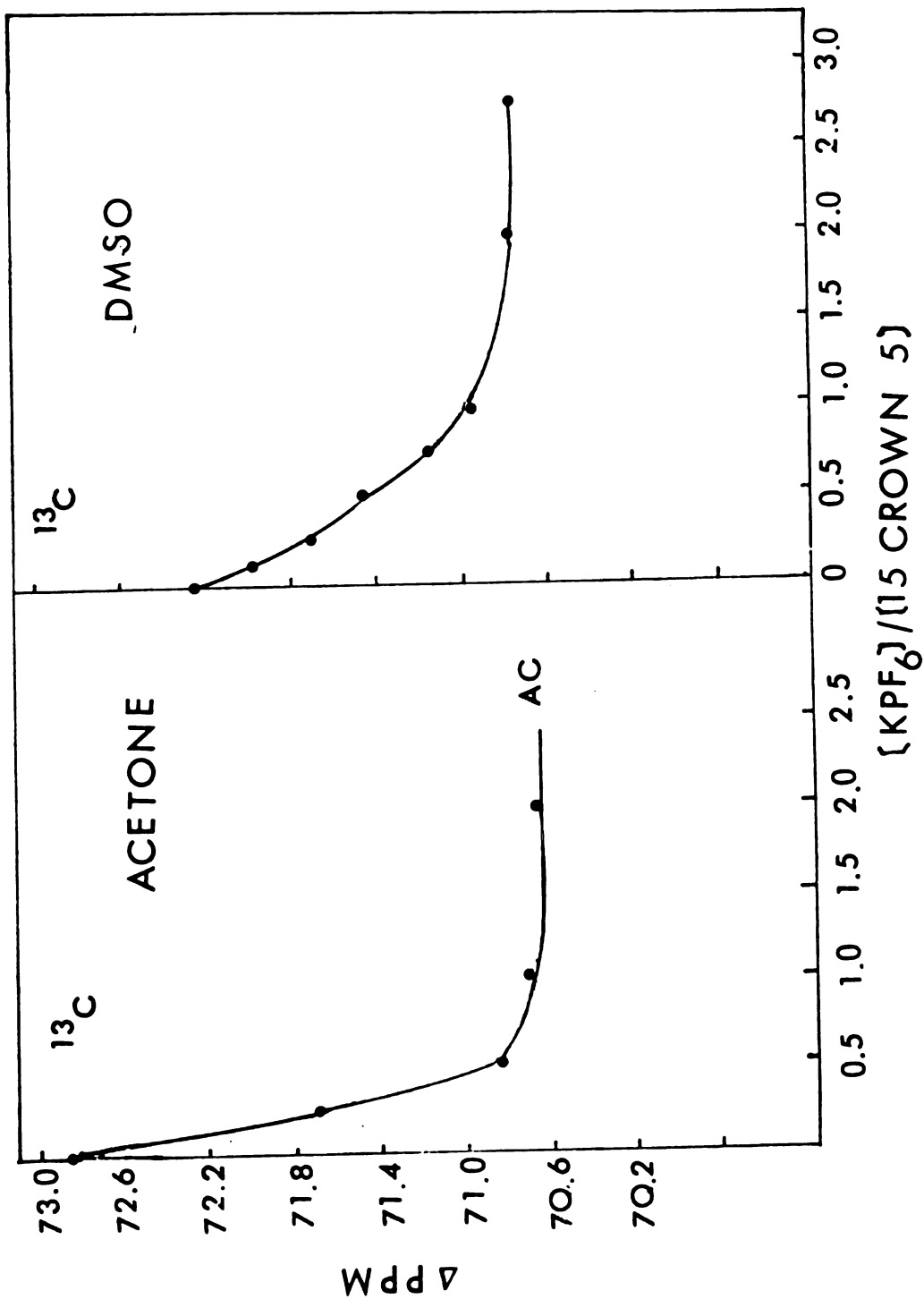


Figure 36. Carbon- $^{13}$  Chemical Shift vs Mole Ratio of  $\text{K}^+$ / $^{15}\text{C}_5$  in Various Solvents.

Table 24. The Limiting Chemical Shifts of  $^{39}\text{K}$  NMR for the Complexes of Potassium Salts with 15-crown-5 in Various Solvents

Solvent	Salts	Chemical Shift (ppm)	Line Width (a) (Hz)
Acetonitrile	KPF <sub>6</sub>	12.6 ± 0.2	34.2
	KSCN	12.6 ± 0.2	39.1
Dimethylformamide	KPF <sub>6</sub>	12.0 ± 0.2	54.7
	KSCN	12.0 ± 0.2	63.5
Methanol	KI	12.0 ± 0.2	68.4
	KSCN	12.5 ± 0.2	34.2
	KI	12.5 ± 0.2	38.8

(a) The line widths of  $^{39}\text{K}$  signals at 15C5/K<sup>+</sup> mole ratio 5.0

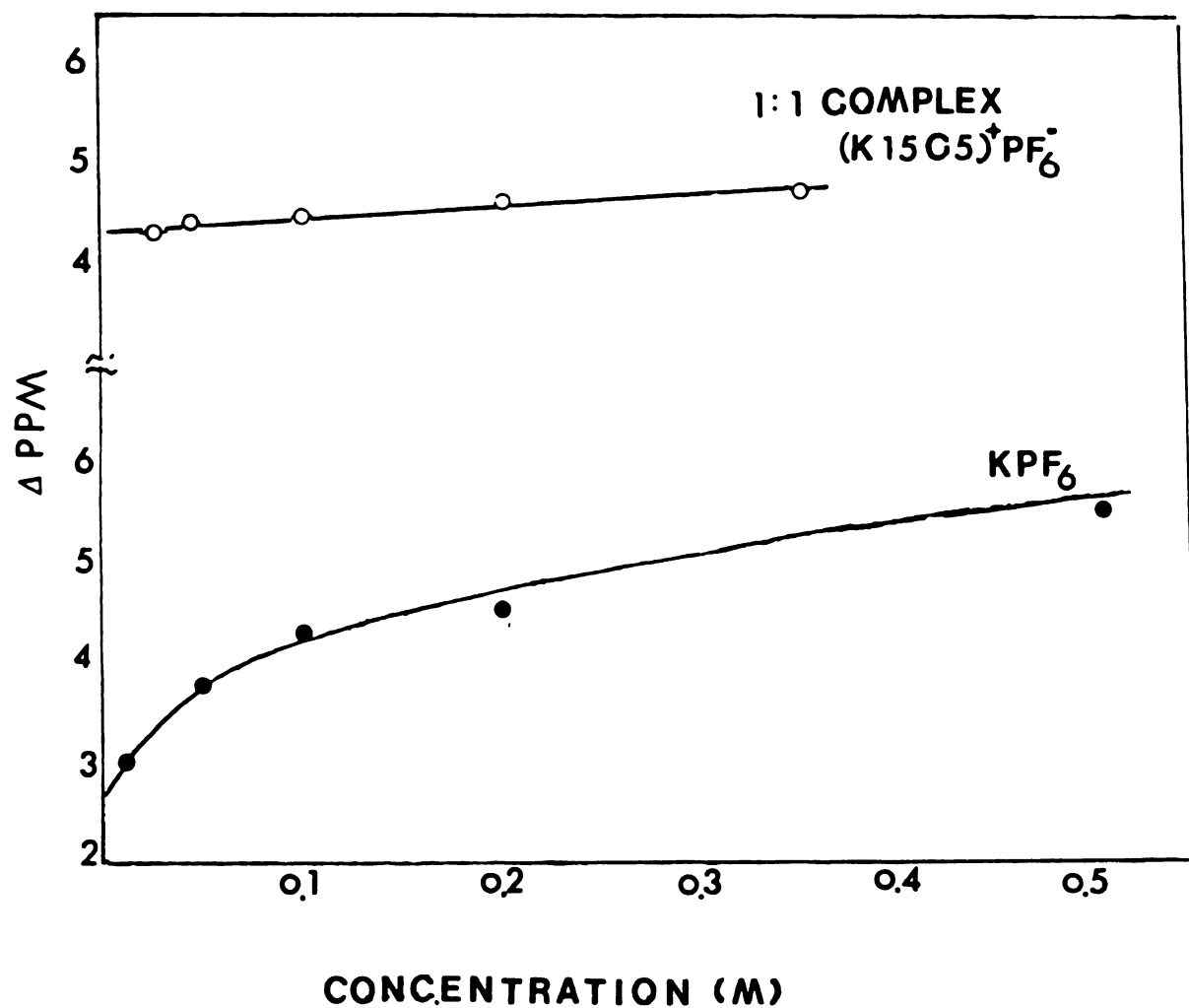


Figure 37.  $^{39}K$  Chemical Shift Variation with the Concentration of 1:1 (15C5)  $KPF_6$  Complex and Potassium Salt in Acetonitrile.

monobenzo -15-crown-5 than with 15-crown-5 would be expected.

As can be seen from Figure 38, in nitromethane and acetonitrile, the limiting chemical shifts seem to reach the same value, which is probably due to the formation of 2:1 sandwich complexes. The formation of both 1:1 and 2:1 complexes of monobenzo-15-crown-5 with  $K^+$  in the methanol-water mixture has been reported by Izatt (105). A solid MB 15 C 5  $KPF_6$  complex was obtained by precipitating it in methanol solution. The melting point was 248 ~250°C and the elemental analysis is given below (Table 25).

Table 25. Elemental Analysis of  $(\text{monobenzo } 15 \text{ C } 5)_2 KPF_6$

	C%	H%	P%
Observation:	46.62	5.54	4.41
Calculation:	46.67	5.55	4.31

The formation constants for both 1:1 and 2:1 complexes obtained are presented in Table 26. In the acetonitrile case, the formation constant of 1:1  $K^+$ -monobenzo 15 C 5 complex is smaller than that of 1:1  $K^+$ -15 C 5 complex. The 2:1 complex, however, shows a formation constant ( $\log K_2$ ) for the MB 15C5- $K^+$  complex which is larger than

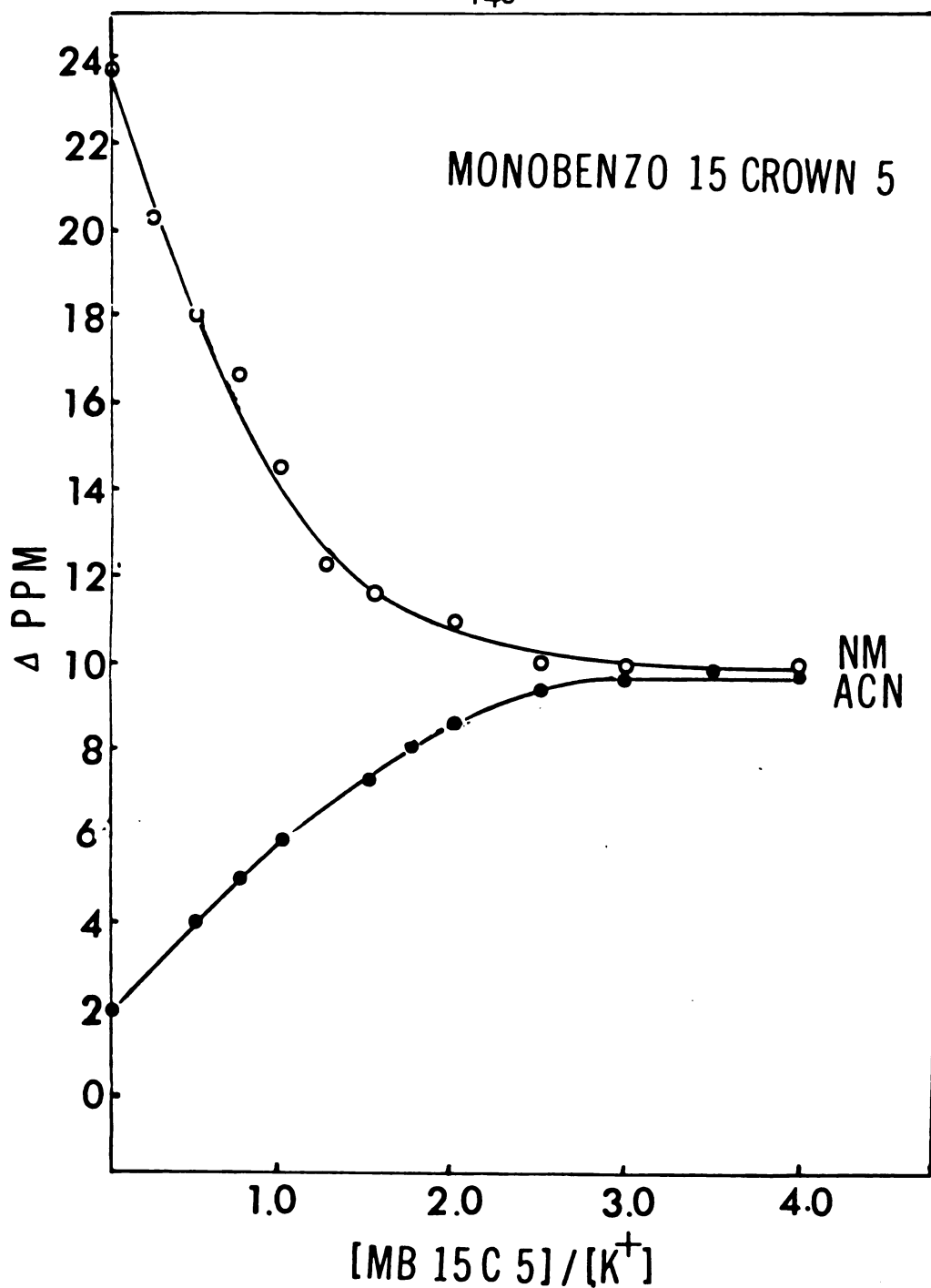


Figure 38.  $^{39}K$  Chemical Shifts vs Mole Ratio of MB 15C5/ $K^+$  in Nitromethane and Acetonitrile.

Table 26. Formation Constants of Complexes of  $\text{KPF}_6$  with Monobenzo-15-crown-5  
in Various Solution

Solvent	Ligand	Log $K_1$	Log $K_2$	$\delta^1$ ppm	$\delta^2$ ppm
Acetonitrile	MB 15 C 5	$2.72 \pm 0.24$	$2.73 \pm 0.17$	6.12	9.59
	15 C 5	> 5	$2.04 \pm 0.11$	4.15	12.95
Nitromethane	MB 15 C 5	> 4	> 4	16.69	9.47
	15 C 5	> 4	$4.17 \pm 0.06$	16.89	11.79

that observed in the 15-crown-5 case. In the nitromethane case, formation constants for 2:1 complexes in both 15-crown-5 and benzo-15-crown-5 cases are large. It is not unexpected since the nitromethane has low donicity of 2.7, it may solvate the  $K^+$  ions weakly.

The complexation of 12-crown-4 and potassium ion in various solvents was studied by K-39 and C-13 NMR, and the results of  $^{39}K$  NMR mole ratio studies are illustrated in Finger 39. As can be seen, in all cases there are no obvious inflection points or breaks in the curves. It is very difficult to say whether or not a 2:1 complex is formed. The cavity size of 12-crown-4 is  $\sim 1.2\overset{\circ}{\text{A}}$  (72) which is very small for the  $K^+$  ion ( $\sim 2.7\overset{\circ}{\text{A}}$ ). Thus it is possible to form both 1:1 and 2:1 ( $12C4/K^+$ ) complexes in these solutions. However, the 2:1 ( $12C4/K^+$ ) complex could not be isolated from  $KPF_6$  methanol solution in the same manner in which we obtained the 2:1 ( $15C5/K^+$ ) complex. Therefore, no evidence of the formation of the 2:1 complex was obtained.

In order to get more information about the behavior of the complexation in this system, the  $^{13}C$  NMR mole ratio study for this system was performed. The data are presented in Table 27. The plot of C-13 chemical shift of 12-crown-4 vs mole ratio of  $K^+/12\text{-crown-4}$  is shown in Figure 40. Since the 12-crown-4 is a symmetric ligand and because the exchange between free ligand and complexed ligand is fast, only one  $^{13}C$  NMR signal was observed at

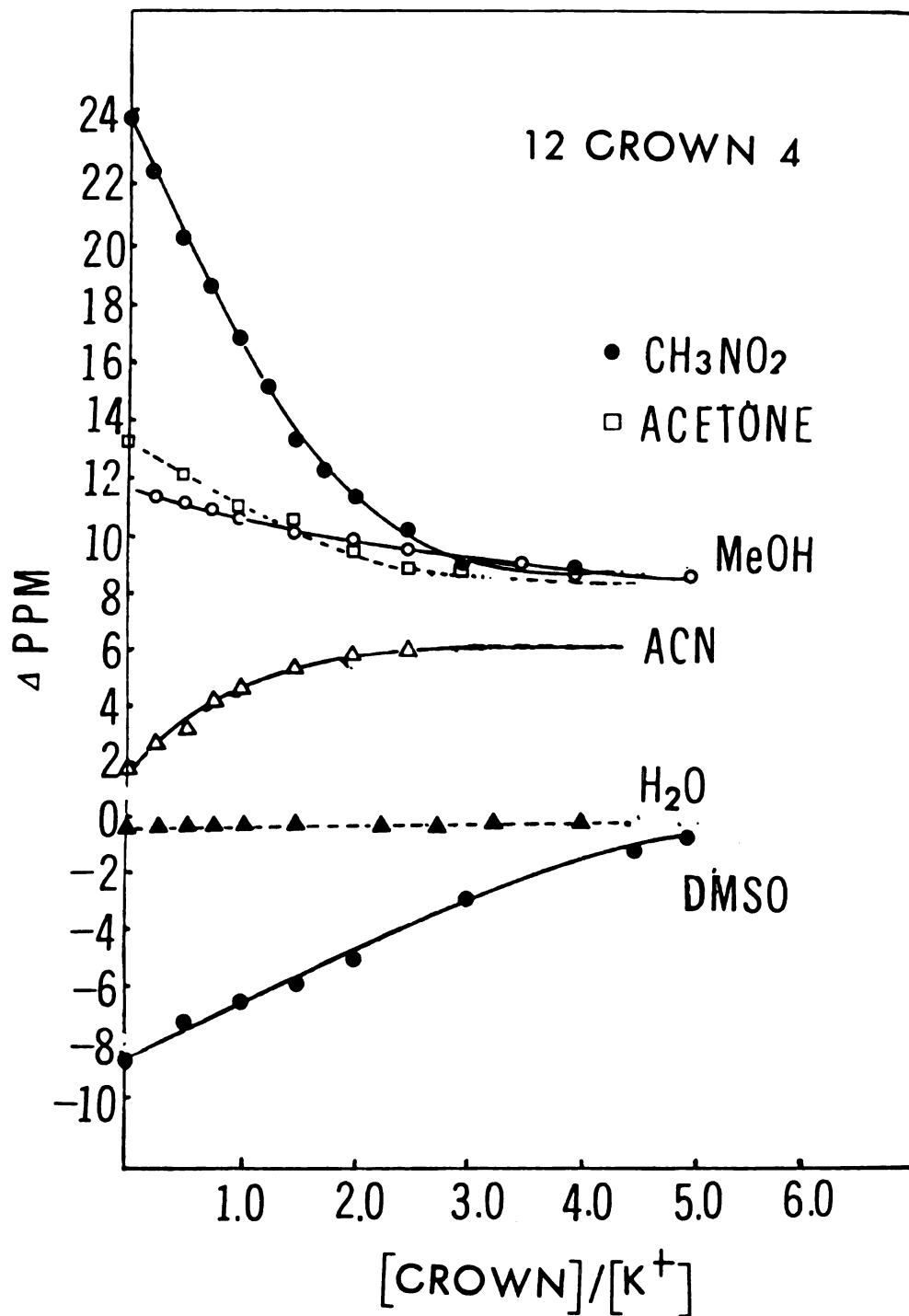


Figure 39. <sup>39</sup>K Chemical Shift vs Mole Ratio of 12-crown-4/K<sup>+</sup> in Various Solvents

Table 27. The C-13 NMR Chemical Shifts of M<sup>+</sup>-12-crown-4 Complexes in Various Solvents (M<sup>+</sup> = K<sup>+</sup>, Cs<sup>+</sup>)

Salt	Solvent	Mole Ratio (M <sup>+</sup> /L)	Δppm	Salt	Solvent	Mole Ratio (M <sup>+</sup> /L)	Δppm
KPF <sub>6</sub>	Acetonitrile	0	71.87	KPF <sub>6</sub>	DMSO	0	73.48
		0.25	70.86			0.5	72.23
		0.50	69.78			1.0	71.74
		0.63	69.38			2.0	70.69
		0.75	69.01			3.5	69.84
KPF <sub>6</sub>	Acetone	1.0	68.57	CsSCN	Methanol	0	71.57
		1.5	67.98			0.5	70.60
		2.0	67.83			1.0	69.88
		0	71.95			1.5	69.41
		0.5	69.79			2.0	69.07
		0.75	69.23	2.5	68.81		
		1.0	67.89				
		1.5	67.48				
		2.0	67.19				

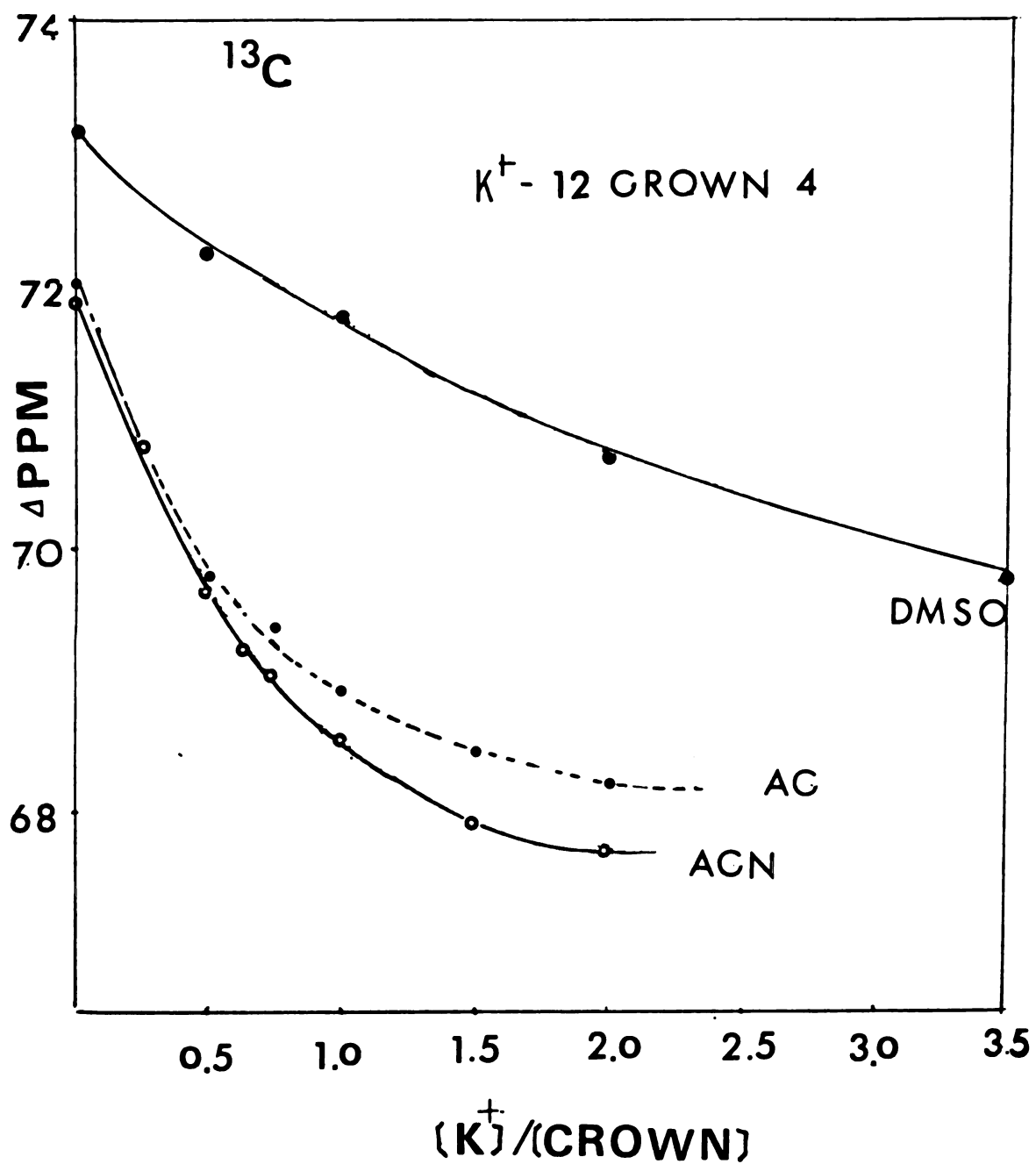


Figure 40. Carbon-13 Chemical Shift vs Mole Ratio of  $K^+/^{12}\text{C}_4$  in Various Solvents.

various mole ratios. Even in the solvents of low donicity, such as acetone and acetonitrile, the  $^{13}\text{C}$  resonance does not tend to reach the limiting value before the mole ratio 2.0, indicative of the formation of a weak 1:1 complex. In the dimethylsulfoxide solutions, the C-13 chemical shift continue to change even after mole ratio 3.0, which suggests that the 1:1 complex is quite weak in this solvent. It is seen that in all cases only evidence for the formation of very weak 1:1 complexes was observed. There is no indication of a 2:1 complex. If only the 1:1 complex is assumed to be present in various solvents, the formation constants of 1:1 complexes can be obtained by fitting the curves for both carbon-13 and potassium-39 NMR and are presented in Table 28. As can be seen, the formation constants of complexes from both C-13 and K-39 NMR studies are in good agreement with each other in acetonitrile, acetone and dimethylsulfoxide cases. The results do not definitely rule out the formation of a very weak 2:1 complex. As Table 28 shows the formation constants of 1:1 complex in methanol and dimethylfoxide are obviously smaller than in acetonitrile, acetone and nitromethane. In the methanol case, it is possible to envisage hydrogen bonding between the methanol molecule and the oxygen of ligand which would probably prevent or reduce the extent of complex formation. The very weak 1:1 complex in DMSO is not unexpected,

Table 28. Formation Constants for the 12-crown-4-K<sup>+</sup> Complexes in Various

Solvent	Method	Formation Constant (Log K)	Limiting Chemical Shift (ppm)
Acetonitrile	K-39 NMR	2.18 ± 0.16	5.67 ± 0.24
	C-13 NMR	2.26 ± 0.07	67.61 ± 0.04
Acetone	K-39	1.79 ± 0.18	7.82 ± 0.40
	C-13	1.87 ± 0.07	67.73 ± 0.23
Nitromethane	K-39	1.67 ± 0.11	5.95 ± 0.77
	K-39	1.05 ± 0.07	6.61 ± 0.36
Dimethylsulfoxide	K-39	0.31 ± 0.04	20.00 ± 0.50
	C-13	0.67 ± 0.14	66.78 ± 1.12

since DMSO has high donicity and can solvate  $K^+$  easily.

It is of interest to study the  $Cs^+$  ion complexation with 12-crown-4, since both  $K^+$  and  $Cs^+$  ions are too large for 12-crown-4 which has about same size as the  $Li^+$  ion. The  $^{13}C$  NMR mole ratio study for 12C4 in the  $Cs^+$  case is shown in Figure 41. In the 12-crown-4 case, the  $^{13}C$  chemical shift of ligand does not tend to reach the limiting value even at mole ratio of 2.5, which is indicative of the formation of a very weak 1:1  $Cs^+$ -12-crown-4 complex. The formation constant ( $\log K$ ) of the 1:1  $Cs^+$ -12-crown-4 complex obtained by fitting the curve is only 1.09 (the data is presented in Table 27, page 144 ). Since the  $Li^+$  ion has about same size as the cavity of 12-crown-4, the  $Li^+$ -12-crown-4 complex would be expected to be strong. Surprising, the  $Li^+$  ion was also reported to form only a weak complex with 12-crown-4 in acetone (106). It may be that due to the very small size of 12-crown-4 (only four oxygen atoms on the crown ether ring), the attraction between the metal ion and the ligand is so weak. As can be seen from Figure 41, in the 15-crown-5 case the curve levels off at mole ratio 1.0, which indicates the formation of strong 1:1 complex (formation constant ( $\log K$ )  $> 4$ ). This is not surprising, since 15-crown-5 is a larger ligand than 12-crown-4 and the attraction between metal ion and ligand is stronger. Even for  $Li^+$ , which is too small for 15-crown-5, the

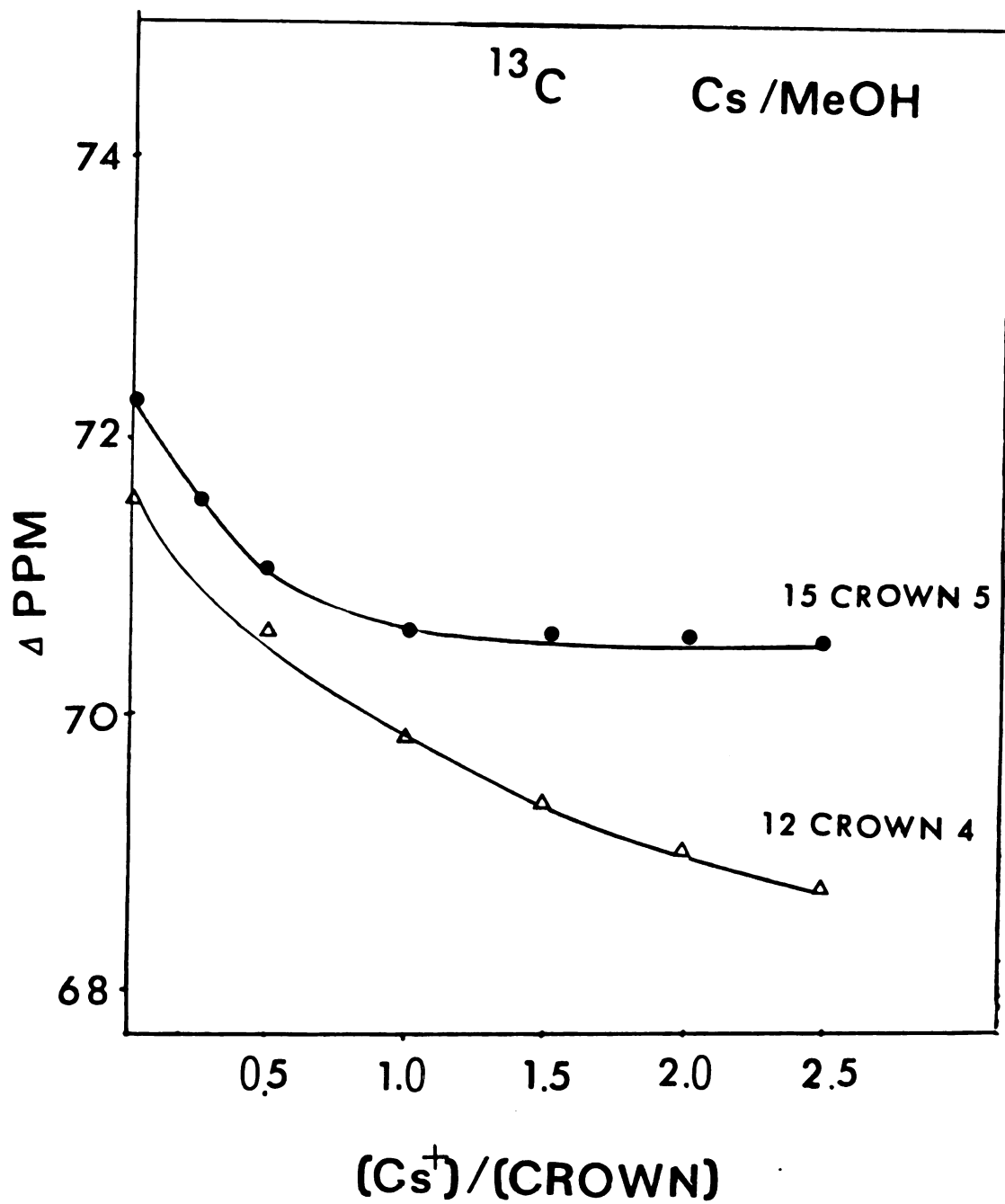


Figure 41. Carbon-13 Chemical Shift vs Mole Ratio of Cs/Ligand in Methanol.

formation of a strong  $\text{Li}^+$ -15-crown-5 complex in acetone was reported (formation constant  $> 10^3$ ) (106).

Haynes, et al (107) found that a good correlation between the  $^{23}\text{Na}$  NMR chemical shift of the complex of the  $\text{Na}^+$  ion with antibiotic ligands such as momensin, enniatin B and valinomycin and the stability constant of the complex formation in the same solvent as

$$\delta_{\text{complex}} = \delta_0 + m \log K_s \quad (\text{IVB.1})$$

where  $\delta_0$  and  $m$  are constants and  $K_s$  is the 'stability constant for the complex. According to the above equation, the strongest complex would be expected to have the largest shift. However, as shown in Figure 42, in acetone solution, DB18C6 has the largest  $^{39}\text{K}$  NMR shift but it does not form the strongest complex as mentioned previously (page 123 ). For cryptands, as shown in Table 29, cryptand C221, not cryptand C222, gives the largest shift ( $\Delta\delta$ ) even though it does not form the more stable complex with the  $\text{K}^+$  ion than cryptand C222. These results indicate that the  $^{39}\text{K}$  NMR chemical shifts of complexes do not correlate with the stabilities of complexes in these macrocyclic polyether systems. This probably suggests that not only  $\text{K}^+$ -ligand attraction force but also another factor such as repulsion force contributes to the paramagnetic shift of  $^{39}\text{K}^+$  upon complexation. The  $\text{K}^+$  ion was reported to nicely fit into

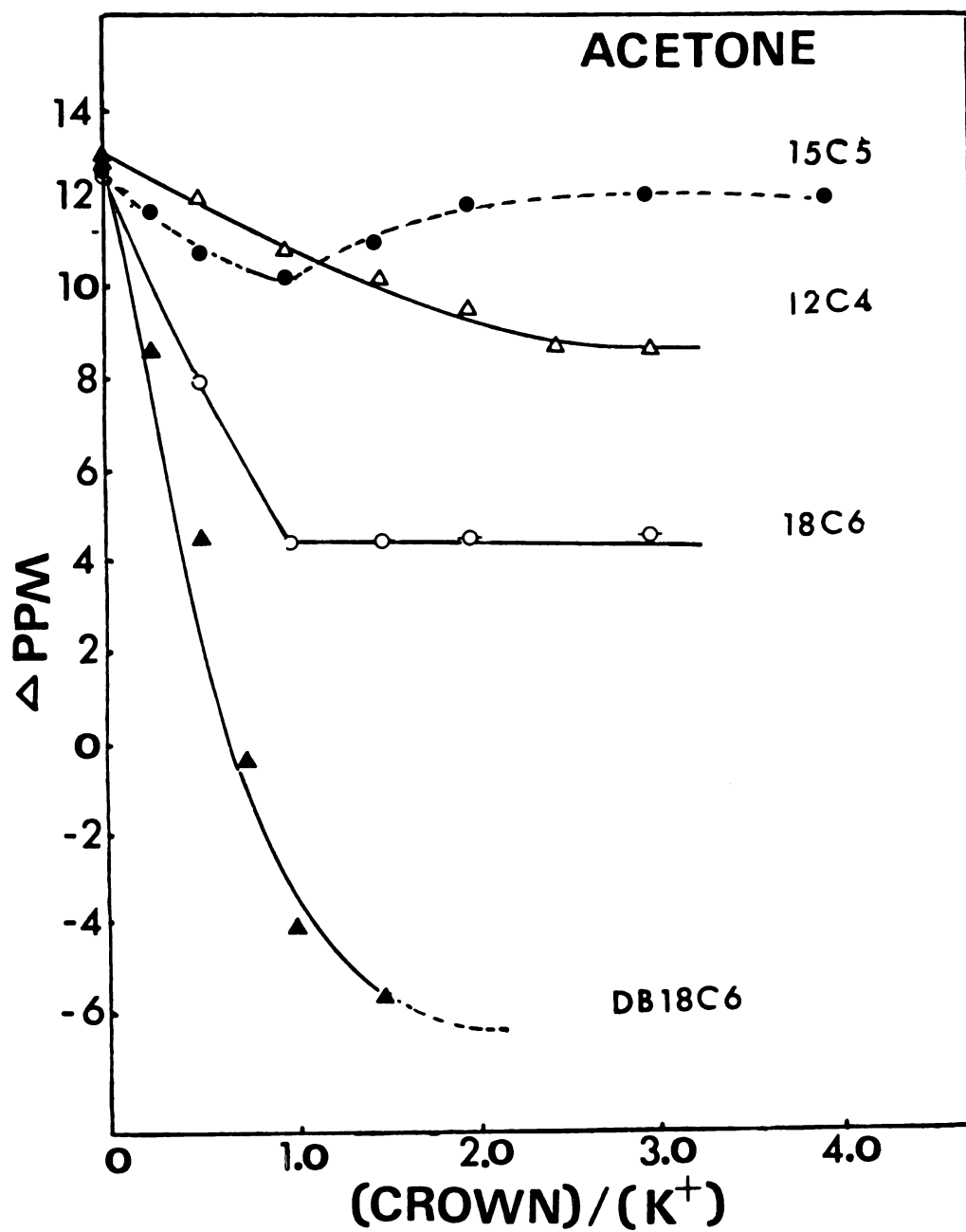


Figure 42. Mole Ratio-<sup>39</sup>K Chemical Shift Study for Various Ligands in Acetone.

Table 29. Limiting Chemical Shifts and Line Widths of K-39 for the Complexation of KPF<sub>6</sub> by Various Macrocyclic Ligands in Acetone

Ligand	Limiting Chemical Shift for 1:1 Complex (ppm)	Line Width ( $\Delta\nu_1$ ) <sup>2</sup> at MR 1.0 (Hz)	T <sub>2</sub> <sup>(b)</sup> (m sec)	$\Delta\delta$ (ppm)(a)
				( $\delta_{limit} - \delta_{free}$ )
Cryptand C222	-2.78	87.9	3.62	-14.79
Cryptand C221	-10.94	53.8	5.92	-23.25
Cryptand C211	-5.44	97.8	3.26	-18.04
18-crown-6	+4.46	131.0	2.43	-8.14
Dibenzo-18-crown-6	-8.26	117	2.72	-20.86
15-crown-5	+9.95	39.1	8.14	-2.07
12-crown-4	+7.82	63.4	5.02	-5.36

(a)  $\Delta\delta = \delta_{limit} - \delta_{free}$ ,  $\delta_{free}$  = chemical shift for free K<sup>+</sup> in acetone

(b) T<sup>\*</sup> is the spin-spin relaxation time including contribution from both natural line width and magnetic field inhomogeneity  $T_2^* = 1 / (\pi\Delta\nu_1/2)$

the cavity of 18 C 6 (81). As mentioned previously, the attachment of the benzo group on the crown ether ring results in decreasing the cavity size of the crown ether (55), the DB18C6 would be expected to have smaller cavity size than 18C6. Therefore, when the  $K^+$  ion is inside of the cavity (81) the repulsive interaction between the  $K^+$  ion and the oxygen atom on the crown ether would be larger in the DBC18C6 case than that in the 18C6 case. The large repulsive interaction probably result in a large paramagnetic shift. The similar behavior is observed in the cryptand C221 case. The cavity of C221 is too large for the  $K^+$  ion, when the  $K^+$  ion tries to fit into the cavity (The  $K^+$  ion was found on the margin of the cavity of C221 from X-ray study of  $K^+$ -C221 complex crystal (108), the repulsive interaction also will be induced.

CHAPTER V

RECOVERY OF CRYPTAND FROM CRYPTATE

## INTRODUCTION

Cryptands C211, C221 and C222 are commercially available but at a rather high price. Therefore, it seemed useful to develop a technique by which the ligands can be recovered from used solutions of their complexes.

It has been shown by Lehn, et al (86) that when the two nitrogen atoms of the bmacrocycle are protonated, the ligand is in the exo-exo form and has very little complexing ability. Lok (109) also reported that the sodium C222 cryptate dissociates into the protonated cryptand and free sodium ion at pH 6.7. The recovery procedure is based on these observations.

## RESULTS AND DISCUSSIONS

The recovery procedure, shown diagrammatically in Figure 43 involves four steps. 1. Recovery of solid cryptate complex from solutions. 2. Preparation of aqueous solutions of the cryptate and release of the captured cation at low pH. 3. Separation of the protonated cryptand from the metal ion(s) on a cation exchange column. 4. Conversion of the protonated cryptand to the basic form and purification.

Solutions of metal cryptates in various solvents were dried in vacuo at  $\sim 10^{-2}$  torr at room temperature (N.B must not be done if the solutions contain  $\text{ClO}_4^-$  anion). The solids (0.1~0.3 g) were dissolved in ~ 20 ml of aqueous 6 M HCl with gentle heating and the solution again

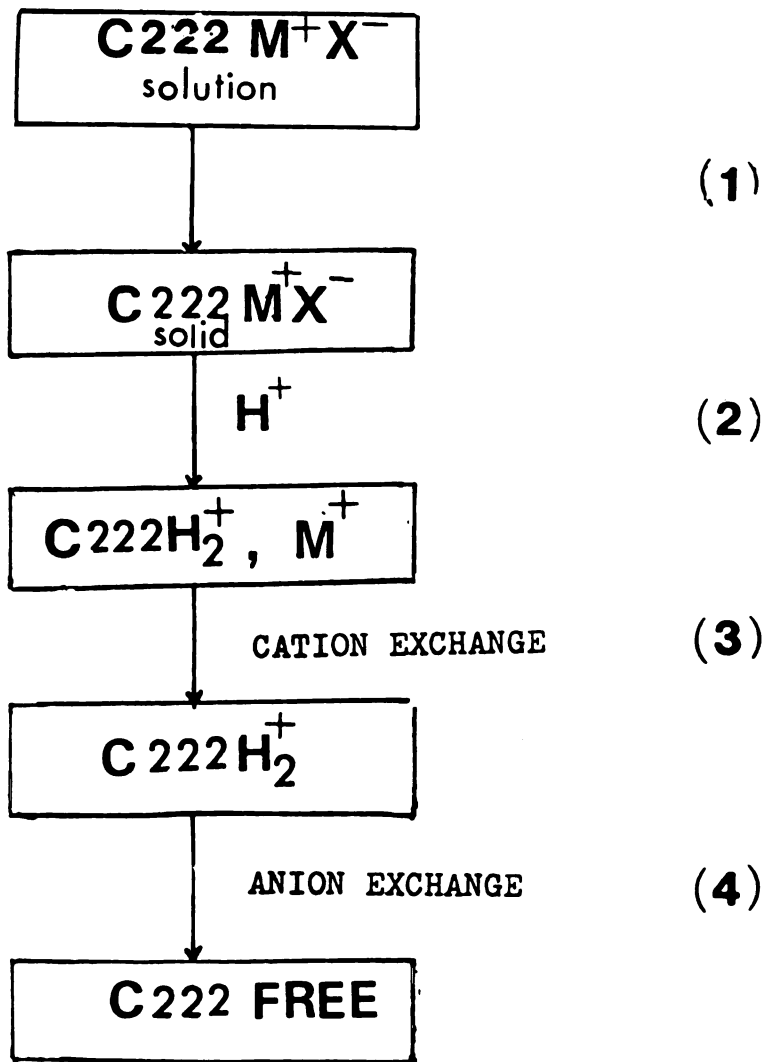


Figure 43. Diagram for Recovery of Cryptand from Cryptate

evaporated to dryness at  $\sim 10^{-2}$  torr. The residue, containing alkali salts and diprotonated cryptand, was dissolved in 20 ml of aqueous 0.1 M HCl. (If the original solutions contain a variety of anions, it is useful at this point to convert the salts to the chloride form by an anion exchange column in  $\text{Cl}^-$  form). The solution was then passed through a cation exchange column in  $\text{H}^+$  form (Dowex 50 x 8, 100  $\sim$  200 mesh, 1.2 x 22 cm column). Metal ions were eluted with 150 ml of 1.0 M HCl while the diprotonated cryptand remained on the column. Second elution was then carried out with  $\sim$  120 ml of 6 M HCl. In an experiment involving sodium-222 cryptate the elution of the alkali cation was followed by atomic absorption while that of the cryptand, by proton NMR. The elution curves are illustrated in Figure 44. The experimental data for atomic absorption and  $^1\text{H}$  NMR are presented in Table 30.

Then, crystals of the diprotonated ligand ( $\text{C222} \cdot 2\text{HCl}$ ) were obtained by evaporating the solvent from the cryptand solution under vacuum. The crystals are redissolved in  $\sim$  2 ml of water, placed on an anion exchange column in the  $\text{OH}^-$  form (Dowex 1 x 2, 100  $\sim$  200 mesh, 1.2 x 45 cm) and the free base eluted with conductance water. Sometimes it is necessary to repeat several times this step until most protonated cryptand was converted to the free cryptand C222. Finally the free cryptand

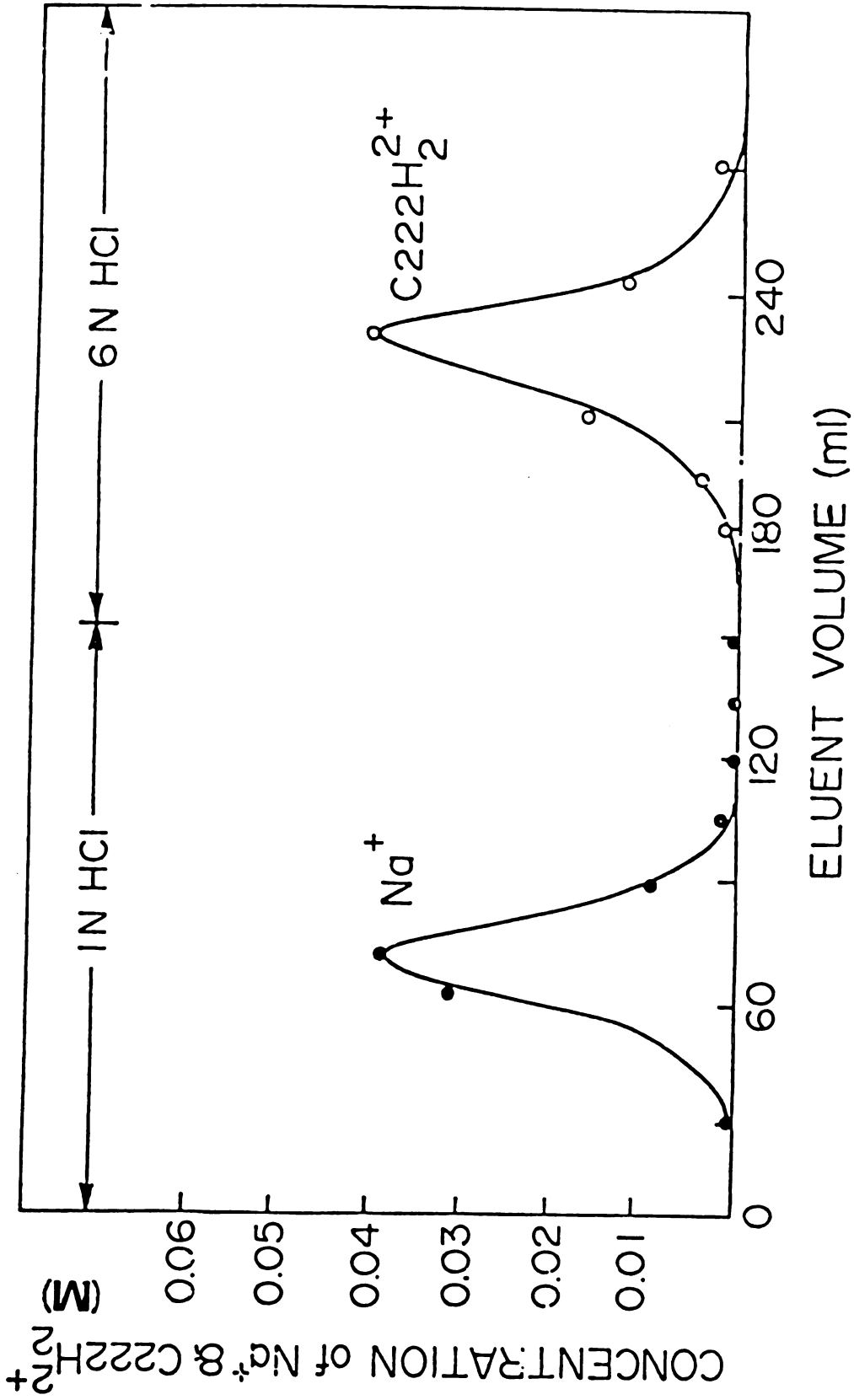


Figure 44. Elution Curve for Separation of C<sub>22</sub>H<sub>2</sub><sup>2+</sup> from Na<sup>+</sup>

Table 30. Concentration of Na<sup>+</sup> and C222 in Elution Solutions

Elution	Volume (ml)	A.E. Intensity (10 <sup>-9</sup> )	NMR Intensity for C222	(a) (Na <sup>+</sup> ) (M)	(C222) (M)
1 NHCl	15	1.8	-	-	-
	30	1.8	-	-	-
	45	5.8	-	0.23 x 10 <sup>-2</sup>	-
	60	90.0	-	3.48 x 10 <sup>-2</sup>	-
	75	100.0	-	3.98 x 10 <sup>-2</sup>	-
	90	17.5	-	0.75 x 10 <sup>-2</sup>	-
	105	4.0	-	0.16 x 10 <sup>-2</sup>	-
	120	3.6	-	0.07 x 10 <sup>-2</sup>	-
	150	-	-	-	-
	6 NHCl	30	1.0	0.05	-
45		3.3	0.1	-	4.28 x 10 <sup>-3</sup>
60		1.1	0.45	-	1.93 x 10 <sup>-2</sup>
75		0.45	1.0	-	4.28 x 10 <sup>-2</sup>
90		-	0.35	-	1.49 x 10 <sup>-2</sup>
120		-	0.05	-	2.14 x 10 <sup>-3</sup>

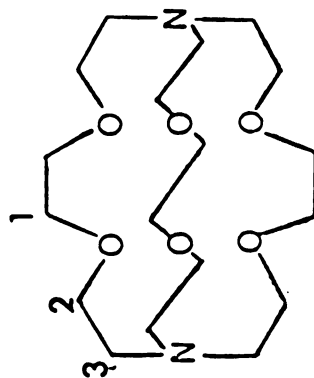
(a) Relative to the 75 ml 6 NHCl elution solution

was obtained by drying in vacuum and recrystallized from hexane. The purity of cryptand C222 was confirmed by melting point, carbon-13 proton-NMR and flame emission technique which was applied to detect the content of  $\text{Na}^+$  impurity. The yield is about 60 ~ 80%. The recovery of the cryptand C211 from cryptate was performed in the similar procedures.

Since the recovery is based on the protonation of cryptand. It was of interest to investigate the protonation of cryptand in more detail. The carbon-13 and  $^1\text{H}$  NMR were applied to study the protonation. These results studies are presented in Table 31 and Figure 45 and 46. As can be seen, both  $^1\text{H}$  and  $^{13}\text{C}$  NMR spectra of protonated cryptand show so much difference from that of free cryptand. As can be seen from Table 31 in the  $\text{H}_2\text{O}$  case the change in C-13 chemical shift by protonation for carbon 1 ( $\text{O}\underline{\text{C}}\text{H}_2$ ), carbon 2 ( $\text{O}\underline{\text{C}}\text{H}_2$ ) and carbon 3 ( $\text{N}\underline{\text{C}}\text{H}_2$ ) are -0.56, 5.34 and -0.66 ppm respectively ("+" means upfield shift). The assignments of peaks for carbons was made by Lehn (86). As can be seen, the one of  $\text{O}\underline{\text{C}}\text{H}_2$  carbon, not  $\text{N}\underline{\text{C}}\text{H}_2$  carbon give the largest shift. The identical phenomenon was also observed by Lehn, et al (110). Since it is well known that the protonation is easier occurred on nitrogen atom, not on oxygen atom, it is reasonable to expect the largest shift for  $\text{N}\underline{\text{C}}\text{H}_2$  carbon. These results are surprising. There are some probable

Table 31. Carbon-13 Chemical Shifts of Protonated Cryptands

Cryptand	Solvent	Free Cryptand	Protonated Cryptand	$\Delta\delta = \delta_{\text{free}} - \delta_{\text{protonated}}$ (ppm)
C222	H <sub>2</sub> O	peak $\Delta$ ppm	$\Delta$ ppm	
		(1) 71.80	72.36	-0.56
		(2) 70.71 $\xrightarrow{\text{H}^+}$	65.37	+5.34 (carbon 2)
C222	MeOH	(3) 54.96	55.62	-0.66
		(1) 72.18	72.46	-0.28
		(2) 71.30 $\xrightarrow{\text{H}^+}$	65.38	+5.92 (carbon 2)
(3) 57.21	56.12	1.09		
Free 222 + Cryptate Protonated MR = 0.5 (K <sup>+</sup> /C222) Cryptand				
C222	DMSO	(1) 72.25	72.46	(1) -0.2 (free)
		(2) 71.56	65.40	-0.41 (complex)
		(3) 57.90 $\xrightarrow{\text{H}^+}$	55.43	(2) +6.16 (F) (3) 2.47 (F) 0.00 (C)



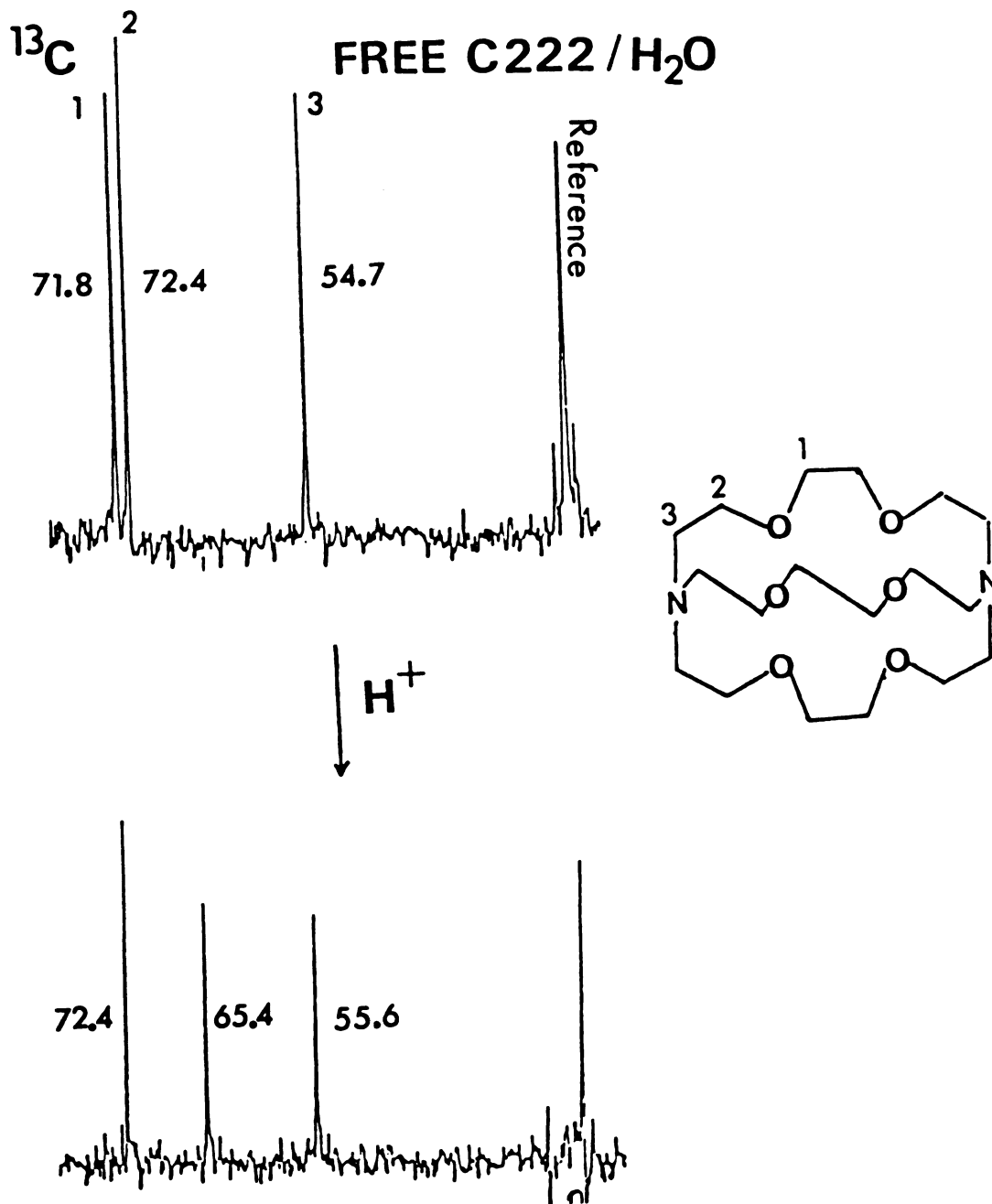


Figure 45. Carbon-13 Spectra of Protonated and Free Cryptands

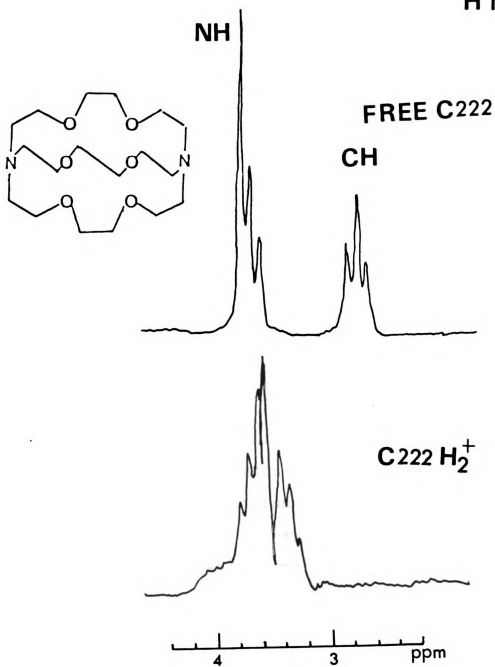
$^1\text{H}$  NMR

Figure 46.  $^1\text{H}$  Spectra of Protonated and Free Cryptands

explanation as following:

(1) It is caused by  $\beta$  effect. The attachment of  $H^+$  on nitrogen causes the big chemical shift for  $\beta$  carbon (carbon (2)) (110).

(2) The assignments of  $^{13}C$  NMR peaks for carbons is probably not correct, however, this is less possible since the  $OCH_2$  carbon, (not  $NCH_2$  carbon) usually resonates around 70 ppm, for example, in the cases of 18-crown-6, 15-crown-5 and 12-crown-4, the  $OCH_2$  carbons all resonated around 70 ppm as mentioned in Chapter IV(B).

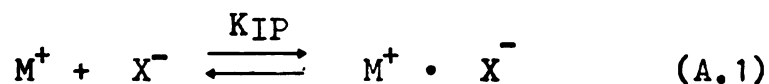
(3) The big change in  $^{13}C$  chemical shift for carbon (2) ( $OCH_2$ ) probably suggest an extremely structure change upon protonation. As also can be seen from the  $^1H$  NMR spectra shown in Figure 46, the peaks for  $NCH_2$  and  $OCH_2$  protons in protonated cryptand show so close, which indicates that the all protons have the similar environments while the so different environments were found for  $NCH_2$  and  $OCH_2$  protons on free cryptand. This is probably another evidence for an extremely cryptand structure change upon protonation.

APPENDICES

APPENDIX I

DESCRIPTION OF COMPUTER PROGRAM KINFIT AND SUBROUTINE  
EQN FOR THE CALCULATION OF ION PAIR FORMATION  
CONSTANTS BY THE NMR TECHNIQUE

The equilibrium for an ion pair reaction can be expressed as



and

$$K_{IP} = \frac{(M^+ \cdot X^-)}{M^+ \cdot X^-} = \frac{C_{(MX)}}{C_{M^+} C_{X^-}} \cdot \frac{1}{\gamma_{\pm}^2}$$

$$= Kc \frac{1}{\gamma_{\pm}^2} \quad (A.2)$$

where Kc is the concentration equilibrium constant,

$\gamma_{\pm}$  is the mean activity coefficient which can be calculated by using Debye-Huckel equation:

$$-\log \gamma_{\pm} = \frac{1.823 \times 10^6}{(DT)^{3/2}} |Z_+ Z_-| \sqrt{I}$$

$$1 + \frac{50.29}{(DT)^{1/2}} \frac{a}{a} \sqrt{I} \quad (A.3)$$

where  $Z_+$  and  $Z_-$  are the charges of the ions, I is the molar ionic strength, D is the dielectric constant of

the solvent,  $T$  is temperature ( $^{\circ}\text{K}$ ),  $\bar{a}$  is the closest distance of approach of the ions in  $\text{\AA}$ . The values of  $\bar{a}$  for  $\text{KPF}_6$ ,  $\text{KI}$  and  $\text{KSCN}$  were used to be 4.0, 3.0 and 3.0  $\text{\AA}$  (102)(111).

The observed chemical shift is a population average of these of the free ion and ion pair

$$\begin{aligned}\delta_{\text{obs}} &= \delta_{\text{F}}X_{\text{F}} + \delta_{\text{ip}}X_{\text{ip}} \\ &= (\delta_{\text{F}} - \delta_{\text{ip}})X_{\text{F}} + \delta_{\text{ip}}\end{aligned}\quad (\text{A.4})$$

where

$$X_{\text{F}} = \frac{C_{\text{F}}^{\text{M}}}{C_{\text{T}}^{\text{M}}}\quad (\text{A.5})$$

Mass balance leads to

$$[\text{M}^+\text{A}^-] = C_{\text{T}}^{\text{M}} - C_{\text{F}}^{\text{M}}\quad (\text{A.6})$$

and charge balance to

$$[\text{M}^+] = [\text{A}^-] = C_{\text{F}}^{\text{M}}\quad (\text{A.7})$$

substitution of (5) (6) (7) into (4) yields

$$C_{\text{F}}^{\text{M}} = \frac{-1 \pm (1 + 4KcC_{\text{T}}^{\text{M}})^{1/2}}{2Kc}\quad (\text{A.8})$$

substitution of (8) to (2) we obtain

$$\delta_{\text{obs}} = \frac{-1 + (1 + 4K_{\text{IP}}C_{\text{T}}^{\text{M}} \gamma_{\pm}^2)^{1/2}}{2K_{\text{IP}}C_{\text{T}}^{\text{M}} \gamma_{\pm}^2} (\delta_{\text{F}} - \delta_{\text{IP}}) + \delta_{\text{IP}}\quad (\text{A.9})$$

In order to fit this equation, four constants and two parameters are used; namely

- Const (1) = chemical shift of free  $K^+$
- Const (2) = dielectric constant of solvent
- Const (3) = temperature of solution ( $^{\circ}K$ )
- Const (4) = ion ion closest distance ( $\overset{0}{A}$ )
- U (1) = chemical shift of ion pair
- U (2) =  $K_{IP}$

In the cases of solvents of low dielectric constant such as acetone, pyridine and ethylenediamine, the Debye-Hukel (DH) equation seems to be invalid at high concentration of the potassium salt ( $>0.2 \text{ M}$ ). For example, the value of  $\gamma_{\pm}$  obtained for  $0.2 \text{ M}$  of  $KPF_6$  in acetone is only 0.17 (activity = 0.034). The value of  $K_{IP}$  for  $KPF_6$  in acetone obtained by fitting the data to equation (A-9) and the DH equation is only 0.03 while the concentration equilibrium constant for ion-pair formation ( $K_c$ ) is  $8.23 \pm 0.17$ .

The value of  $K_c$  can be obtained using equation (A-9) with  $\gamma_{\pm} = 1.0$  and only one constant (ie: chemical shift of free  $K^+$ ). The subroutine EQN for calculations of  $K_{IP}$  and  $K_c$  are listed the next two pages.

K<sub>i</sub>p

```

SUBROUTINE EON
COMMON KOUNT,ITAPE,JTAPE,INT,LAP,XINCE,NOPT,NOVAR,NM,NK,K
1 WTA,TEXT,I,AV,REGID,IAR,EPS,IYF,XX,RY,YY, ZI,COB,COF,CO,
2 IGVAL,YST,T,DT,L,M,I,J,Y,DY,VECT,NCST,CONST,NOAT,NOATM,NOI,
3 YYY,CONSTS
COMMON/PREDI/IMETH
COMMON/POINT/KCPT,JOPT,XXX
DIMENSION X(4,300),U(20),NTX(6,100),X1(4),FOP(300),CO(1,10),
1 P(2,21),VECT(20,21),ZL(100),I1(20),IGV(20),YST(100),Y1
2 DY(13),CONSTS(50,16),NCST(50),IOPIN(50),IOP(50),XK(1,50),
3 NOPT(50),LOPT(50),YYY(50),CONST(16),XXX(15)
GO TO (2,3,4,5,1,7,8,9,10,11,12) IYF
1 CONTINUE
ITAPE=40
JTAPE=61
WRITE (JTAPE,6)
6 FORMAT(//////////,* KINFIT CURVE EXTRA-POLA:OP*)
NOUNK=2
NOVAR=2
RETURN
7 CONTINUE
RETURN
8 CONTINUE
RETURN
9 CONTINUE
IF (IMETH.NE.-1) GO TO 35
RETURN
35 CONTINUE
CONST(1)=S OF FREE K
CONST(2)=DIEL . CONST. OF SOLVENT
CONST(3)=TEMP. OF SOL.
CONST(4)=ION ION DIST. (A) CM
XX(1)=CONC. OF K
XX(2)=ONS. CHEM. SHIF
III(1)=S OF ION PAIR
III(2)=KIP
ANY=XX(1)
CONCK=XX(1)
DO 20 JPH=1,10
SINH=CONCK
IF (SINH.GT.83.83)
A7 WRITE (ITAPE,85) XX(1),JPH,U(2),GAMMA
85 FORMAT(6X,E14.6,15,F14.7,E14.5)
STOP
A3 CONTINUE
SINH=SQRT(SINH)
H10=1.72
V10=1.72
H10A=-1.823E+06/(CONST(2)*CONST(3))*F10
H10R=5.029E+09/(CONST(2)*CONST(3))*VECT
GAMLOG=(H10A*SINH)/(1.0+H10R*CONST(4)*SINH)
GAMMA=10.0**GAMLOG
C1P=U(2)*GAMMA**2
CONCK=(1.-SQRT(ABS(1.+4.*C1P**XX(1))))/(2.*C1P)
DIFF=ABS(CONCK-ANY)
F10=ANY**0.05
IF (DIFF.LT.F10) GO TO 250
ANY=CONCK
200 XX=CONCK/XX(1)
250 DELOHS=XX*CONST(1)+(1.-XX)*U(1)
H10=DELOHS-XX(2)
RETURN
3 CONTINUE
RETURN
4 CONTINUE
RETURN
5 CONTINUE
IF (IMETH.NE.-1) GO TO 20
RETURN
20 CONTINUE
RETURN
9 CONTINUE
RETURN
10 CONTINUE
RETURN
11 CONTINUE
RETURN

```



## APPENDIX II

### DESCRIPTION OF COMPUTER PROGRAM KINFIT AND SUBROUTINE EQN FOR THE EXTRAPOLATION OF NMR CHEMICAL SHIFTS TO INFINITELY DILUTE CONCENTRATION

It was discovered that the curves described by the chemical shift vs concentration plots could be adequately described using a simple power series in concentration

$$\delta_{\text{obs}} = \delta_0 + AC + BC^2 + DC^3 + EC^4 + FC^5 + GC^6 + HC^7$$

where  $\delta_{\text{obs}}$  is the observed chemical shift, C is the salt concentration in molarity, A. B. D. E. F. G. and H are unknowns and  $\delta_0$  is the chemical shift at infinite dilution, which is also unknown. The above equations expressed in Fortran notation are as follows:

$$S = U(1) + U(2)*XX(1) + U(3)*XX(1)**2 + U(4)*XX(1)**3 + U(5)*XX(1)**4 + U(6)*XX(1)**5 + U(7)*XX(1)**6 + U(8)*XX(1)**7$$

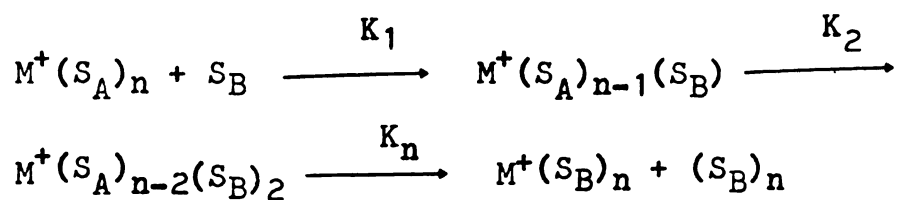
Subroutine EQN of this calculation is listed on the next page



APPENDIX III

DESCRIPTION OF COMPUTER PROGRAM KINFIT AND SUBROUTINE  
EQN FOR THE EQUILIBRIUM CONSTANT OF PREFERENTIAL  
SOLVATION IN BINARY SOLVENT MIXTURES

The equilibria in mixed solvents can be expressed  
as



(B.1)

where  $S_A$  and  $S_B$  are the solvent A and B respectively  
 $n$  is the solvation number  $K_1 \dots \dots \dots K_n$  are the  
equilibrium constants for each step. If  $\delta_p$  is the total  
shift in the resonance of  $M^+$  from pure A to pure B  
solvents. Hence, the intrinsic shifts of the various  
solvated species was assumed to be proportional to the  
amount of B which they contain and then

$$\delta_{MA_n} = 0; \delta_{MA_{n-1}B} = \frac{1}{n} \delta_p, \dots \dots \delta_{MB_n} = \delta_p \quad (B.2)$$

$$\text{Let } K' = K^{1/n} = (K_1 K_2 K_3 \dots \dots \dots K_n)^{1/n} \quad (B.3)$$

$$K_1 = nK', K_n = \frac{1}{n} K' \quad (B.4)$$

The final equation in this treatment allows calculation  
of  $K^{1/n}$  as follows:

$$\frac{1}{\delta} = \frac{1}{\delta_p} \left( 1 + \frac{1}{K^{1/n} \frac{X_B}{X_A}} \right)$$

$\delta$  = observed chemical shift relative to the resonance  
of  $M^+$  in pure A

$$\delta_p = \delta_M^{\circ}(\text{solv A}) - \delta_{M^+}^{\circ}(\text{solv B})$$

$K^{1/n}$  = the geometric equilibrium constant

$n$  = solvation number

$X_A$  ,  $X_B$  = the mole fractions of A and B respectively

The subroutine equation is listed on the next page.

```

SUBROUTINE EQU
COMMON KOUNT,ITAPE,JTAPE,IWT,LAP,XINCR,NOPT,NOVAR,NOUN
IWA,TEST,1,AV,RESID,IAR,EPS,ITYP,XX,RXTYP,DX11,FOP,FO,
EIGVAL,AST,T,DT,L,M,JJJ,Y,DY,VECT,NCST,CONST,NJAT,JUAT,
JYY,CONSTS
COMMON/FREDT/METH
COMMON/POINT/KOPT,JOP1,XXX
DIMENSION X(4,300),U(20),WTA(4,300),XX(4),FOP(300),FO(
1,P(20,21),VECT(20,21),ZL(300),IU(20),EIGVAL(20),AST(30
2UY(10),CONSTS(50,16),NCST(50),ISMIN(50),RXTYP(50),DX11
3,NUPT(50),LUPT(50),YYY(50),CONST(16),XXX(15)
DIMENSION DIFF(200),C(200)
GO TO (2,3,4,5,1,7,8,9,10,11,12)  ITYP
1 CONTINUE
ITAPE=0
JTAPE=1
NUNK=0
NOVAR=0
RETURN
7 CONTINUE
RETURN
4 CONTINUE
RETURN
7 CONTINUE
IF(METH.NE.-1) GO TO 35
RETURN
35 CONTINUE
XA(1)=X(A)/X(B)
XA(2)=SH=1/S , S=CHEM. SHIFT OF K 39 RELATIVE TO S OF
U(1) = 1/(S(A)-(B))
U(2) = K(1/N) , EQUIM. CONST.
NE=OLVATION NO.
AF=0+XX(1)/U(2)
SH=A*U(1)
RESID=SH-XX(2)
RETURN
3 CONTINUE
RETURN
4 CONTINUE
RETURN
5 CONTINUE
IF(METH.NE.-1) GO TO 20
RETURN
2 CONTINUE
RETURN
6 CONTINUE
RETURN
1 CONTINUE
RETURN
11 CONTINUE
RETURN
12 CONTINUE
RETURN
END

```

## APPENDIX IV

### DESCRIPTION OF COMPUTER SUBROUTINE EQN FOR THE CALCULATION OF FORMATION STANTS FOR ONLY ONE STEP REACTION

When the exchange between the free and complexed  $K^+$  ion is fast on the NMR time scale, only a population averaged chemical shift is observed

$$\delta_{\text{Obs}} = \delta_F' X_F' + \delta_C X_C \quad (\text{D.1})$$

where  $\delta_F' X_F' = \delta_F X_F + \delta_{IP} X_{IP}$  (D.2)

In which  $\delta_F$ ,  $\delta_{IP}$  and  $\delta_C$  are the chemical shifts for free, ion pair and complexed  $K^+$  ions respectively and  $X_F$ ,  $X_{IP}$  and  $X_C$  are the relative mole fractions for each species. Since

$$C_M^T = C_M + C_{ML} \quad (\text{D.3})$$

and  $C_L^T = C_{ML} + C_L$  (D.4)

Substitution of (D.3), (D.4) and (D.2) to (D.1) yields

$$\begin{aligned} \delta_{\text{obs}} = & [R \cdot \delta_{M^+} + (K_f \cdot R \cdot C_L^T \cdot \delta_{MX})] / [(1 + \delta_{MX} \cdot R) \\ & + (K_{IP} \cdot R \cdot C_M^T \cdot \delta_{IP}) / (1 + K_{IP} \cdot R)] / C_M^T \end{aligned} \quad (\text{D.5})$$

where  $R = C_M^T / (K_f \cdot K_{IP}) - C_L^T (1 + K_f) + (1/K_{IP})$  (D.6)

In which  $C_M^T$  and  $C_L^T$  are the total concentration of metal and ligand respectively.  $K_f$  and  $K_{IP}$  are the formation constant of complex and ion-pair respectively.

In order to fit these equations, four constants and two parameters are used; namely

Const (1) = Ion pair formation constant

Const (2) = Total conc of ion pair

Const (3) = Chemical shift of ion pair

Const (4) = Chemical shift of metal

U (1) = Chemical constant of complexed

U (2) = Formation constant of complex

If only very small amount of the ion pair formation is in the solution, the (C.6) equation can be simplified to

$$\begin{aligned} \delta_{\text{obs}} = & (K_f C_M^T - K C_L^T - 1) + (K_f^2 C_L^T{}^2 + K_f^2 C_M^T{}^2 \\ & - 2K_f^2 C_L^T C_M^T + 2K_f C_L^T C_M^T + 2K_f C_L^T \\ & + 2K_f C_M^T + 1)^{1/2} \frac{\delta_f - \delta_c}{2K C_T^M} + \delta_c \end{aligned}$$

Subroutine EQN of the calculation of  $K_f$  with and without ion pairing consideration are listed on the next two pages.



SUBROUTINE EON 73/73 OPT=1 FTN 4.6\*433 01/05/78 .

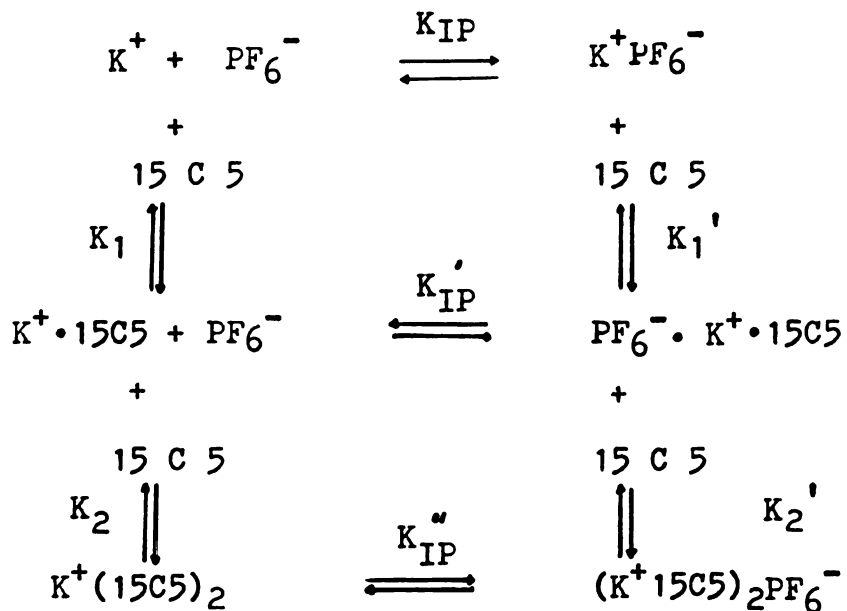
```

1      SUBROUTINE EON
      COMMON KOUNT,ITAPE,JTAPE,IWT,LAP,XINCR,NOPT,NQVAR,NQUNK,X,U,ITMAX, EON4
      IWT,TEST,I,AV,RESID,IAR,EPS,ITYP,XX,RXTYP,DXII,FOP,FQ,FU,P,ZL,TU,E EON4
      ZIGVAL,XST,T,DT,L,M,J,JJ,Y,DY,VECT,NCST,CONST,NDAT,JDAT,MOPT,LOPT, EON4
5      3YYY,CONSTS
      COMMON/FREIT/INETH
      COMMON/POINT/KOPT,JOPT,XXX
      DIMENSION X(4,300),U(20),WTX(4,300),XX(4),FOP(300),FQ(300),FU(300) EO
1)      I,J(21),VFCT(2),ZL(30),TO(20),EIGVAL(20),XST(300),Y(10),
      ZDY(10),CONSTS(50,15),NCST(50),ISHIP(50),RXTYP(50),DXII(50),IRX(50)
      3,NOPT(50),LOPT(50),YYY(50),CONST(16),XXX(15)
      DIMENSION DIFF(20),C(20)
      GO TO (2,3,4,5,1,7,8,9,13,11,12) ITYP
15     ? CONTINUE
      I=ITAPE
      J=JTAPE
      W=WTX(JTAPE,A)
      4 FORMAT(////////,*, FORMATION CONSTANT *)
      NQUNK=
      NQVAR=
      R=ITYP
      7 CONTINUE
      R=ITYP
      4 CONTINUE
      R=ITYP
      2 CONTINUE
      IF(INETH.NE.-1) GO TO 35
      R=ITYP
35     ? CONTINUE
      AF=U(21)*XX(1)*XX(1)
      HF=U(21)*XX(1)*CONST(11)*XX(1)
      CF=U(21)*XX(1)*XX(1)*CONST(11)
      UF=U(21)*XX(1)
      FF=U(21)*XX(1)*CONST(11)
      AA=U(21)*XX(1)
      HH=U(21)*XX(1)
      CF=COF*(U(21)-1)/(2.*CONST(11)*U(21))
      SF=(AA*HH-1)*SQRT(AA*(AA*U(21)+1)+CC)*U(1)
      W=DIFF(2)
      R=ITYP
      3 CONTINUE
      R=ITYP
      4 CONTINUE
      R=ITYP
      5 CONTINUE
      IF(INETH.NE.-1) GO TO 35
      R=ITYP
      2 CONTINUE
      NQUNK=
      NQVAR=
      R=ITYP
      1 CONTINUE
      W=ITYP
      11 CONTINUE
      R=ITYP
      1 CONTINUE
      W=ITYP
  
```

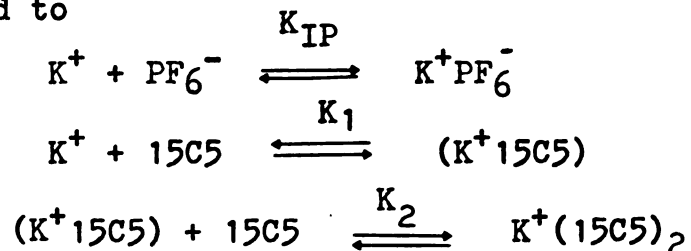
APPENDIX V

DESCRIPTION OF COMPUTER PROGRAM KINFIT AND SUBROUTINE  
 EQN FOR THE CALCULATION OF FORMATION CONSTANTS  
 FOR TWO-STEP REACTION

The equilibria for this two step reaction can be  
 expresses as



As shown in Figure 37, the 1:1 complex of 15 C 5 with  $K^+$  gives no evidence for contact ion pair formation. That is,  $K_{IP}' \sim 0$ . Also, as can be seen from Table 24, anions show no interaction with 2:1 complexes, it suggested  $K_{IP}'' \sim 0$  too. Therefore the above scheme can be simplified to

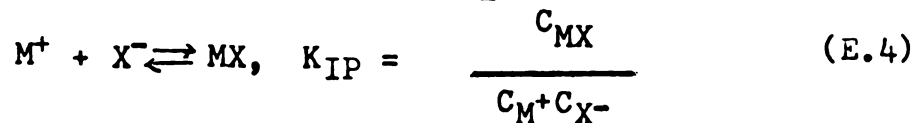
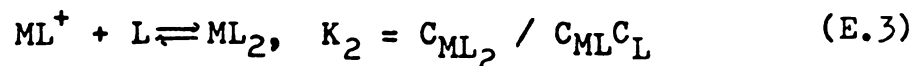
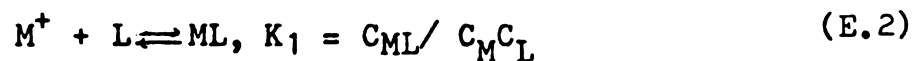


The observed chemical shift can be expressed as

$$\delta_{\text{obs}} = \delta_{\text{F}}X_{\text{F}} + \delta_{\text{IP}}X_{\text{IP}} + \delta_{\text{C}_1}X_{\text{C}_1} + \delta_{\text{C}_2}X_{\text{C}_2} \quad (\text{E.1})$$

Where F, IP, C<sub>1</sub>, C<sub>2</sub> denote uncomplexed K<sup>+</sup>, ion-paired K<sup>+</sup>, (K<sup>+</sup>15C5) and K<sup>+</sup>(15C5)<sub>2</sub> respectively.

The equilibria for two step reaction can be rewritten in general form:



The concentration balance leads to

$$C_{\text{M}}^{\text{T}} = C_{\text{M}} + C_{\text{ML}} + C_{\text{ML}_2} + C_{\text{MX}} \quad (\text{E.5})$$

$$C_{\text{L}}^{\text{T}} = C_{\text{L}} + C_{\text{ML}} + 2C_{\text{ML}_2} \quad (\text{E.6})$$

$$C_{\text{M}}^{\text{T}} = C_{\text{X}}^{\text{T}} = C_{\text{X}} + C_{\text{MX}} \quad (\text{E.7})$$

substitution of (E.2) (E.7) to (E.5) and (E.6) to (E.3) yields

$$C_{\text{M}}^{\text{T}} = C_{\text{M}}(1 + K_1C_{\text{L}} + K_1K_2C_{\text{L}}^2 + K_{\text{IP}}C_{\text{X}}) \quad (\text{E.8})$$

and

$$C_{\text{L}}^{\text{T}} = C_{\text{L}} + K_1C_{\text{M}}C_{\text{L}} + 2K_1K_2C_{\text{M}}C_{\text{L}}^2 \quad (\text{E.9})$$

substitution of (D.8) to (D.9) we obtain

$$C_{\text{L}} = \frac{-1(1 + K_1C_{\text{M}}) + [(1 + K_1C_{\text{M}})^2 + 8K_1K_2C_{\text{M}}C_{\text{L}}^{\text{T}}]^{\frac{1}{2}}}{4K_1K_2C_{\text{M}}} \quad (\text{E.10})$$

and also since

$$X_{C_1} = K_1 C_M C_L \quad (E.11)$$

$$X_{C_2} = K_1 K_2 C_M C_L^2 / C_M^T \quad (E.12)$$

$$X_F = C_M / C_M^T \quad (E.13)$$

$$X_{IP} = K_{IP} C_M C_{X^-} / C_M^T \quad (E.14)$$

In most solvents,  $KPF_6$  show very weak ionic association, in addition, the results from  $^{13}C$  NMR study (shown in Figure 36) indicate that the formation constant for 1:1 complex always large, therefore ion pair formation can not compete with the complexation formation. Therefore in most solvents, the ion pairing formation can be neglect ( $X_{IP} \approx 0$ ). In this case, in order to fit these above equations, four parameters and two constants are used

Const (1) = total concentration of metal

Const (2) = chemical shift of free metal

U (1) = formation of 1:1 complex

U (2) = Chemical shift of 1:1 complex

U (3) = Formation constant of 2:1 complex

U (4) = chemical shift of 2:1 complex

subroutine EQN of the calculation for with and without ion pairing are listed on the next two pages.





## REFERENCES

- 1 J. N. Shoolery and B. J. Alder, *J. Chem. Phys.*,  
23, 805 (1955)
- 2 B. P. Fabrikand, S. S. Goldberg, R. Leifer and  
S. G. Agen., *Mol. Phys.*, 7, 425 (1963)
- 3 A. Fratiello, R. E. Lee, D. P. Miller and  
V. M. Nishida, *Mol. Phys.*, 10, 551 (1966)
- 4 B. W. Maxey and A. I. Popov, *J. Amer. Chem. Soc.*,  
90, 4470 (1968)
- 5 E. Schasched and M. C. Day, *J. Amer. Chem. Soc.*,  
10, 503 (1968)
- 6 R. E. Connick and R. E. Poulson, *J. Phys. Chem.*,  
62, 1002 (1958)
- 7 W. DeWitte and A. I. Popov, *J. Solution Chem.*,  
5, 231, (1976)
- 8 A. Carrington, F. Dravnick and M. C. R. Symons,  
*Mol. Phys.*, 3, 174 (1960)
- 9 J. P. K. Tong and C. H. Langford, *Can. J. Chem.*,  
52. 1721 (1974)
- 10 L. S. Frankel, C. H. Langford and T. R. Stengle,  
*J. Phys. Chem.*, 74, 1376 (1976)
- 11 A. K. Covington, T. H. Lieley and G. A. Porthouse,  
*Trans. Faraday Soc. I.*, 69, 963 (1973)
- 12 T. R. Stengle and C. H. Langford, *J. Phys. Chem.*,  
69, 3299 (1965)
- 13 C. Deverell and R. E. Richards, *Mol. Phys.*, 16,  
421 (1969)

14. J. S. Stengle, Y. E. Pan and C. H. Langford, J. Amer. Chem. Soc., 94, 9037 (1972)
15. A. I. Popov and R. G. Baum, J. Solution Chem., 4, 441 (1975)
16. H. A. Berman and T. R. Stengle, J. Phys. Chem., 79, 2551 (1975)
17. J. Sadley and A. J. Sadeley, J. Mag. Res., 14 (97), 103 (1974)
18. A. I. Popov, in "Solute-Solvent Interactions" M. Dekker, New York, N.Y. (1976), Vol. II. pp 271-330
19. R. E. Maciel, J. K. Hancock, L. E. Lafferty, P. A. Muller and W. K. Musker, Inorg. Chem., 5, 554 (1966)
20. E. M. Kosower, J. Amer. Chem. Soc., 80, 3253 (1958)
21. R. H. Erlich, E. Roach and A. I. Popov, J. Amer. Chem. Soc., 92, 4989 (1970)
22. Y. M. Cahen, P. R. Handy, E. T. Roach and A. I. Popov, J. Phys. Chem., 79, 80 (1975)
23. A. I. Mishystin and Y. M. Kessler, J. Solution Chem., 4, 799 (1975)
24. V. Gutmann "Coordination Chemistry in Nonaqueous Solvents" Springer Vienna, (1968)
25. H. G. Hertz and H. Weingartner, J. Solution Chem., 4, 790 (1975)
26. C. A. Melendres and H. G. Hertz, J. Chem. Phys., 61, 4156 (1974)

- 27 J. P. Oliver, P. A. Scherr and A. J. Weibel,  
J. Organometal Chem., 85, 265 (1975)
- 28 K. Covington, R. Lamtzkea and J. M. Thain, J. Chem.  
Soc. Faraday, 70, 1869 (1974)
- 29 M. S. Greenberg, Ph.D thesis, Michigan State University  
(1974)
- 30 Y. M. Kessler, A. I. Mishnstim and A. I. Podkovyrin,  
J. Solution Chem., 6, 111 (1977)
- 31 G. Olofsson, Acta. Chem. Scan., 22, 1352 (1968)
- 32 E. G. Bloor and G. R. Kidd, Can. J. Chem. 46,  
3425 (1968)
- 33 W. J. DeWitte, L. Liu , E. Mei, J. C. Dye and  
A. I. Popov, J. Solution Chem., 6, 337 (1977)
- 34 J. D. Halleday, R. E. Richards and R. R. Sharp,  
Proc. Roy. Soc. London, A313, 45 (1969)
- 35 M. S. Greenberg, R. L. Bondner and A. I. Popov,  
J. Phys. Chem., 77, 2449 (1973)
- 36 C. Deverell and R. E. Richards, Mol. Phys., 10,  
551 (1966)
- 37 J. W. Crawford and R. P. Gasser, Trans. Faraday  
Soc., 63, 2758 (1967)
- 38 P. Neggla, M. Holtz and H. G. Hertz, J. Chim. Phys.,  
71, 56 (1974)
- 39 G. W. Stockton and J. S. Martin, Can. J. Chem.,  
52, 744 (1974)

- 40 T. L. Collins, *Phys. Rev.*, 103, 80 (1950)
- 41 H. Sommer, H. A. Thomas and J. A. Hipple, *Phys. Rev.*, 82, 697 (1951)
- 42 E. Brun, J. Oeser, H. H. Stans and C. G. Telschow, *Phys. Rev.*, 93, 172 (1953)
- 43 J. C. Hindman, *J. Chem. Phys.*, 36, 1000 (1962)
- 44 E. G. Bloor and R. G. Kidd, *Can. J. Chem.*, 50, 3926 (1972)
- 45 W. Sahn and A. Schweenk, *Z. Naturforsch.*, 29A, 1754 (1974)
- 46 M. Shporer and Z. Luz, *J. Amer. Chem. Soc.*, 97, 665 (1975)
- 47 F. W. Cope and R. Damadian, *Nature*, 228, 76 (1970)
- 48 M. Goldsmith and R. Domadian, *Physiol. Chem. & Physics*, 7, 263 (1975)
- 49 R. Damadian and F. W. Cope, *Physiol Chem. & Physics*, 5, 511 (1973)
- 50 F. W. Cope and R. Damadian, *Physiol Chem. & Physics*, 6, 17 (1974)
- 51 N. F. Ramsey, *Phys. Rev.*, 78, 699 (1950)
- 52 J. Kondo and J. Yamashita, *J. Phys. Chem. Solids*, 10, 245 (1959)
- 53 D. Ikenberry and T. P. Das, *Chem. Phys.*, 43, 2199 (1965)
- 54 C. Moore and B. C. Pressman, *Biochem. Biophys. Res. Commun.*, 15, 562 (1964)

- 55 C. J. Pedersen, J. Amer. Chem. Soc., 89, 7071 (1967)
- 56 C. J. Pedersen, J. Amer. Chem. Soc., 92, 391 (1970)
- 57 S. Ciani, G. Eisenman and G. Szabo, J. Membrane Biol. 1 294 (1969)
- 58 D. C. Tostenson, Fred. Proc. Rad. Amer. Soc. Exp. Bio., 27, 1269 (1968)
- 59 H. Lardy, Ibid., 27, 1278 (1968)
- 60 F. L. Cook, T. C. Caruso and C. L. Liotta, Tetrahedron. Lett., 4029 (1974)
- 61 K. H. Wong, G. Knoizer and J. Smid, J. Amer. Chem. Soc., 92, 666 (1970)
- 62 M. J. Maskornick, Tetrahedron Lett., 1797 (1972)
- 63 S. G. Smith and M. P. Hanson, J. Org. Chem., 36, 1931 (1971)
- 64 D. J. Samand and H. E. Simmons, J. Amer. Chem. Soc., 94, 4024 (1972)
- 65 R. M. Izatt, D. T. Eatough and J. J. Christensen, Structure and Bonding, 16, 161 (1973)
- 66 J. M. Lehn, Ibid, 16, 1 (1973)
- 67 J. J. Christensen, D. J. Eatough and R. M. Izatt, Chem. Rev., 74, 351 (1974)
- 68 J. S. Bradshaw and J. Y. Hui, Review, 649 (1974)
- 69 G. W. Gokel and H. D. Durst, Synthesis, 168 (1976)
- 70 A. I. Popov and J. M. Lehn, Chapter in Chemistry of Macrocyclic Compounds, Gordon A. Melson, Editor Plenum Publishing, N. Y, in press.

- 71 J. D. Lamb, R. M. Izatt, J. J. Christensen and D. J. Eatough, "Thermodynamics and Kinetics of Cation-Macrocyclic Interaction" Chapter in Chemistry of Macrocyclic compounds, Gordon A. Melson, Editor, Plenum Publishing, N. Y. in press.
- 72 H. F. Frensdorff, J. Amer. Chem. Soc., 93, 600 (1971)
- 73 R. M. Izatt, R. E. Terry, B. L. Haymore, L. D. Hansen, N. K. Dalley, A. G. Avondet and J. J. Christensen, J. Amer. Chem. Soc., 98, 7620 (1976)
- 74 J. R. Lotz, B. P. Block and W. C. Fermelius, J. Phys. Chem., 63, 541 (1959)
- 75 D. T. Cram, R. C. Helgeson, L. R. Sousa and K. Kaplan, Pure Appl. Chem., 43, 327 (1975)
- 76 S. C. Shah, K. Kopolow and J. Smid, J. Polym. Sci., 14, 2023 (1976)
- 77 E. Mei, A. I. Popov and J. L. Dye, J. Phys. Chem., 81, 1677 (1977)
- 78 N. Matsura and A. Sasaki, Bull. Chem. Soc., Jap. 49 1246 (1976)
- 79 D. F. Evans and E. L. Cusseler, J. Solution Chem., 1, 499 (1972)
- 80 E. M. Arnett and T. C. Moriavity, J. Amer. Chem. Soc., 93, 4908 (1971)
- 81 M. R. Truter, Structure and Bonding, 16, 71 (1973)

- 82 F. P. Boer, M. A. Neuman, F. P. Van-Remortere  
and E. C. Steiner, *Inorg. Chem.*, 13, 2826 (1974)
- 83 F. P. Vanremoortere and F. P. Boer, *Inorg. Chem.*,  
13, 2071 (1974)
- 84 C. Riche and C. P. Billy, *J. C. S. Chem. Comm.*,  
183 (1977)
- 85 M. A. Busch and M. R. Truter, *Chem. Commun.*,  
1349 (1970)
- 86 B. Dietrich, J. M. Lehn and J. P. Sauvage,  
*Tetrahedron Lett.*, 2885 (1969)
- 87 D. Moras, B. Metz and R. Weiss, *Acta Cryst.*,  
B29, 388 (1973)
- 88 B. Metz, D. Moras and R. Weiss, *Chem. Commun.*,  
440 (1971)
- 89 E. Mei, A. I. Popov and J. L. Dye, *J. Amer. Chem.  
Soc.*, 99 6532 (1977)
- 90 P. B. Dietrich, J. M. Lehn and J. P. Sauvage,  
*Tetrahedron Lett.*, 34, 2889 (1969)
- 91 P. B. Dietrich, J. M. Lehn and J. P. Sauvage,  
*Chem. Commun.*, 1055 (1970)
- 92 Y. M. Cahen, J. L. Dye and A. I. Popov, *J. Phys.  
Chem.*, 79 1289 (1975)
- 93 Y. M. Cahen, J. L. Dye and A. I. Popov, *J. Phys.  
Chem.*, 79, 1292 (1975)
- 94 J. L. Dye, C. W. Andrews and S. E. Mathews, *J.  
Phys.*, 79, 3065 (1975)

- 95 J. M. Lehn, *Pure and appl. Chem.*, 49, 857 (1977)
- 96 J. M. Lehn and J. Simon, *Hel. Chim. Acta*, 60,  
141 (1977)
- 97 D. H. Live and S. I. Chan., *Anal. Chem.*, 42, 791  
(1970)
- 98 G. J. Templeman and A. L. VanGeet, *J. Amer.  
Chem. Soc.*, 94, 5578 (1972)
- 99 G. Foex, C. J. Gorter and L. J. Smiths, "Constants  
Selectionnees, Diamagnetisme et. Paramagnetism,  
Relaxation Paramagnetique" Masson & Cie Editeurs  
Paris (1957)
- 100 C. W. Gokel, D. J. Cram, C. L. Liotta, H. P. Harris  
and F. L. Cook, *J. Org. Chem.*, 39, 2445 (1974)
- 101 V. A. Nicely and J. L. Dye, *J. Chem. Educ.*, 48,  
443 (1971)
- 102 R. A. Robinson, J. M. Stokes and R. H. Stokes  
*J. Phys. Chem.*, 65, 542 (1961)
- 103 L. S. Frankel, T. R. Stengle and C. H. Langford  
*Chem. Commun.*, 393 (1965)
- 104 R. G. pearson, *J. Amer. Chem. Soc.*, 85, 3533 (1963)
- 105 R. M. Izatt, R. E. Terry and J. J. Christensen  
*J. Amer. Chem. Soc.* 98 7626 (1976)
- 106 A. Smetana, Private communication
- 107 D. H. Haynes, B. C. Presman and A. K. Walsky,  
*Biochem.*, 10 852 (1971)
- 108 R. Weiss private communication

- 109 W. Lok, Ph.D Thesis Michigan State University (1973)  
110 J. M. Lehn, private communication  
111 J. Kielland, J. Amer. Chem. Soc. 59, 1675 (1937)